

21
152

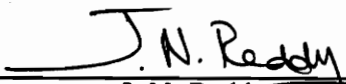
**A STUDY OF VIBRATIONS IN ROTATING LAMINATED COMPOSITE PLATES
ACCOUNTING FOR SHEAR DEFORMATION AND ROTARY INERTIA**

by

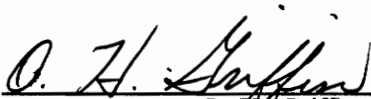
Ravinder Bhumbra

Thesis submitted to the Faculty of the
Virginia Polytechnic Institute and State University
in partial fulfillment of the requirements for the degree of
Master of Science
in
Engineering Mechanics

APPROVED:




J. N. Reddy, Chairman



O. H. Griffin



S. L. Hendricks



J. B. Kosmatka

April 21, 1989

Blacksburg, Virginia

LD
5655
V855
1989
B485

c.2

A STUDY OF VIBRATIONS IN ROTATING LAMINATED COMPOSITE PLATES ACCOUNTING FOR SHEAR DEFORMATION AND ROTARY INERTIA

by

Ravinder Bhumbla

J. N. Reddy, Chairman

Engineering Mechanics

(ABSTRACT)

A first-order shear deformation plate theory is used to predict free vibration frequencies in rotating laminated composite plates. The theory accounts for geometric non-linearity in the form of von Kármán strains. The plate is permitted to have arbitrary orientation and offset from the axis of rotation.

A finite element model is developed to obtain a solution to the problem. The model is validated by comparing the results for free vibration of non-rotating plates for various boundary conditions and material properties with the exact results based on the classical plate theory and the first-order shear deformable plate theory. Results are presented for free vibration of isotropic and laminated composite plates rotating at different angular velocities. A study has also been made on the change in the free vibration frequencies of the plate with angular velocity for different plate thicknesses and for different modulus ratios.

Acknowledgements

I would like to express my gratitude to Dr. J. N. Reddy for his guidance throughout this study.

I also thank Dr. O. H. Griffin and Dr. S. L. Hendricks for their helpful comments and for serving on the thesis committee.

Special thanks are due to Dr. J. B. Kosmatka of Mechanical Engineering Department without whom this study would not have been conceived and could not have been executed. His advice was available at all stages in the study and he was always forthcoming with his helpful suggestions and with literature which proved extremely useful in the research.

I am also grateful to the staff of the Computing Services User Services Department and, in particular, Mr. William Richardson for their help in overcoming difficulties involved in the computational portions of the research.

I am forever indebted to my parents, Mrs. and Dr. D. R. Bhumbla, to my brother, Devinder K. Bhumbla, and, to my sister-in-law, Saroj Bhumbla for their love, support and encouragement.

Table of Contents

- 1.0 INTRODUCTION 1
- 2.0 THEORETICAL DEVELOPMENT 7
 - 2.1 Strain-Displacement Relations 8
 - 2.2 Stresses and Stress Resultants 12
 - 2.2.1 Constitutive relations 12
 - 2.2.2 Stress Resultants 16
 - 2.3 Hamilton’s Principle 20
 - 2.3.1 Strain Energy (U) 20
 - 2.3.2 Kinetic Energy (T) 26
 - 2.3.3 External Work (W_e) 37
 - 2.4 Governing Equations 38
- 3.0 FINITE ELEMENT MODELLING 41
 - 3.1 Static Analysis 42
 - 3.1.1 Newton-Raphson Method 44
 - 3.1.1.1 Tangent Stiffness Matrix 46

3.2 Dynamic Analysis 48

3.2.1 Numerical Integration 51

4.0 RESULTS AND DISCUSSION 53

4.1 Non-Rotating Plates 55

4.1.1 Free Plates 55

4.1.2 Simply-Supported Plates 56

4.1.3 Cantilever Plates 58

4.2 Rotating Plates 73

5.0 CONCLUSIONS 101

REFERENCES 102

Appendix A. Element Matrices 105

A.1.1 Stiffness Matrix : 106

A.1.1.1 Linear Stiffness Matrix (K^L) : 106

A.1.1.2 Non-Linear Stiffness Matrix (K^{NL}) : 106

A.1.1.3 Centrifugal Stiffness Matrix (K^{CF}) : 107

A.1.2 Coriolis Matrix : 107

A.1.3 Mass Matrix : 108

A.2 Centrifugal Stiffness Matrix (K^{CF}) 108

A.3 Coriolis Matrix (C) 111

A.4 Mass Matrix (M) 113

Vita 116

List of Illustrations

Figure 1. Laminate Coordinate System	14
Figure 2. Laminate and Material Principal Directions	15
Figure 3. Translational offsets of the orthogonal axes	27
Figure 4. Rotational offsets of the orthogonal axes	28
Figure 5. Simply Supported Isotropic Plate. Mode 1	61
Figure 6. Simply Supported Isotropic Plate. Mode 1	62
Figure 7. Simply Supported Isotropic Plate. Mode 2	63
Figure 8. Simply Supported Isotropic Plate. Mode 2	64
Figure 9. Simply Supported Isotropic Plate. Mode 3	65
Figure 10. Simply Supported Isotropic Plate. Mode 3	66
Figure 11. Simply Supported [0/90/90/0] Laminated Composite Plate. Mode 1	67
Figure 12. Simply Supported [0/90/90/0] Laminated Composite Plate. Mode 1	68
Figure 13. Simply Supported [0/90/90/0] Laminated Composite Plate. Mode 2	69
Figure 14. Simply Supported [0/90/90/0] Laminated Composite Plate. Mode 2	70
Figure 15. Simply Supported [0/90/90/0] Laminated Composite Plate. Mode 3	71
Figure 16. Simply Supported [0/90/90/0] Laminated Composite Plate. Mode 3	72
Figure 17. Cantilever Isotropic Plate. Mode 1	76
Figure 18. Cantilever Isotropic Plate. Mode 1	77
Figure 19. Cantilever Isotropic Plate. Mode 2	78
Figure 20. Cantilever Isotropic Plate. Mode 2	79
Figure 21. Cantilever Isotropic Plate. Mode 3	80

Figure 22. Cantilever Isotropic Plate. Mode 3	81
Figure 23. Cantilever Laminated Composite [0/90/90/0] Plate. Mode 1	82
Figure 24. Cantilever Laminated Composite [0/90/90/0] Plate. Mode 1	83
Figure 25. Cantilever Laminated Composite [0/90/90/0] Plate. Mode 2	84
Figure 26. Cantilever Laminated Composite [0/90/90/0] Plate. Mode 2	85
Figure 27. Cantilever Laminated Composite [0/90/90/0] Plate. Mode 3	86
Figure 28. Cantilever Laminated Composite [0/90/90/0] Plate. Mode 3	87
Figure 29. Orientation of Plate with Respect to Axis of Rotation	89
Figure 30. Rotating Cantilever Isotropic Plates - Verification of Results	91
Figure 31. Variation in Frequency of Rotating Isotropic Plate with Angular Velocity for First 5 modes	93
Figure 32. Variation in Frequency of Rotating Composite Plate with Angular Velocity for First 5 modes	95
Figure 33. Variation in Fundamental Frequency of Rotating Plate with Angular Velocity for Different Side-to-Thickness Ratios	97
Figure 34. Variation in Fundamental Frequency of Rotating Plate with Angular Velocity for Different Modulus Ratios	100

List of Tables

Table 1. Vibration of Free Isotropic Plates	57
Table 2. Vibration of Simply Supported Isotropic Plates	59
Table 3. Vibration of Simply Supported Laminated Composite Plates	60
Table 4. Vibration of Cantilever Isotropic Plates	74
Table 5. Vibration of Cantilever Laminated Composite Plates	75
Table 6. Rotating Cantilever Isotropic Plates - Verification of Results	90
Table 7. Vibration of Rotating Cantilever Isotropic Plates	92
Table 8. Vibration of Rotating Cantilever Laminated Composite Plates	94
Table 9. Variation in Fundamental Frequency of Rotating Plate with Side-to-Thickness Ratio	96
Table 10. Variation in Fundamental Frequency of Rotating Plate with Modulus Ratio	99

1.0 INTRODUCTION

In recent years, there has been a renewed interest in the design of aircraft turbo-propellers which have much higher fuel efficiency than present aircraft engines. This is because of the availability of composite materials which have a high strength-to-weight ratio, and thus provide quiet and more efficient propellers than other available materials. In this study, an analysis has been made of vibrations in rotating plates to provide a basis for future vibration analysis of rotating turbo-propellers with more complicated geometries.

Earlier studies of vibrations in turbo-propellers used beam models for their analyses. Since low aspect ratio blades are expected to behave like plates rather than like beams, it is hoped that a plate model will provide better results for propellers with high width-to-length ratios.

Chen and Chen [1] studied the vibration and stability of cracked rotating blades. They considered the effects of transverse shear deformation and rotatory inertia. Hodges and Rutkowski [2] made an analysis of free vibrations in rotating beams. Their analysis dealt with rotating beams with both translational and rotational offsets from the axis of rotation. In their paper they have given both the eigenvalues and the mode shapes associated with the rotation of a cantilever beam.

Dokainish and Rawtani [3] used a finite element technique to determine the natural frequencies and mode shapes of an isotropic cantilever plate mounted on a rotating disk and assumed to make any arbitrary angle with the plane of rotation of the disc. Their study assumed geometrically linear strains.

Gupta [4-7], Meirovitch [8], and Bauchau [9] have developed algorithms to solve the eigenvalue problem associated with the undamped free vibration of spinning structures. Bauchau found that the stiffness matrix for the problem was composed of three components : the linear stiffness matrix, the non-linear stiffness matrix due to spin-induced loads, and the centrifugal stiffness matrix. The non-linear and the centrifugal stiffnesses vanish when the plate is not spinning. Besides this, there is a gyroscopic matrix due to the Coriolis acceleration. The stiffness and mass matrices for this problem are symmetric, while the gyroscopic matrix is skew-symmetric.

Gupta was the first to develop an algorithm for this problem which, however, was not very efficient for systems with large bandwidth. Meirovitch offered an alternative solution which took advantage of the symmetric and the skew-symmetric nature of the matrices for this problem, but this procedure destroys the sparsity of the system and, hence, can not be used for large problems. In the present analysis, it has not been possible to use any of the above algorithms because of their unavailability, and only the commonly available subroutines have been used to solve the eigenvalue problem.

Because of the presence of a gyroscopic matrix, the problem has complex roots, occurring in conjugate pairs, with the real part representing the exponential decay (if negative) or exponential growth (if positive), and, the imaginary part representing the frequency of vibration. However, for an undamped vibration problem, as would be expected, the eigenvalues are purely imaginary and the imaginary part of the eigenvalue is the frequency of free vibration of the structure.

Meirovitch [10] showed that for a rotating cantilever beam, the lowest natural frequency of out-of-plane vibration increases with the angular velocity and in such a way that it is always higher than

the angular rotation. Gupta [5] showed that if the non-linear and the centrifugal stiffnesses are omitted in the analysis, the eigenvalues remain almost unchanged for various unchanged spin rates.

In the present study, a finite element model has been developed to study vibration of plates made of laminated composite materials. Some features of this model are :

1. The plate is permitted to have any arbitrary orientation about the inertial reference frame, and any arbitrary displacement from the axis of rotation
2. The laminated composite plate is permitted to have plies with arbitrary orientation, and, each ply is permitted to have different material properties.
3. Aerodynamic loads on the plate have not been considered. So, the plate modelled is physically equivalent to one rotating in a vacuum. (In future studies, aerodynamic loads can be brought into consideration by making minor alterations to the present development.)
4. A first-order non-linear theory of plates with transverse shear deformation has been used for the analysis. This theory incorporates geometrical non-linearity in the form of von Kármán strains.

In earlier analyses of plates, the **classical plate theory** was frequently used. It is a thin plate theory, in that, it considers, and is reasonably accurate for, plates with thickness-to-side ratios of less than 1/20. It is based on the following assumptions:

1. Planes normal to the mid-plane remain plane and normal after deformation, i.e., transverse shear strains are neglected.
2. The mid-plane of the plate remains unstretched after deformation, i.e., the mid-plane of the plate is the neutral plane.
3. Transverse normal stresses are assumed to small and hence are neglected, i.e., a state of plane stress is assumed

This theory can be extended to allow for moderate transverse deflections (of the order of the plate thickness). This can be done by considering the second-order terms in the expressions for the displacements in the plate. One way of doing this is to use the von Kármán theory of plates which considers the products of derivatives of displacements. The von Kármán theory of plates assumes the derivatives of in-plane displacements to be much smaller than the corresponding out of plane terms, and, thus neglects products and squares of derivatives of the in-plane displacements.

However, it is found that the classical plate theory (CPT) under-predicts deflections and over-predicts the natural frequencies. This is attributed to the fact that the transverse shear strains are omitted in the classical plate theory. This assumption is valid for thin plates where transverse shear strains are indeed negligible. However, when transverse shear strains are not negligible, as in the case of thick plates or plates made of composites, the classical plate theory can prove to be inaccurate. Also, the effect of transverse shear deformation is more significant at the higher modes. Thus an alternate theory which allows for transverse shear deformation is required for the analysis of plates made of composite materials.

Reissner [11], Mindlin [12], and others developed a plate theory which allows for transverse shear strains and, hence, is known as the **first- order shear deformation plate theory** (see Reddy [13]). This theory yields much better results for thick plates and for laminated composite plates, and, therefore has been used in the present analysis. The first-order shear deformation plate theory is based on the following assumptions :

1. Planes normal to the mid-plane remain plane but not necessarily normal after deformation.
2. The mid-plane of the plate remains unstretched after deformation, i.e., the mid-plane of the plate remains the neutral plane.
3. Transverse normal stresses are assumed to be negligible compared to the in-plane and the transverse shear stresses.

The first-order shear deformation plate theory has two independent in-plane displacement variables (u, v), and three independent out of plane displacement variables (w, ψ_x, ψ_y). In this theory the displacements are assumed to vary linearly through the thickness. Also, the transverse shear strains, and hence the transverse shear stresses are assumed to be constant through the thickness. This is incorrect as, actually, the transverse shear stresses are observed to vary parabolically through the thickness and are zero at the plate surfaces. Reissner, and Mindlin have attempted to correct this shortcoming by multiplying the transverse shear forces by a constant, called the **shear correction factor**. This makes the strain energy of the plate closer to the exact value though it still does not accurately represent the distribution of the transverse shear stresses through the thickness of the plate. Reissner gave the value of the shear correction factor to be $5/6$ while Mindlin gave it to be $\pi^2/12$ for isotropic rectangular plates. The value given by Reissner has been used in the present study.

In this analysis, four-node bilinear and nine-node quadratic elements have been used for the finite element analysis. Here the Gauss-Legendre quadrature was used for the numerical evaluation of mass, stiffness and coriolis matrices. For a polynomial of degree n , a Gauss-Legendre using $(n + 1)/2$ Gauss points integrates the polynomial exactly. The above integration is referred to as full integration. It is observed, however, that when full integration is carried out on the transverse shear coefficient terms to obtain the element stiffness matrix, there appears to be an over-stiffening of the plate, resulting in under-prediction of deflections and over-prediction of frequencies. This apparent over-stiffening is due to the difference in magnitudes of the transverse shear and the in-plane terms.

To get around the problem, an accepted mathematical *trick* is performed in the integration by using reduced integration on the transverse shear coefficients. In this so-called reduced integration, Gauss quadrature using 1 point less than the full integration is employed for the transverse shear terms. This seems to give acceptable results for static and dynamic analysis of plates. However, it was first observed by Hughes [14,15] that the reduced integration results in rank deficient stiffness and mass matrices for the four-node element. This problem was later observed for the 8-node and 9-node elements also by Verhegghe and Powell [16]. This rank deficiency results in the appearance of some

spurious zero-energy modes. It was observed that this problem manifests only in very thick plates and here only in some special cases. The boundary conditions and the mode shapes associated with this kind of a problem are discussed later. Hughes suggested correcting this error by modifying the reduced integration. Verhegghe and Powell [16] have also discussed techniques to deal with this problem.

Levinson [17], Murthy [18], Reddy [19,20], and others have introduced **higher order shear deformation plate theories**. These theories are based on the same assumptions as the first-order shear deformation plate theory, but allow for a parabolic variation of the transverse shear strains through the thickness, and vanish on the bounding planes. As in the first-order theory, there are two independent in-plane displacement variables (u , v), and three independent out of plane variables (w , ψ_x , ψ_y). Reddy's theory is a variationally consistent theory, whereas Levinson's and Murthy's are not.

The higher order shear deformation plate theories are even more accurate than the first-order plate theory in the analysis of composite plates, but are beyond the scope of this study.

2.0 THEORETICAL DEVELOPMENT

In the displacement-based theories, one assumes that the displacement field can be expressed as a linear combination of unknown functions of (x, y) and the thickness coordinate, z :

$$u(x, y, z, t) = u_0(x, y, t) + z\psi_x(x, y, t) + z^2\xi_x(x, y, t) + z^3\eta_x(x, y, t) + \dots$$

$$v(x, y, z, t) = v_0(x, y, t) + z\psi_y(x, y, t) + z^2\xi_y(x, y, t) + z^3\eta_y(x, y, t) + \dots$$

$$w(x, y, z, t) = w_0(x, y, t) + z\psi_z(x, y, t) + z^2\xi_z(x, y, t) + z^3\eta_z(x, y, t) + \dots$$

where, u , v , and w denote the displacement components of a point along x , y , and z directions, respectively. $u_0, v_0, w_0, \psi_x, \psi_y, \psi_z, \xi_x, \xi_y, \xi_z, \eta_x, \eta_y, \eta_z$ are independent displacement variables.

According to the **first-order shear deformation plate theory (FSDPT)** developed by Reissner [11], Mindlin [12], and others, the inplane displacements are assumed to vary linearly through the thickness, i.e. displacements are functions of first order powers of z . Thus, the displacement field for a first-order shear deformation theory can be expressed as:

$$u(x, y, z, t) = u_0(x, y, t) + z\psi_x(x, y, t)$$

$$v(x, y, z, t) = v_0(x, y, t) + z\psi_y(x, y, t)$$

$$w(x, y, z, t) = w_0(x, y, t) \quad [2.1.1]$$

where, ψ_x and ψ_y are the rotations about y and x axes, respectively. Note that w is assumed to be constant through the thickness, implying that the transverse normal strain is negligible.

2.1 Strain-Displacement Relations

In general, the strain-displacement relations can be written as:

$$\varepsilon_{ij} = \frac{1}{2}(V_{i,j} + V_{j,i} + V_{r,i}V_{r,j})$$

where the indices vary from 1 to 3, and, repeated indices indicate summation over the index (Ex:

$$l_{rr} = l_{11} + l_{22} + l_{33}), \text{ and,}$$

$$V_1 = u, \quad V_2 = v, \quad V_3 = w$$

Thus, for example,

$$\varepsilon_{11} = V_{1,1} + \frac{1}{2}(V_{1,1}^2 + V_{2,1}^2 + V_{3,1}^2)$$

However, for plates, the inplane displacements and their derivatives are much smaller in magnitude compared to the corresponding out of plane terms. So, according to von Kármán's hypothesis, terms containing products or squares of derivatives of inplane displacements can be neglected in comparison with the corresponding out of plane terms. Thus, for example,

$$\varepsilon_{11} = V_{1,1} + \frac{1}{2}(V_{3,1})^2$$

or, writing the relations in terms of u, v, w, x, y, and z,

$$\varepsilon_{xx} = \frac{\partial u}{\partial x} + \frac{1}{2} \left(\frac{\partial w}{\partial x} \right)^2$$

$$\varepsilon_{yy} = \frac{\partial v}{\partial y} + \frac{1}{2} \left(\frac{\partial w}{\partial y} \right)^2$$

$$\varepsilon_{zz} = 0$$

$$\gamma_{xy} = \frac{\partial u}{\partial y} + \frac{\partial v}{\partial x} + \frac{\partial w}{\partial x} \frac{\partial w}{\partial y}$$

$$\gamma_{yz} = \frac{\partial v}{\partial z} + \frac{\partial w}{\partial y}$$

$$\gamma_{xz} = \frac{\partial u}{\partial z} + \frac{\partial w}{\partial x}$$

Using the displacement field [2.1.1], the following strain-displacement relations can be derived :

$$\varepsilon_{xx} = \frac{\partial u_0}{\partial x} + z \frac{\partial \psi_x}{\partial x} + \frac{1}{2} \left(\frac{\partial w_0}{\partial x} \right)^2$$

$$\varepsilon_{yy} = \frac{\partial v_0}{\partial y} + z \frac{\partial \psi_y}{\partial y} + \frac{1}{2} \left(\frac{\partial w_0}{\partial y} \right)^2$$

$$\varepsilon_{zz} = 0$$

$$\gamma_{xy} = \frac{\partial u_0}{\partial y} + \frac{\partial v_0}{\partial x} + z \left(\frac{\partial \psi_x}{\partial y} + \frac{\partial \psi_y}{\partial x} \right) + \frac{\partial w_0}{\partial x} \frac{\partial w_0}{\partial y}$$

$$\gamma_{yz} = \psi_y + \frac{\partial w_0}{\partial y}$$

$$\gamma_{xz} = \psi_x + \frac{\partial w_0}{\partial x}$$

[2.1.2]

In the classical plate theory, the normality of cross-section (Assumption 1 on page 3) implies that the rotations ψ_x and ψ_y are related to the derivatives of the transverse deflection by :

$$\psi_y = -\frac{\partial w_0}{\partial y}, \quad \psi_x = -\frac{\partial w_0}{\partial x}$$

$$\text{So, } \gamma_{yz} = \gamma_{xz} = 0$$

Writing in a condensed form, the FSDPT strain-displacement relations can be written as,

$$\begin{bmatrix} \varepsilon_1 \\ \varepsilon_2 \\ \varepsilon_6 \\ \varepsilon_4 \\ \varepsilon_5 \end{bmatrix} = \begin{bmatrix} \varepsilon_{xx} \\ \varepsilon_{yy} \\ \gamma_{xy} \\ \gamma_{yz} \\ \gamma_{xz} \end{bmatrix} = \begin{bmatrix} \varepsilon_0 \\ \gamma_0 \end{bmatrix} + z \begin{bmatrix} \kappa \\ 0 \end{bmatrix} + \begin{bmatrix} \varepsilon^{NL} \\ 0 \end{bmatrix} \quad [2.1.3]$$

where,

$\{\varepsilon_0\}$ are the mid-plane strains given by:

$$\{\varepsilon_0\} = \begin{bmatrix} \frac{\partial u_0}{\partial x} \\ \frac{\partial v_0}{\partial y} \\ \frac{\partial u_0}{\partial y} + \frac{\partial v_0}{\partial x} \end{bmatrix} \quad [2.1.4]$$

$\{\gamma_0\}$ are the shearing strains given by:

$$\{\gamma_0\} = \begin{bmatrix} \psi_y + \frac{\partial w_0}{\partial y} \\ \psi_x + \frac{\partial w_0}{\partial x} \end{bmatrix} \quad [2.1.5]$$

$\{\kappa\}$ are the bending curvatures given by

$$\{\kappa\} = \begin{bmatrix} \frac{\partial \psi_x}{\partial x} \\ \frac{\partial \psi_y}{\partial y} \\ \frac{\partial \psi_x}{\partial y} + \frac{\partial \psi_y}{\partial x} \end{bmatrix} \quad [2.1.6]$$

$\{\varepsilon_{NL}\}$ are the non-linear mid-plane strains given by

$$\{\varepsilon^{NL}\} = \begin{bmatrix} \frac{1}{2} \left(\frac{\partial w_0}{\partial x} \right)^2 \\ \frac{1}{2} \left(\frac{\partial w_0}{\partial y} \right)^2 \\ \frac{\partial w_0}{\partial x} \frac{\partial w_0}{\partial y} \end{bmatrix} \quad [2.1.7]$$

2.2 Stresses and Stress Resultants

2.2.1 Constitutive relations

For an **orthotropic** material, the relations between the stresses and the strains, called the constitutive relations, are given by:

$$\begin{bmatrix} \sigma_1 \\ \sigma_2 \\ \sigma_3 \\ \tau_{23} \\ \tau_{13} \\ \tau_{12} \end{bmatrix} = \begin{bmatrix} C_{11} & C_{12} & C_{13} & 0 & 0 & 0 \\ C_{12} & C_{22} & C_{23} & 0 & 0 & 0 \\ C_{13} & C_{23} & C_{33} & 0 & 0 & 0 \\ 0 & 0 & 0 & C_{44} & 0 & 0 \\ 0 & 0 & 0 & 0 & C_{55} & 0 \\ 0 & 0 & 0 & 0 & 0 & C_{66} \end{bmatrix} \begin{bmatrix} \varepsilon_1 \\ \varepsilon_2 \\ \varepsilon_3 \\ \gamma_{23} \\ \gamma_{13} \\ \gamma_{12} \end{bmatrix} \quad [2.2.1]$$

where, C_{ij} are independent material constants obtained from the generalized Hooke's law.

For the first order shear deformation plate theory, transverse normal stress, σ_3 is assumed to be zero.

Thus,

$$\sigma_3 = C_{13}\varepsilon_1 + C_{23}\varepsilon_2 + C_{33}\varepsilon_3 = 0$$

Or,

$$\varepsilon_3 = -\frac{C_{13}}{C_{33}}\varepsilon_1 - \frac{C_{23}}{C_{33}}\varepsilon_2$$

Substituting the above relation into the constitutive relations, the constitutive relations can be written in the material principal directions for a single ply as [22]:

$$\begin{bmatrix} \sigma_1 \\ \sigma_2 \\ \tau_{12} \\ \tau_{23} \\ \tau_{13} \end{bmatrix} = \begin{bmatrix} Q_{11} & Q_{12} & 0 & 0 & 0 \\ Q_{12} & Q_{22} & 0 & 0 & 0 \\ 0 & 0 & Q_{66} & 0 & 0 \\ 0 & 0 & 0 & Q_{44} & 0 \\ 0 & 0 & 0 & 0 & Q_{55} \end{bmatrix} \begin{bmatrix} \varepsilon_1 \\ \varepsilon_2 \\ \gamma_{12} \\ \gamma_{23} \\ \gamma_{13} \end{bmatrix} \quad [2.2.2]$$

where,

$$Q_{11} = C_{11} - \frac{C_{13} C_{13}}{C_{33}}$$

$$Q_{12} = C_{12} - \frac{C_{13} C_{23}}{C_{33}}$$

$$Q_{22} = C_{22} - \frac{C_{23} C_{23}}{C_{33}}$$

$$Q_{44} = C_{44}, Q_{55} = C_{55}, Q_{66} = C_{66}$$

$$\text{Or, } Q_{ij} = C_{ij} - \frac{C_{i3} C_{j3}}{C_{33}} \quad i, j = 1, 2$$

Q is known as the "reduced" stiffness matrix for the laminate.

If the material principal directions are considered to be at an arbitrary angle θ to the laminate principal directions, as shown in Figure 1 on page 14 and Figure 2 on page 15, then the above constitutive relations for the m^{th} ply are given in the global coordinates as:

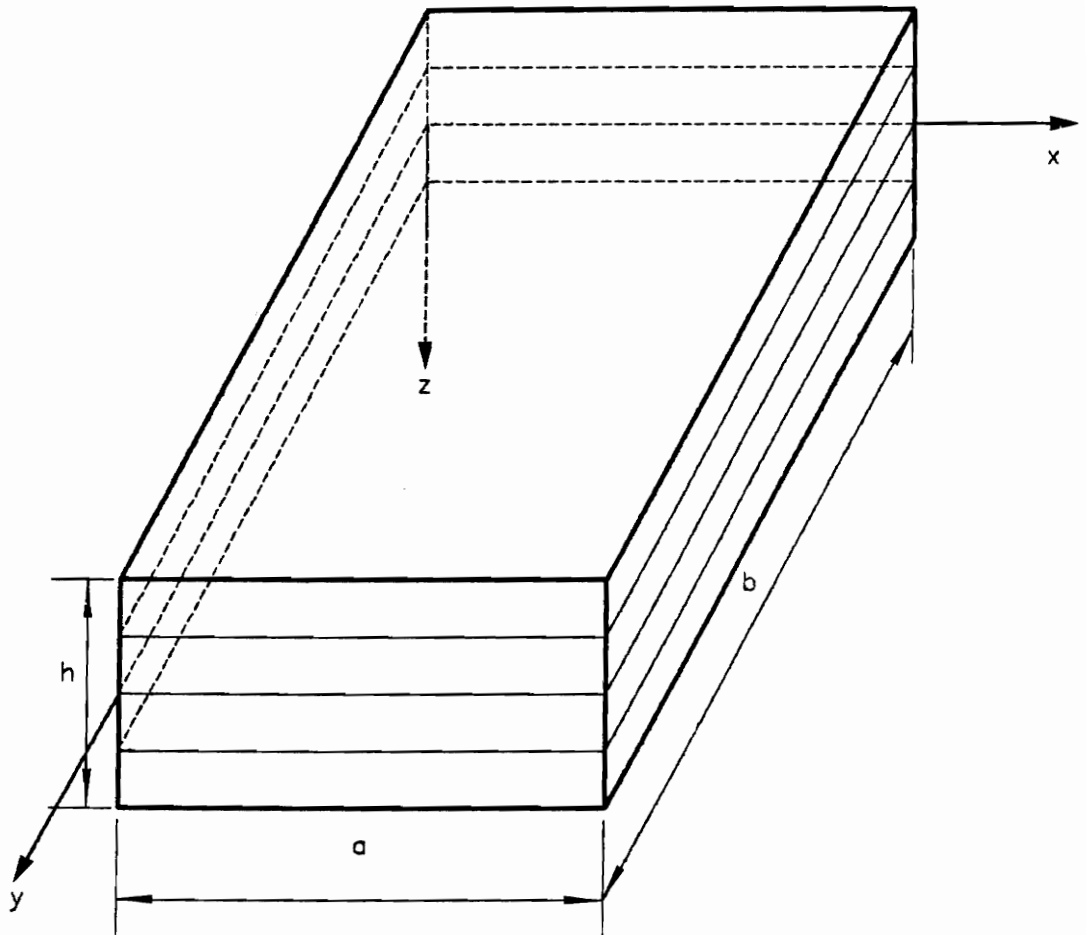
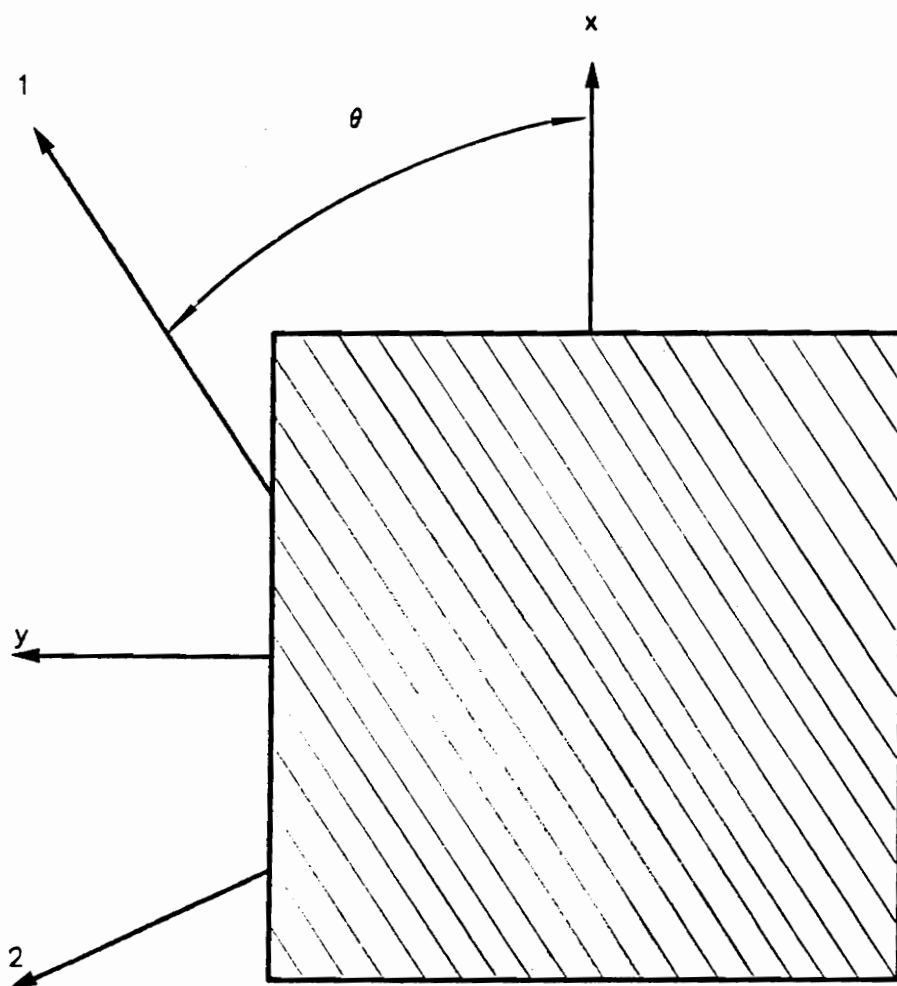


Figure 1. Laminate Coordinate System



- $1, 2$ - Material Principle Directions
 x, y - Laminate Principle Directions

Figure 2. Laminate and Material Principle Directions

$$\begin{bmatrix} \sigma_x \\ \sigma_y \\ \tau_{xy} \\ \tau_{yz} \\ \tau_{xz} \end{bmatrix}^{(m)} = \begin{bmatrix} \bar{Q}_{11} & \bar{Q}_{12} & \bar{Q}_{16} & 0 & 0 \\ \bar{Q}_{12} & \bar{Q}_{22} & \bar{Q}_{26} & 0 & 0 \\ \bar{Q}_{16} & \bar{Q}_{26} & \bar{Q}_{66} & 0 & 0 \\ 0 & 0 & 0 & \bar{Q}_{44} & \bar{Q}_{45} \\ 0 & 0 & 0 & \bar{Q}_{45} & \bar{Q}_{55} \end{bmatrix}^{(m)} \begin{bmatrix} \varepsilon_x \\ \varepsilon_y \\ \gamma_{xy} \\ \gamma_{yz} \\ \gamma_{xz} \end{bmatrix}^{(m)} \quad [2.2.3]$$

where,

$$\begin{bmatrix} \bar{Q}_{11} & \bar{Q}_{12} & \bar{Q}_{16} \\ \bar{Q}_{12} & \bar{Q}_{22} & \bar{Q}_{26} \\ \bar{Q}_{16} & \bar{Q}_{26} & \bar{Q}_{66} \end{bmatrix} = \begin{bmatrix} m^2 & n^2 & 2mn \\ n^2 & m^2 & -2mn \\ -mn & mn & m^2 - n^2 \end{bmatrix}^{-1} \begin{bmatrix} Q_{11} & Q_{12} & 0 \\ Q_{12} & Q_{22} & 0 \\ 0 & 0 & Q_{66} \end{bmatrix} \begin{bmatrix} m^2 & n^2 & mn \\ n^2 & m^2 & -mn \\ -2mn & 2mn & m^2 - n^2 \end{bmatrix}$$

$$\begin{bmatrix} \bar{Q}_{44} & \bar{Q}_{45} \\ \bar{Q}_{45} & \bar{Q}_{55} \end{bmatrix} = \begin{bmatrix} m & -n \\ n & m \end{bmatrix}^{-1} \begin{bmatrix} Q_{44} & Q_{45} \\ Q_{45} & Q_{55} \end{bmatrix}^{(m)} \begin{bmatrix} m & -n \\ n & m \end{bmatrix}$$

where, $m = \cos \theta$, and, $n = \sin \theta$

2.2.2 Stress Resultants

The stress resultants are given by

$$\begin{bmatrix} N_x \\ N_y \\ N_{xy} \end{bmatrix} = \int_{-h/2}^{h/2} \begin{bmatrix} \sigma_x \\ \sigma_y \\ \tau_{xy} \end{bmatrix} dz = \sum_{m=1}^n \int_{z_m}^{z_{m+1}} \begin{bmatrix} \sigma_x \\ \sigma_y \\ \tau_{xy} \end{bmatrix}^{(m)} dz$$

$$= \sum_{m=1}^n \int_{z_m}^{z_{m+1}} \begin{bmatrix} \bar{Q}_{11} & \bar{Q}_{12} & \bar{Q}_{16} \\ \bar{Q}_{12} & \bar{Q}_{22} & \bar{Q}_{26} \\ \bar{Q}_{16} & \bar{Q}_{26} & \bar{Q}_{66} \end{bmatrix}^{(m)} \begin{bmatrix} \varepsilon_x \\ \varepsilon_y \\ \gamma_{xy} \end{bmatrix}^{(m)} dz \quad [2.2.4]$$

where, z_m is the distance of the bottom of the m^{th} ply from the mid-plane of the plate.

Similarly,

$$\begin{bmatrix} M_x \\ M_y \\ M_{xy} \end{bmatrix} = \sum_{m=1}^n \int_{z_m}^{z_{m+1}} \begin{bmatrix} \bar{Q}_{11} & \bar{Q}_{12} & \bar{Q}_{16} \\ \bar{Q}_{12} & \bar{Q}_{22} & \bar{Q}_{26} \\ \bar{Q}_{16} & \bar{Q}_{26} & \bar{Q}_{66} \end{bmatrix}^{(m)} \begin{bmatrix} \varepsilon_x \\ \varepsilon_y \\ \gamma_{xy} \end{bmatrix}^{(m)} z \, dz$$

$$\begin{Bmatrix} Q_y \\ Q_x \end{Bmatrix} = \sum_{m=1}^n \int_{z_m}^{z_{m+1}} k^2 \begin{bmatrix} \bar{Q}_{44} & \bar{Q}_{45} \\ \bar{Q}_{45} & \bar{Q}_{55} \end{bmatrix}^{(m)} \begin{Bmatrix} \gamma_{yz} \\ \gamma_{xz} \end{Bmatrix}^{(m)} dz \quad [2.2.5]$$

Substituting for the ply strains in terms of the mid-ply strains and curvatures,

$$\begin{bmatrix} N_x \\ N_y \\ N_{xy} \end{bmatrix} = \sum_{m=1}^n \int_{z_m}^{z_{m+1}} \begin{bmatrix} \bar{Q}_{11} & \bar{Q}_{12} & \bar{Q}_{16} \\ \bar{Q}_{12} & \bar{Q}_{22} & \bar{Q}_{26} \\ \bar{Q}_{16} & \bar{Q}_{26} & \bar{Q}_{66} \end{bmatrix} \left[\begin{Bmatrix} \varepsilon_0 \end{Bmatrix} + z \begin{Bmatrix} \kappa \end{Bmatrix} + \begin{Bmatrix} \varepsilon^{NL} \end{Bmatrix} \right] dz$$

$$= \begin{bmatrix} A_{11} & A_{12} & A_{16} \\ A_{12} & A_{22} & A_{26} \\ A_{16} & A_{26} & A_{66} \end{bmatrix} \left[\begin{Bmatrix} \varepsilon_0 \end{Bmatrix} + \begin{Bmatrix} \varepsilon^{NL} \end{Bmatrix} \right] + \begin{bmatrix} B_{11} & B_{12} & B_{16} \\ B_{12} & B_{22} & B_{26} \\ B_{16} & B_{26} & B_{66} \end{bmatrix} \begin{Bmatrix} \kappa \end{Bmatrix} \quad [2.2.6]$$

where,

$$A_{ij} = \sum_{m=1}^n \int_{z_m}^{z_{m+1}} \bar{Q}_{ij} \, dz \quad i, j = 1, 2, 6$$

$$= \sum_{m=1}^n (\bar{Q}_{ij})^{(m)} (z_{m+1} - z_m) \quad [2.2.7]$$

$$\begin{aligned}
B_{ij} &= \sum_{m=1}^n \int_{z_m}^{z_{m+1}} \bar{Q}_{ij} z dz \quad i, j = 1, 2, 6 \\
&= \sum_{m=1}^n (\bar{Q}_{ij})^{(m)} \left(\frac{z_{m+1}^2 - z_m^2}{2} \right)
\end{aligned} \tag{2.2.8}$$

and, $\{\varepsilon_0\}$, $\{\varepsilon^{NL}\}$, $\{\kappa\}$ are as defined earlier. Similarly,

$$\begin{aligned}
\begin{bmatrix} M_x \\ M_y \\ M_{xy} \end{bmatrix} &= \sum_{m=1}^n \int_{z_m}^{z_{m+1}} \begin{bmatrix} \bar{Q}_{11} & \bar{Q}_{12} & \bar{Q}_{16} \\ \bar{Q}_{12} & \bar{Q}_{22} & \bar{Q}_{26} \\ \bar{Q}_{16} & \bar{Q}_{26} & \bar{Q}_{66} \end{bmatrix} \left[\begin{Bmatrix} \varepsilon_0 \end{Bmatrix} + z \begin{Bmatrix} \kappa \end{Bmatrix} + \begin{Bmatrix} \varepsilon^{NL} \end{Bmatrix} \right] z dz \\
&= \begin{bmatrix} B_{11} & B_{12} & B_{16} \\ B_{12} & B_{22} & B_{26} \\ B_{16} & B_{26} & B_{66} \end{bmatrix} \left[\begin{Bmatrix} \varepsilon_0 \end{Bmatrix} + \begin{Bmatrix} \varepsilon^{NL} \end{Bmatrix} \right] + \begin{bmatrix} D_{11} & D_{12} & D_{16} \\ D_{12} & D_{22} & D_{26} \\ D_{16} & D_{26} & D_{66} \end{bmatrix} \begin{Bmatrix} \kappa \end{Bmatrix}
\end{aligned}$$

where,

$$\begin{aligned}
D_{ij} &= \sum_{m=1}^n \int_{z_m}^{z_{m+1}} \bar{Q}_{ij} z^2 dz \quad i, j = 1, 2, 6 \\
&= \sum_{m=1}^n \bar{Q}_{ij}^{(m)} \left(\frac{z_{m+1}^3 - z_m^3}{3} \right)
\end{aligned}$$

And,

$$\begin{Bmatrix} Q_y \\ Q_x \end{Bmatrix} = \sum_{m=1}^n \int_{z_m}^{z_{m+1}} k^2 \begin{bmatrix} \bar{Q}_{44} & \bar{Q}_{45} \\ \bar{Q}_{45} & \bar{Q}_{55} \end{bmatrix} \begin{Bmatrix} \gamma_0 \end{Bmatrix} dz$$

$$= \begin{bmatrix} \bar{A}_{44} & \bar{A}_{45} \\ \bar{A}_{45} & \bar{A}_{55} \end{bmatrix} \begin{Bmatrix} \gamma_0 \end{Bmatrix}$$

where, k^2 is the shear correction factor given by Reissner to be 5/6, and

$$\begin{aligned} A_{ij} &= \sum_{m=1}^n \int_{z_m}^{z_{m+1}} k^2 \bar{Q}_{ij} dz \quad i, j = 4, 5 \\ &= \sum_{m=1}^n k^2 \bar{Q}_{ij}^{(m)} (z_{m+1} - z_m) \end{aligned}$$

Thus, the following expressions are obtained for the stress resultants:

$$\begin{bmatrix} N_x \\ N_y \\ N_{xy} \\ M_x \\ M_y \\ M_{xy} \\ Q_y \\ Q_x \end{bmatrix} = \begin{bmatrix} A_{11} & A_{12} & A_{16} & B_{11} & B_{12} & B_{16} & 0 & 0 \\ A_{12} & A_{22} & A_{26} & B_{12} & B_{22} & B_{26} & 0 & 0 \\ A_{16} & A_{26} & A_{66} & B_{16} & B_{26} & B_{66} & 0 & 0 \\ B_{11} & B_{12} & B_{16} & D_{11} & D_{12} & D_{16} & 0 & 0 \\ B_{12} & B_{22} & B_{26} & D_{12} & D_{22} & D_{26} & 0 & 0 \\ B_{16} & B_{26} & B_{66} & D_{16} & D_{26} & D_{66} & 0 & 0 \\ 0 & 0 & 0 & 0 & 0 & 0 & \bar{A}_{44} & \bar{A}_{45} \\ 0 & 0 & 0 & 0 & 0 & 0 & \bar{A}_{45} & \bar{A}_{55} \end{bmatrix} \begin{bmatrix} \left\{ \varepsilon_0 + \varepsilon^{NL} \right\} \\ \left\{ \kappa \right\} \\ \left\{ \gamma_0 \right\} \end{bmatrix} \quad [2.2.9]$$

2.3 *Hamilton's Principle*

Hamilton's principle is used to obtain the equations of motion by setting the variation in the integral of the Lagrangian function equal to zero.

$$0 = \delta \int_{t_1}^{t_2} L dt = \delta \int_{t_1}^{t_2} (U - T - W_e) dt \quad [2.3.1]$$

where,

U = Plate Strain Energy

T = Plate Kinetic Energy

W_e = Plate External Work

2.3.1 Strain Energy (U)

The strain energy for an elastic system is given by

$$U = \frac{1}{2} \int_V (\sigma_x \epsilon_x + \sigma_y \epsilon_y + \sigma_z \epsilon_z + \tau_{xy} \gamma_{xy} + \tau_{yz} \gamma_{yz} + \tau_{xz} \gamma_{xz}) dV \quad [2.3.2]$$

For plain stress assumption, $\sigma_z = 0$.

Therefore,

$$U = \frac{1}{2} \int_V (\sigma_x \epsilon_x + \sigma_y \epsilon_y + \tau_{xy} \gamma_{xy} + \tau_{yz} \gamma_{yz} + \tau_{xz} \gamma_{xz}) dV$$

$$= \frac{1}{2} \int_A \int_{-h/2}^{h/2} (\sigma_x \varepsilon_x + \sigma_y \varepsilon_y + \tau_{xy} \gamma_{xy} + \tau_{yz} + \tau_{xz} \gamma_{xz}) dV$$

$$= \frac{1}{2} \int_A \int_{-h/2}^{h/2} \begin{bmatrix} \varepsilon_x \\ \varepsilon_y \\ \gamma_{xy} \\ \gamma_{yz} \\ \gamma_{xz} \end{bmatrix}^T \begin{bmatrix} \sigma_x \\ \sigma_y \\ \tau_{xy} \\ \tau_{yz} \\ \tau_{xz} \end{bmatrix} dz dA$$

Thus, using the first order shear deformation plate theory relations,

$$U = \frac{1}{2} \int_A \int_{-h/2}^{h/2} \left[\begin{bmatrix} \{\varepsilon_0\} \\ \{\gamma_0\} \end{bmatrix} + z \begin{bmatrix} \{\kappa\} \\ \{0\} \end{bmatrix} + \begin{bmatrix} \{\varepsilon^{NL}\} \\ \{0\} \end{bmatrix} \right]^T \begin{bmatrix} \sigma_x \\ \sigma_y \\ \tau_{xy} \\ \tau_{yz} \\ \tau_{xz} \end{bmatrix} dz dA$$

$$= \frac{1}{2} \int_A \int_{-h/2}^{h/2} \left[\begin{bmatrix} \{\varepsilon_0\} \\ \{\gamma_0\} \end{bmatrix} + \begin{bmatrix} \{\varepsilon^{NL}\} \\ \{0\} \end{bmatrix} \right]^T \begin{bmatrix} \sigma_x \\ \sigma_y \\ \tau_{xy} \\ \tau_{yz} \\ \tau_{xz} \end{bmatrix} dz dA + \frac{1}{2} \int_A \int_{-h/2}^{h/2} z \begin{bmatrix} \{\kappa\} \\ \{0\} \end{bmatrix}^T \begin{bmatrix} \sigma_x \\ \sigma_y \\ \tau_{xy} \\ \tau_{yz} \\ \tau_{xz} \end{bmatrix} dz dA$$

$$\begin{aligned}
&= \frac{1}{2} \int_A \left[\begin{array}{c} \{\varepsilon_0\} \\ \{\gamma_0\} \end{array} \right] + \left[\begin{array}{c} \{\varepsilon^{NL}\} \\ \{0\} \end{array} \right] \left[\begin{array}{c} N_x \\ N_y \\ N_{xy} \\ Q_y \\ Q_x \end{array} \right]^T dA + \frac{1}{2} \int_A \{\kappa\}^T \left[\begin{array}{c} M_x \\ M_y \\ M_{xy} \end{array} \right] dA \\
&= \frac{1}{2} \int_A \left[\begin{array}{c} \{\varepsilon_0\} + \{\varepsilon^{NL}\} \\ \{\kappa\} \\ \{\gamma_0\} \end{array} \right]^T \left[\begin{array}{c} N_x \\ N_y \\ N_{xy} \\ M_x \\ M_y \\ M_{xy} \\ Q_y \\ Q_x \end{array} \right] dA \quad [2.3.3]
\end{aligned}$$

But, from [2.2.9],

$$\left[\begin{array}{c} N_x \\ N_y \\ N_{xy} \\ M_x \\ M_y \\ M_{xy} \\ Q_y \\ Q_x \end{array} \right] = \left[\begin{array}{ccc} \left[\begin{array}{c} A \end{array} \right] & \left[\begin{array}{c} B \end{array} \right] & \left[\begin{array}{c} 0 \end{array} \right] \\ \left[\begin{array}{c} B \end{array} \right] & \left[\begin{array}{c} D \end{array} \right] & \left[\begin{array}{c} 0 \end{array} \right] \\ \left[\begin{array}{c} 0 \end{array} \right] & \left[\begin{array}{c} 0 \end{array} \right] & \left[\begin{array}{c} \bar{A} \end{array} \right] \end{array} \right] \left[\begin{array}{c} \{\varepsilon_0\} + \{\varepsilon^{NL}\} \\ \{\kappa\} \\ \{\gamma_0\} \end{array} \right]$$

Substituting [2.2.9] into [2.3.3] and taking the variation of the strain energy will produce the following relation :

$$\therefore \delta U = \int_A \begin{bmatrix} \left\{ \delta \varepsilon_0 \right\} + \left\{ \delta \varepsilon^{NL} \right\} \\ \left\{ \delta \kappa \right\} \\ \left\{ \delta \gamma_0 \right\} \end{bmatrix} \begin{bmatrix} N_x \\ N_y \\ N_{xy} \\ M_x \\ M_y \\ M_{xy} \\ Q_y \\ Q_x \end{bmatrix} dA \quad [2.3.4]$$

Using definitions from [2.1.3], [2.1.4], [2.1.5], [2.1.6],

$$[\delta \varepsilon_0] = \begin{bmatrix} \frac{\partial \delta u_0}{\partial x} \\ \frac{\partial \delta v_0}{\partial y} \\ \frac{\partial \delta u_0}{\partial y} + \frac{\partial \delta v_0}{\partial x} \end{bmatrix}$$

$$[\delta \kappa] = \begin{bmatrix} \frac{\partial \delta \psi_x}{\partial x} \\ \frac{\partial \delta \psi_y}{\partial y} \\ \frac{\partial \delta \psi_x}{\partial y} + \frac{\partial \delta \psi_y}{\partial x} \end{bmatrix}$$

$$[\delta \gamma_0] = \begin{bmatrix} \delta \psi_y + \frac{\partial \delta w_0}{\partial y} \\ \delta \psi_x + \frac{\partial \delta w_0}{\partial x} \end{bmatrix}$$

$$[\delta \varepsilon^{NL}] = \begin{bmatrix} \frac{\partial w_0}{\partial x} \frac{\partial \delta w_0}{\partial x} \\ \frac{\partial w_0}{\partial y} \frac{\partial \delta w_0}{\partial y} \\ \frac{\partial w_0}{\partial x} \frac{\partial \delta w_0}{\partial y} + \frac{\partial w_0}{\partial y} \frac{\partial \delta w_0}{\partial x} \end{bmatrix} \quad [2.3.5]$$

Thus using [2.3.4] and [2.3.5], the following expression is obtained for the variation in Strain Energy.

$$\begin{aligned}
 \therefore \delta U = & \int_A \left[N_x \left(\frac{\partial \delta u_0}{\partial x} + \frac{\partial w_0}{\partial x} \frac{\partial \delta w_0}{\partial x} \right) + N_y \left(\frac{\partial \delta v_0}{\partial y} + \frac{\partial w_0}{\partial y} \frac{\partial \delta w_0}{\partial y} \right) \right. \\
 & + N_{xy} \left(\frac{\partial \delta u_0}{\partial y} + \frac{\partial \delta v_0}{\partial x} + \frac{\partial w_0}{\partial x} \frac{\partial \delta w_0}{\partial y} + \frac{\partial w_0}{\partial y} \frac{\partial \delta w_0}{\partial x} \right) \\
 & + M_x \left(\frac{\partial \delta \psi_x}{\partial x} \right) + M_y \left(\frac{\partial \delta \psi_y}{\partial y} \right) + M_{xy} \left(\frac{\partial \delta \psi_y}{\partial x} + \frac{\partial \delta \psi_x}{\partial y} \right) \\
 & \left. + Q_y \left(\delta \psi_y + \frac{\partial \delta w_0}{\partial y} \right) + Q_x \left(\delta \psi_x + \frac{\partial \delta w_0}{\partial x} \right) \right] dA \quad [2.3.6]
 \end{aligned}$$

Integrating by parts, one will get the final form of the variation of the total strain energy.

$$\begin{aligned}
 \delta U = & - \int_A \left\{ \left[\frac{\partial N_x}{\partial x} + \frac{\partial N_{xy}}{\partial y} \right] \delta u_0 + \left[\frac{\partial N_y}{\partial y} + \frac{\partial N_{xy}}{\partial x} \right] \delta v_0 \right. \\
 & + \left[\frac{\partial}{\partial x} \left(N_x \frac{\partial w_0}{\partial x} + N_{xy} \frac{\partial w_0}{\partial y} \right) + \frac{\partial Q_x}{\partial x} \right. \\
 & \left. + \frac{\partial}{\partial y} \left(N_y \frac{\partial w_0}{\partial y} + N_{xy} \frac{\partial w_0}{\partial x} \right) + \frac{\partial Q_y}{\partial y} \right] \delta w_0 \\
 & \left. + \left[\frac{\partial M_x}{\partial x} + \frac{\partial M_{xy}}{\partial y} - Q_x \right] \delta \psi_x \right.
 \end{aligned}$$

$$+ \left[\frac{\partial M_y}{\partial y} + \frac{\partial M_{xy}}{\partial x} - Q_y \right] \delta \psi_y \Bigg\} dA \quad [2.3.7]$$

2.3.2 Kinetic Energy (T)

The total Kinetic Energy of a plate can be expressed as :

$$T = \frac{1}{2} \int_V \rho \hat{V} \cdot \hat{V} dV \quad [2.3.8]$$

where, ρ is the mass density of the plate and \hat{V} is the velocity vector of an arbitrary point on the plate with respect to the inertial reference frame $(\tilde{i}, \tilde{j}, \tilde{k})$

It has been assumed that the plate rotates about the inertial coordinate system $(\tilde{i}, \tilde{j}, \tilde{k})$, with an angular velocity Ω about the \tilde{k} axis.

$$\therefore \hat{V} = \dot{\hat{r}} + \Omega \hat{k} \times \hat{r} \quad [2.3.9]$$

where, \hat{r} is the position vector from the origin of the inertial reference frame to a point on the deformed plate

From Figure 3 on page 27,

$$\hat{r} = \begin{pmatrix} h_i & h_j & h_k \end{pmatrix} \begin{bmatrix} \hat{i} \\ \hat{j} \\ \hat{k} \end{bmatrix} + \begin{pmatrix} x + u & y + v & w \end{pmatrix} \begin{bmatrix} \hat{e}_x \\ \hat{e}_y \\ \hat{e}_z \end{bmatrix} \quad [2.3.10]$$

The plate element is in $\hat{e}_x - \hat{e}_y$ plane. Therefore, $z = 0$ for each element.

For first-order shear deformation plate theory,

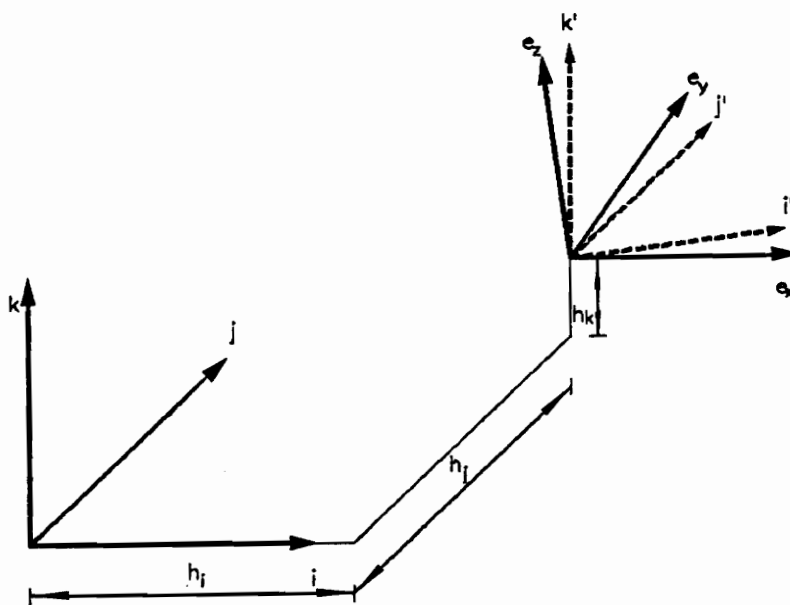


Figure 3. Translational offsets of the orthogonal axes $(\hat{e}_x, \hat{e}_y, \hat{e}_z)$ from the inertial axes $(\hat{i}, \hat{j}, \hat{k})$

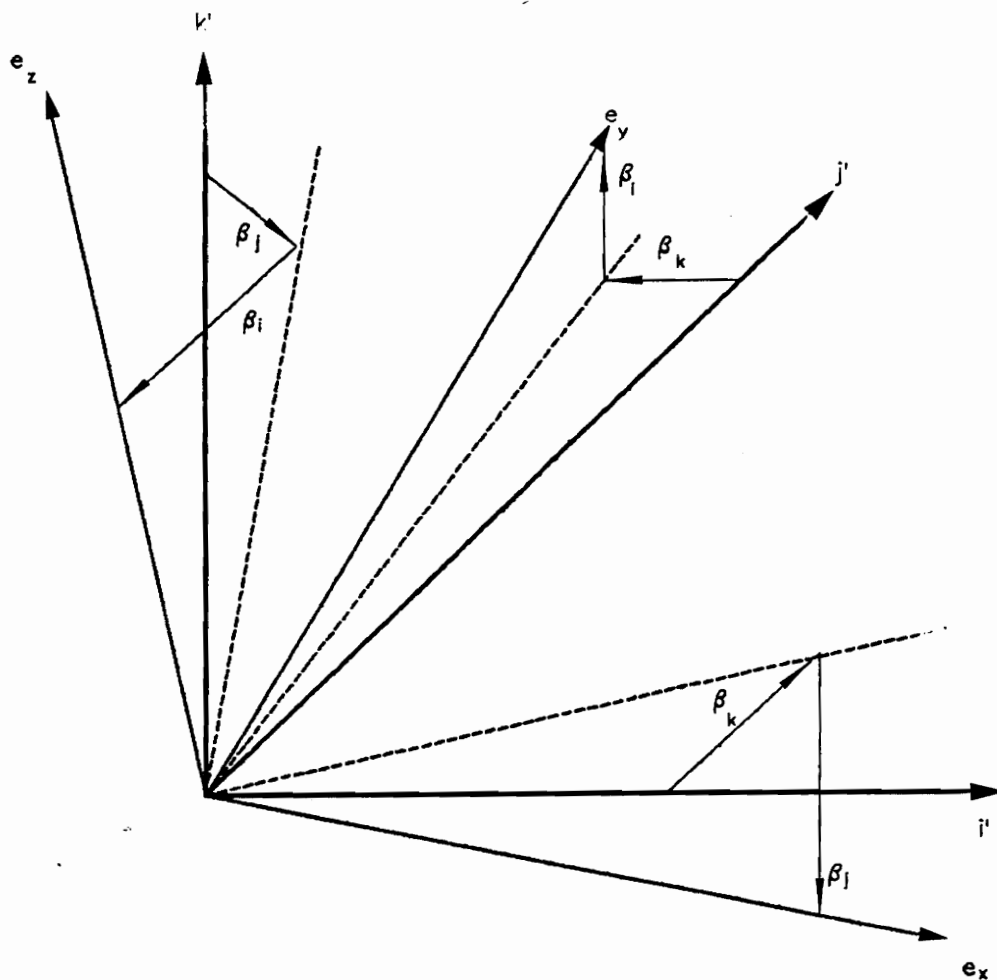


Figure 4. Rotational offsets of the orthogonal axes $(\hat{e}_x, \hat{e}_y, \hat{e}_z)$ from the inertial axes $(\hat{i}, \hat{j}, \hat{k})$. The order of the Euler angles is $\beta_k, \beta_j, \beta_i$

$$u = u_0 + z\psi_x$$

$$v = v_0 + z\psi_y$$

$$w = w_0$$

Substituting the displacement definitions from [2.1.1] into position vector [2.3.1] and transforming to the local inertial frame $(\hat{e}_x, \hat{e}_y, \hat{e}_z)$,

$$\therefore \hat{r} = (h_x + x + u_0 + z\psi_x, \quad h_y + y + v_0 + z\psi_y, \quad h_z + w_0) \begin{bmatrix} \hat{e}_x \\ \hat{e}_y \\ \hat{e}_z \end{bmatrix} \quad [2.3.11]$$

where,

$$(h_x, h_y, h_z) = (h_i, h_j, h_k) [T_{LG}]^T \quad [2.3.12]$$

$$[T_{LG}] = \begin{bmatrix} 1 & 0 & 0 \\ 0 & \cos \beta_i & \sin \beta_i \\ 0 & -\sin \beta_i & \cos \beta_i \end{bmatrix} \begin{bmatrix} \cos \beta_j & 0 & -\sin \beta_j \\ 0 & 1 & 0 \\ \sin \beta_j & 0 & \cos \beta_j \end{bmatrix} \begin{bmatrix} \cos \beta_k & \sin \beta_k & 0 \\ -\sin \beta_k & \cos \beta_k & 0 \\ 0 & 0 & 1 \end{bmatrix} \quad [2.3.13]$$

and, the Euler angles, β_i , β_j , and β_k are defined in figure, and the order of rotations is β_k β_j , and β_i , as shown in figure 4. The above transformation is orthogonal such that :

$$\begin{bmatrix} \hat{e}_x \\ \hat{e}_y \\ \hat{e}_z \end{bmatrix} = [T_{LG}] \begin{bmatrix} \hat{i} \\ \hat{j} \\ \hat{k} \end{bmatrix} \Rightarrow \begin{bmatrix} \hat{i} \\ \hat{j} \\ \hat{k} \end{bmatrix} = [T_{LG}]^T \begin{bmatrix} \hat{e}_x \\ \hat{e}_y \\ \hat{e}_z \end{bmatrix}$$

Also, $\Omega \hat{k}$ can be written in the plate coordinate system as :

$$\Omega \hat{k} = \Omega_x \hat{e}_x + \Omega_y \hat{e}_y + \Omega_z \hat{e}_z \quad [2.3.14]$$

where,

$$(\Omega_x, \Omega_y, \Omega_z) = (0, 0, \Omega) [T_{LG}]^T$$

$$\therefore \dot{\hat{r}} = (\dot{u}_0 + z \dot{\psi}_x, \dot{v}_0 + z \dot{\psi}_y, \dot{w}_0) \begin{bmatrix} \hat{e}_x \\ \hat{e}_y \\ \hat{e}_z \end{bmatrix} \quad [2.3.15]$$

Similarly,

$$\begin{aligned} \Omega \hat{k} \times \hat{r} &= (\Omega_x, \Omega_y, \Omega_z) \begin{bmatrix} \hat{e}_x \\ \hat{e}_y \\ \hat{e}_z \end{bmatrix} \times \hat{r} \\ &= \begin{vmatrix} \hat{e}_x & \hat{e}_y & \hat{e}_z \\ \Omega_x & \Omega_y & \Omega_z \\ h_x + x + u_0 + z \psi_x & h_y + y + v_0 + z \psi_y & h_z + w_0 \end{vmatrix} \\ &= \hat{e}_x \{ \Omega_y (h_z + w_0) - \Omega_z (h_y + y + v_0 + z \psi_y) \} \\ &+ \hat{e}_y \{ \Omega_z (h_x + x + u_0 + z \psi_x) - \Omega_x (h_z + w_0) \} \\ &+ \hat{e}_z \{ \Omega_x (h_y + y + v_0 + z \psi_y) - \Omega_y (h_x + x + u_0 + z \psi_x) \} \end{aligned} \quad [2.3.16]$$

$$\begin{aligned} \therefore \hat{V} &= \dot{\hat{r}} + \Omega \hat{k} \times \hat{r} \\ &= \hat{e}_x \{ (\dot{u}_0 + z \dot{\psi}_x) + \Omega_y (h_z + w_0) - \Omega_z (h_y + y + v_0 + z \psi_y) \} \end{aligned}$$

$$\begin{aligned}
& + \hat{e}_y \{ (\dot{v}_0 + z \dot{\psi}_y) + \Omega_z (h_x + x + u_0 + z \psi_x) - \Omega_x (h_z + w_0) \} \\
& + \hat{e}_z \{ \dot{w}_0 + \Omega_x (h_y + y + v_0 + z \psi_y) - \Omega_y (h_x + x + u_0 + z \psi_x) \} \quad [2.3.17]
\end{aligned}$$

Writing the variation of the total Kinetic Energy :

$$\delta T = \int_V \rho \hat{V} \cdot \delta \hat{V} dV \quad [2.3.18]$$

From equation [2.3.17],

$$\begin{aligned}
\delta \hat{V} &= \hat{e}_x \{ (\delta \dot{u}_0 + z \delta \dot{\psi}_x) + \Omega_y \delta w_0 - \Omega_z (\delta v_0 + z \delta \psi_y) \} \\
&+ \hat{e}_y \{ (\delta \dot{v}_0 + z \delta \dot{\psi}_y) + \Omega_z (\delta u_0 + z \delta \psi_x) - \Omega_x \delta w_0 \} \\
&+ \hat{e}_z \{ \delta \dot{w}_0 + \Omega_x (\delta v_0 + z \delta \psi_y) - \Omega_y (\delta u_0 + z \delta \psi_x) \} \quad [2.3.19]
\end{aligned}$$

Thus,

$$\begin{aligned}
\delta T &= \int_V \rho \hat{V} \cdot \delta \hat{V} dV = \int_A \int_{-h/2}^{h/2} \rho \hat{V} \cdot \delta \hat{V} dz dA \\
&= \sum_{m=1}^n \int_A \int_{z_m}^{z_{m+1}} \rho_m \hat{V} \cdot \delta \hat{V} dz dA
\end{aligned}$$

$$\begin{aligned}
\delta T = & \sum_{m=1}^n \int_A \int_{z_m}^{z_{m+1}} \rho_m \\
& \left\{ (\delta \dot{u}_0 + z \delta \dot{\psi}_x) \left[(\dot{u}_0 + z \dot{\psi}_x) + \Omega_y (h_z + w_0) - \Omega_z (h_y + y + v_0 + z \psi_y) \right] \right. \\
& + \Omega_z (\delta u_0 + z \delta \psi_x) \left[(\dot{v}_0 + z \dot{\psi}_y) + \Omega_z (h_x + x + u_0 + z \psi_x) - \Omega_x (h_z + w_0) \right] \\
& - \Omega_y (\delta u_0 + z \delta \psi_x) \left[\dot{w}_0 + \Omega_x (h_y + y + v_0 + z \psi_y) - \Omega_y (h_x + x + u_0 + z \psi_x) \right] \\
& + (\delta \dot{v}_0 + z \delta \dot{\psi}_y) \left[(\dot{v}_0 + z \dot{\psi}_y) + \Omega_z (h_x + x + u_0 + z \psi_x) - \Omega_x (h_z + w_0) \right] \\
& - \Omega_z (\delta v_0 + z \delta \psi_y) \left[(\dot{u}_0 + z \dot{\psi}_x) + \Omega_y (h_z + w_0) - \Omega_z (h_y + y + v_0 + z \psi_y) \right] \\
& + \Omega_x (\delta v_0 + z \delta \psi_y) \left[\dot{w}_0 + \Omega_x (h_y + y + v_0 + z \psi_y) - \Omega_y (h_x + x + u_0 + z \psi_x) \right] \\
& + \delta \dot{w}_0 \left[\dot{w}_0 + \Omega_x (h_y + y + v_0 + z \psi_y) - \Omega_y (h_x + x + u_0 + z \psi_x) \right] \\
& + \Omega_y \delta w_0 \left[(\dot{u}_0 + z \dot{\psi}_x) + \Omega_y (h_z + w_0) - \Omega_z (h_y + y + v_0 + z \psi_y) \right] \\
& \left. - \Omega_x \delta w_0 \left[(\dot{v}_0 + z \dot{\psi}_y) + \Omega_z (h_x + x + u_0 + z \psi_x) - \Omega_x (h_z + w_0) \right] \right\} dV
\end{aligned}
\tag{2.3.20}$$

Integrating by parts with respect to time for time dependent variations, and using the Hamilton's principle such that,

$$\delta ()_{t_1} = \delta ()_{t_2} = 0 ,$$

$$\int_{t_1}^{t_2} \delta T = \int_{t_1}^{t_2} \sum_{m=1}^n \int_A \int_{z_m}^{z_{m+1}} \rho_m$$

$$\left\{ \begin{aligned} & - (\ddot{u}_0 + z \ddot{\psi}_x) - \Omega_y \dot{w}_0 + \Omega_z (\dot{v}_0 + z \dot{\psi}_y) \\ & + \Omega_z (\dot{v}_0 + z \dot{\psi}_y) + \Omega_z (h_x + x + u_0 + z \psi_x) - \Omega_x (h_z + w_0) \\ & - \Omega_y (\dot{w}_0 + \Omega_x (h_y + y + v_0 + z \psi_y) - \Omega_y (h_x + x + u_0 + z \psi_x)) \end{aligned} \right] (\delta u_0 + z \delta \psi_x) \\ + \left[\begin{aligned} & - (\ddot{v}_0 + z \ddot{\psi}_y) - \Omega_z (\dot{u}_0 + z \psi_x) + \Omega_x \dot{w}_0 \\ & + \Omega_z (\dot{u}_0 + z \dot{\psi}_x) + \Omega_y (h_z + w_0) - \Omega_z (h_y + y + v_0 + z \psi_y) \\ & - \Omega_x (\dot{w}_0 + \Omega_x (h_y + y + v_0 + z \psi_y) - \Omega_y (h_x + x + u_0 + z \psi_x)) \end{aligned} \right] (\delta v_0 + z \delta \psi_y) \\ + \left[\begin{aligned} & - \ddot{w}_0 - \Omega_x (\dot{v}_0 + z \psi_y) + \Omega_y (\dot{u}_0 + z \psi_x) \\ & + \Omega_y (\dot{u}_0 + z \dot{\psi}_x) + \Omega_y (h_z + w_0) - \Omega_z (h_y + y + v_0 + z \psi_y) \\ & + \Omega_x (\dot{v}_0 + z \dot{\psi}_y) + \Omega_z (h_x + x + u_0 + z \psi_x) - \Omega_x (h_z + w_0) \end{aligned} \right] \delta w_0 \end{aligned} \right\} dz dA \quad [2.3.21]$$

Substituting for the position vector r_x , r_y , r_z , integrating over the plate thickness and rearranging,

$$\delta T =$$

$$\begin{aligned}
& \int_A \left\{ \left[I_1 \left(-\ddot{u}_0 - 2\Omega_y \dot{w}_0 + 2\Omega_z \dot{v}_0 + (\Omega_y^2 + \Omega_z^2)(h_x + x + u_0) \right. \right. \right. \\
& \quad \left. \left. - \Omega_z \Omega_x (h_z + w_0) - \Omega_y \Omega_x (h_y + y + v_0) \right) \right. \\
& \quad \left. + I_2 \left(-\ddot{\psi}_x + 2\Omega_z \dot{\psi}_y + (\Omega_y^2 + \Omega_z^2)\psi_x - \Omega_y \Omega_x \psi_y \right) \right] \delta u_0 \\
& + \left[I_1 \left(-\ddot{v}_0 - 2\Omega_z \dot{u}_0 + 2\Omega_x \dot{w}_0 + (\Omega_z^2 + \Omega_x^2)(h_y + y + v_0) \right. \right. \\
& \quad \left. \left. - \Omega_z \Omega_y (h_z + w_0) - \Omega_x \Omega_y (h_x + x + u_0) \right) \right. \\
& \quad \left. + I_2 \left(-\ddot{\psi}_y - 2\Omega_z \dot{\psi}_x + (\Omega_z^2 + \Omega_x^2)\psi_x - \Omega_x \Omega_y \psi_x \right) \right] \delta v_0 \\
& + \left[I_1 \left(-\ddot{w}_0 - 2\Omega_x \dot{v}_0 + 2\Omega_y \dot{u}_0 + (\Omega_x^2 + \Omega_y^2)(h_z + w_0) \right. \right. \\
& \quad \left. \left. - \Omega_y \Omega_z (h_y + y + v_0) - \Omega_x \Omega_z (h_x + x + u_0) \right) \right. \\
& \quad \left. + I_2 \left(-2\Omega_x \dot{\psi}_y + 2\Omega_y \dot{\psi}_x - \Omega_y \Omega_z \psi_y - \Omega_x \Omega_z \psi_x \right) \right] \delta w_0 \\
& + \left[I_2 \left(-\ddot{u}_0 - 2\Omega_y \dot{w}_0 + 2\Omega_z \dot{v}_0 + (\Omega_y^2 + \Omega_z^2)(h_x + x + u_0) \right. \right. \\
& \quad \left. \left. - \Omega_z \Omega_x (h_z + w_0) - \Omega_y \Omega_x (h_y + y + v_0) \right) \right. \\
& \quad \left. + I_3 \left(-\ddot{\psi}_x + 2\Omega_z \dot{\psi}_y + (\Omega_y^2 + \Omega_z^2)\psi_x - \Omega_y \Omega_x \psi_y \right) \right] \delta \psi_x \\
& + \left[I_2 \left(-\ddot{v}_0 - 2\Omega_z \dot{u}_0 + 2\Omega_x \dot{w}_0 + (\Omega_z^2 + \Omega_x^2)(h_y + y + v_0) \right. \right. \\
& \quad \left. \left. - \Omega_z \Omega_y (h_z + w_0) - \Omega_x \Omega_y (h_x + x + u_0) \right) \right. \\
& \quad \left. + I_3 \left(-\ddot{\psi}_y - 2\Omega_z \dot{\psi}_x + (\Omega_z^2 + \Omega_x^2)\psi_x - \Omega_x \Omega_y \psi_x \right) \right] \delta \psi_y \} dA \quad [2.3.22]
\end{aligned}$$

where

$$(I_1, I_2, I_3) = \sum_{m=1}^n \int_{z_m}^{z_{m+1}} \rho_m(1, z, z^2) dz \quad [2.3.23]$$

Defining $\bar{Z}_{u_0}, \bar{Z}_{v_0}, \bar{Z}_{w_0}, \bar{Z}_{\psi_x}, \bar{Z}_{\psi_y}$ to be the coefficients of $u_0, v_0, w_0, \psi_x, \psi_y$ in the above expression, the variation in Kinetic Energy can be rewritten as :

$$\delta T = \int_A \{ \bar{Z}_{u_0} \delta u_0 + \bar{Z}_{v_0} \delta v_0 + \bar{Z}_{w_0} \delta w_0 + \bar{Z}_{\psi_x} \delta \psi_x + \bar{Z}_{\psi_y} \delta \psi_y \} dA \quad [2.3.24]$$

2.3.3 External Work (W_e)

The external work contribution is given by

$$W_e = \int_A \begin{bmatrix} p_x \\ p_y \\ p_z \end{bmatrix}^T \begin{bmatrix} u_0 \\ v_0 \\ w_0 \end{bmatrix} dA$$

where, p_x , p_y , p_z are the distributed loads (pressures) acting on the plate in the x, y, and z directions respectively.

Thus, the variation in the external work can be written as:

$$\delta W_e = \int_A \begin{bmatrix} p_x \\ p_y \\ p_z \end{bmatrix}^T \begin{bmatrix} \delta u_0 \\ \delta v_0 \\ \delta w_0 \end{bmatrix} dA \quad [2.3.25]$$

2.4 Governing Equations

From Hamilton's Principle,

$$0 = \delta \int_{t_1}^{t_2} (U - T - W_e) dt \quad [2.4.1]$$

Thus, using equations [2.3.7], [2.3.24], [2.3.25], assuming no external forces, and using the fact that the variations $\delta u_0, \delta v_0, \delta w_0, \delta \psi_x, \delta \psi_y$ vary independently, the following governing equations are obtained:

$$\delta u_0: \frac{\partial N_x}{\partial x} + \frac{\partial N_{xy}}{\partial y} + \bar{Z}_{u_0} = 0$$

$$\delta v_0: \frac{\partial N_y}{\partial y} + \frac{\partial N_{xy}}{\partial x} + \bar{Z}_{v_0} = 0$$

$$\begin{aligned} \delta w_0: \frac{\partial}{\partial x} \left(N_x \frac{\partial w_0}{\partial x} + N_{xy} \frac{\partial w_0}{\partial y} \right) + \frac{\partial}{\partial y} \left(N_y \frac{\partial w_0}{\partial y} + N_{xy} \frac{\partial w_0}{\partial x} \right) \\ + \frac{\partial Q_y}{\partial y} + \frac{\partial Q_x}{\partial x} + Z_{w_0} = 0 \end{aligned}$$

$$\delta \psi_x: \frac{\partial M_x}{\partial x} + \frac{\partial M_{xy}}{\partial y} - Q_x - \bar{Z}_{\psi_x} = 0$$

$$\delta \psi_y: \frac{\partial M_y}{\partial y} + \frac{\partial M_{xy}}{\partial x} - Q_y - \bar{Z}_{\psi_y} = 0 \quad [2.4.2]$$

where,

$$\begin{aligned}
N_x = & A_{11} \left(\frac{\partial u_0}{\partial x} + \frac{1}{2} \frac{\partial w_0^2}{\partial x} \right) + A_{12} \left(\frac{\partial v_0}{\partial y} + \frac{1}{2} \frac{\partial w_0^2}{\partial y} \right) \\
& + A_{16} \left(\frac{\partial u_0}{\partial y} + \frac{\partial v_0}{\partial x} + \frac{\partial w_0}{\partial x} \frac{\partial w_0}{\partial y} \right) \\
& + B_{11} \frac{\partial \psi_x}{\partial x} + B_{12} \frac{\partial \psi_y}{\partial y} + B_{16} \left(\frac{\partial \psi_x}{\partial y} + \frac{\partial \psi_y}{\partial x} \right)
\end{aligned}$$

$$\begin{aligned}
N_y = & A_{12} \left(\frac{\partial u_0}{\partial x} + \frac{1}{2} \frac{\partial w_0^2}{\partial x} \right) + A_{22} \left(\frac{\partial v_0}{\partial y} + \frac{1}{2} \frac{\partial w_0^2}{\partial y} \right) \\
& + A_{26} \left(\frac{\partial u_0}{\partial y} + \frac{\partial v_0}{\partial x} + \frac{\partial w_0}{\partial x} \frac{\partial w_0}{\partial y} \right) \\
& + B_{12} \frac{\partial \psi_x}{\partial x} + B_{22} \frac{\partial \psi_y}{\partial y} + B_{26} \left(\frac{\partial \psi_x}{\partial y} + \frac{\partial \psi_y}{\partial x} \right)
\end{aligned}$$

$$\begin{aligned}
N_{xy} = & A_{16} \left(\frac{\partial u_0}{\partial x} + \frac{1}{2} \frac{\partial w_0^2}{\partial x} \right) + A_{26} \left(\frac{\partial v_0}{\partial y} + \frac{1}{2} \frac{\partial w_0^2}{\partial y} \right) \\
& + A_{66} \left(\frac{\partial u_0}{\partial y} + \frac{\partial v_0}{\partial x} + \frac{\partial w_0}{\partial x} \frac{\partial w_0}{\partial y} \right) \\
& + B_{16} \frac{\partial \psi_x}{\partial x} + B_{26} \frac{\partial \psi_y}{\partial y} + B_{66} \left(\frac{\partial \psi_x}{\partial y} + \frac{\partial \psi_y}{\partial x} \right)
\end{aligned}$$

$$Q_x = \bar{A}_{45} \left(\psi_y + \frac{\partial w_0}{\partial y} \right) + \bar{A}_{55} \left(\psi_x + \frac{\partial w_0}{\partial x} \right)$$

$$Q_y = \bar{A}_{44} \left(\psi_y + \frac{\partial w_0}{\partial y} \right) + \bar{A}_{45} \left(\psi_x + \frac{\partial w_0}{\partial x} \right)$$

$$\begin{aligned}
M_x &= B_{11} \left(\frac{\partial u_0}{\partial x} + \frac{1}{2} \frac{\partial w_0^2}{\partial x} \right) + B_{12} \left(\frac{\partial v_0}{\partial y} + \frac{1}{2} \frac{\partial w_0^2}{\partial y} \right) \\
&+ B_{16} \left(\frac{\partial u_0}{\partial y} + \frac{\partial v_0}{\partial x} + \frac{\partial w_0}{\partial x} \frac{\partial w_0}{\partial y} \right) \\
&+ D_{11} \frac{\partial \psi_x}{\partial x} + D_{12} \frac{\partial \psi_y}{\partial y} + D_{16} \left(\frac{\partial \psi_x}{\partial y} + \frac{\partial \psi_y}{\partial x} \right) \\
M_y &= B_{12} \left(\frac{\partial u_0}{\partial x} + \frac{1}{2} \frac{\partial w_0^2}{\partial x} \right) + B_{22} \left(\frac{\partial v_0}{\partial y} + \frac{1}{2} \frac{\partial w_0^2}{\partial y} \right) \\
&+ B_{26} \left(\frac{\partial u_0}{\partial y} + \frac{\partial v_0}{\partial x} + \frac{\partial w_0}{\partial x} \frac{\partial w_0}{\partial y} \right) \\
&+ D_{12} \frac{\partial \psi_x}{\partial x} + D_{22} \frac{\partial \psi_y}{\partial y} + D_{26} \left(\frac{\partial \psi_x}{\partial y} + \frac{\partial \psi_y}{\partial x} \right) \\
M_{xy} &= B_{16} \left(\frac{\partial u_0}{\partial x} + \frac{1}{2} \frac{\partial w_0^2}{\partial x} \right) + B_{26} \left(\frac{\partial v_0}{\partial y} + \frac{1}{2} \frac{\partial w_0^2}{\partial y} \right) \\
&+ B_{66} \left(\frac{\partial u_0}{\partial y} + \frac{\partial v_0}{\partial x} + \frac{\partial w_0}{\partial x} \frac{\partial w_0}{\partial y} \right) \\
&+ D_{16} \frac{\partial \psi_x}{\partial x} + D_{26} \frac{\partial \psi_y}{\partial y} + D_{66} \left(\frac{\partial \psi_x}{\partial y} + \frac{\partial \psi_y}{\partial x} \right)
\end{aligned}$$

3.0 FINITE ELEMENT MODELLING

In the present analyses, a Ritz-Galerkin formulation has been used. The Ritz approximation assumes displacements at any point in an element to be a linear combination of the corresponding displacements at the nodes of the element. Thus the displacements u_0 , v_0 , w_0 , ψ_x , and ψ_y can be written in the form:

$$u_0 = \sum_j \Delta_j^1 \phi_j$$

$$v_0 = \sum_j \Delta_j^2 \phi_j$$

$$w_0 = \sum_j \Delta_j^3 \phi_j$$

$$\psi_x = \sum_j \Delta_j^4 \phi_j$$

$$\psi_y = \sum_j \Delta_j^5 \phi_j \quad [3.1.1]$$

where, ϕ_j are shape functions discussed later, and, Δ_j^i are respectively u_0 , v_0 , w_0 , ψ_x , and ψ_y on the j^{th} node of the element.

Substituting the above displacement relations into the previously defined energy variations, the following non-linear expression of motion is obtained.

$$[M] \{\ddot{\Delta}\} + [C] \{\dot{\Delta}\} + [K^{CF} + K^L + K^{NL}(\Delta)] \{\Delta\} = \{F^{CF}\}$$

where the submatrices associated with each matrix is given in Appendix A. In order to solve this equation, one must divide the solution into two parts, the determination of the static shape and the vibrations about this non-linear static position.

3.1 Static Analysis

For the static analysis of the problem, the time-dependent terms are neglected. Then, the governing equations for static analysis are obtained from equation [2.4.2] as follows

$$\delta u_0: \frac{\partial N_x}{\partial x} + \frac{\partial N_{xy}}{\partial y} = 0$$

$$\delta v_0: \frac{\partial N_y}{\partial y} + \frac{\partial N_{xy}}{\partial x} = 0$$

$$\delta w_0: \frac{\partial}{\partial x} \left(N_x \frac{\partial w_0}{\partial x} + N_{xy} \frac{\partial w_0}{\partial y} \right) + \frac{\partial}{\partial y} \left(N_y \frac{\partial w_0}{\partial y} + N_{xy} \frac{\partial w_0}{\partial x} \right)$$

$$+ \frac{\partial Q_y}{\partial y} + \frac{\partial Q_x}{\partial x} = 0$$

$$\delta\psi_x: \frac{\partial M_x}{\partial x} + \frac{\partial M_{xy}}{\partial y} - Q_x = 0$$

$$\delta\psi_y: \frac{\partial M_y}{\partial y} + \frac{\partial M_{xy}}{\partial x} - Q_y = 0 \quad [3.1.2]$$

Then, following the Galerkin variational formulation, the governing equations yield :

$$\int_{\Omega} \phi_i \left(\frac{\partial N_x}{\partial x} + \frac{\partial N_{xy}}{\partial y} \right) d\Omega = 0$$

$$\int_{\Omega} \phi_i \left(\frac{\partial N_y}{\partial y} + \frac{\partial N_{xy}}{\partial x} \right) d\Omega = 0$$

$$\begin{aligned} \int_{\Omega} \phi_i \left(\frac{\partial}{\partial x} \left(N_x \frac{\partial w_0}{\partial x} + N_{xy} \frac{\partial w_0}{\partial y} \right) + \frac{\partial}{\partial y} \left(N_y \frac{\partial w_0}{\partial y} + N_{xy} \frac{\partial w_0}{\partial x} \right) \right. \\ \left. + \frac{\partial Q_y}{\partial y} + \frac{\partial Q_x}{\partial x} \right) d\Omega = 0 \end{aligned}$$

$$\int_{\Omega} \phi_i \left(\frac{\partial M_x}{\partial x} + \frac{\partial M_{xy}}{\partial y} - Q_x \right) d\Omega = 0$$

$$\int_{\Omega} \phi_i \left(\frac{\partial M_y}{\partial y} + \frac{\partial M_{xy}}{\partial x} - Q_y \right) d\Omega = 0 \quad [3.1.3]$$

Using the Ritz approximation for the displacements, and using the stress-displacement relations, the following final form is obtained for the equations of motion for static analysis:

$$[K^{CF} + K^L + K^{NL}(\Delta_s)] \{\Delta_s\} = \{F^{CF}\}$$

where,

K^L are the geometrically linear stiffness terms obtained from the strain energy expression,

K^{NL} are the geometrically non-linear stiffness terms obtained from the strain energy expression,

K^{CF} and F^{CF} are the stiffness's and forces, respectively, obtained from the kinetic energy expression (centrifugal terms), and,

Δ_s is the static component of the deflections

3.1.1 Newton-Raphson Method

The Newton-Raphson Method is an efficient technique to obtain a converging solution for non-linear differential equations. The above equation of motion for the static problem can be rewritten in the form :

$$[K(u_s)] \{u_s\} = \{F^{CF}\} \quad [3.1.4]$$

where, $[K(u_s)]$ is the non-linear expression for the stiffness matrix for the problem, and,
 $u_s \equiv \Delta_s$ is the static component of the deflection.

Or,

$$[K(u_s)] \{u_s\} - \{F^{CF}\} \equiv \{R\} = \{0\} \quad [3.1.5]$$

Expanding $\{R\}$ in a Taylor series expansion in terms of the displacements Δ_s ,

$$\{0\} = \{R\}^r + \left[\left(\frac{\partial \{R\}}{\partial \{u_s\}} \right)_r \right] \{\Delta u\} + \dots$$

where the superscript r denotes the value of the function evaluated at the solution obtained in the previous iteration.

Considering only the first-order terms,

$$\{0\} = \{R\}^r + \left[\left(\frac{\partial \{R\}}{\partial \{u_s\}} \right)_r \right] \{\Delta u\}$$

where, Δu is the change in the solution from the previous iteration.

Defining,

$$\left[\left(\frac{\partial \{R\}}{\partial \{u_s\}} \right)_r \right] \equiv [K^T],$$

$$[K^T] \{\Delta u\} = -\{R\}^r = -[K(u_s^r)] \{u_s^r\} + \{F^{CF}\} \quad [3.1.6]$$

The above differential equation is solved numerically for the unknowns, Δu , and after each iteration, the solution u_s is updated as:

$$\{u_s\}^{r+1} = \{u_s\}^r + \{\Delta u\}$$

The solution is assumed to have converged when

$$\sqrt{\frac{\sum_j |\Delta u_j|^2}{\sum_j |u_j^r|^2}} < \varepsilon$$

for a sufficiently small $\varepsilon > 0$

$\{R\}$ is called the Residual, and , $\{K^T\}$ is known as the tangent stiffness matrix for the Newton-Raphson method.

3.1.1.1 Tangent Stiffness Matrix

The tangent stiffness matrix is evaluated as follows:

$$[K^T] = (K_{ij}^{\alpha\beta})^{\tan} = \frac{\partial R_i^\alpha}{\partial \Delta_j^\beta} \quad [3.1.7]$$

where,

$$R_i^\alpha = \sum_{k=1}^n \sum_{\gamma=1}^5 K_{ik}^{\alpha\gamma} \Delta_k^\gamma - F_i^\alpha$$

where, $K_{ik}^{\alpha\gamma}$ is the element stiffness sub-matrix, the coefficient of Δ_k^γ in the α^{th} equation of motion , γ is the number of degrees of freedom, and, n is the number of nodes in each element in the finite element mesh. F_i^α is the force on the i^{th} node in the finite element mesh. Therefore, the coefficients of the tangent stiffness matrix, $[K^T]$, are defined by :

$$\left(K_{ij}^{\alpha\beta}\right)^{\text{tan}} = \frac{\partial R_i^\alpha}{\partial \Delta_j^\beta} = K_{ij}^{\alpha\beta} + \sum_{\gamma=1}^5 \sum_{k=1}^n \frac{\partial K_{ik}^{\alpha\gamma}}{\partial \Delta_j^\beta} \Delta_k^\gamma \quad [3.1.8]$$

3.2 Dynamic Analysis

For dynamic analysis, both the static, and the time dependent components of displacement are considered. Following the approach used for static analysis, the following equations of motion are obtained:

$$[M] \{\ddot{\Delta}\} + [C] \{\dot{\Delta}\} + [K^{CF} + K^L + K^{NL}(\Delta)] \{\Delta\} = \{F^{CF}\} \quad [3.1.9]$$

where $[M]$ is the mass, and $[C]$ the coriolis matrix, and

Δ is the deflection, involving both static and time-dependent terms.

Any displacement Δ can be expressed as the sum of a static and a dynamic term. Thus,

$$\Delta = \Delta_s + \delta$$

where, Δ_s is the static deflection as a result of the centrifugal load, and, δ is the dynamic displacement, or the vibration about the static displaced position. For centrifugal loads, the dynamic displacements are much smaller than the corresponding static displacements.

Thus,

$$\Delta = \Delta_s + \delta$$

$$\dot{\Delta} = \dot{\delta}$$

$$\ddot{\Delta} = \ddot{\delta} \quad [3.2.10]$$

where, it is assumed that Δ_s is not a function of time.

Thus, the equations of motion can be written in terms of the static and dynamic terms as:

$$[M] \{\ddot{\delta}\} + [C] \{\dot{\delta}\} + [K^{CF} + K^L + K^{NL}(\Delta_s + \delta)] \{\Delta_s + \delta\} = \{F^{CF}\} \quad [3.2.11]$$

where, K^L are the geometrically linear stiffness terms obtained from the strain energy expression K^{NL} are the geometrically non-linear stiffness terms obtained from the strain energy expression, and, K^{CF} and F^{CF} are the stiffness's and forces, respectively, obtained from the kinetic energy expression (centrifugal terms).

Consider $K^{NL}(\Delta_s + \delta)$:

$$K^{NL}(\Delta_s + \delta) = K^{NL}(\Delta_s) + \delta \frac{\partial}{\partial \Delta_s} K^{NL}(\Delta_s) + \delta^2 \frac{\partial^2}{\partial^2 \Delta_s} K^{NL}(\Delta_s) + \dots$$

Ignoring the δ^2 and higher order terms (as δ , the dynamic deflections, are much smaller than the corresponding static deflections), the following equations are obtained :

$$\begin{aligned} [M] \{\ddot{\delta}\} + [C] \{\dot{\delta}\} + [K^{CF} + K^L + K^{NL}(\Delta_s)] \{\delta\} + \left[\delta \frac{\partial}{\partial \Delta_s} (K^{NL}(\Delta_s)) \right] \{\delta\} \\ + [K^{CF} + K^L + K^{NL}(\Delta_s)] \{\Delta_s\} + \left[\delta \frac{\partial}{\partial \Delta_s} (K^{NL}(\Delta_s)) \right] \{\Delta_s\} = \{F^{CF}\} \end{aligned}$$

Or, simplifying the above expression,

$$\begin{aligned} [M] \{\ddot{\delta}\} + [C] \{\dot{\delta}\} + \left[K^{CF} + K^L + K^{NL}(\Delta_s) + \Delta_s \frac{\partial}{\partial \Delta_s} (K^{NL}(\Delta_s)) \right] \{\delta\} \\ + [K^{CF} + K^L + K^{NL}(\Delta_s)] \{\Delta_s\} = \{F^{CF}\} \end{aligned} \quad [3.2.12]$$

However, from the earlier static analysis,

$$[K^{CF} + K^L + K^{NL}(\Delta_s)] \{\Delta_s\} = \{F^{CF}\}$$

and, $\left[K^{CF} + K^L + K^{NL}(\Delta_s) + \Delta_s \frac{\partial}{\partial \Delta_s} (K^{NL}(\Delta_s)) \right]$ is the tangent stiffness matrix obtained in the Newton-Raphson technique to solve a non-linear equation.

Thus,

$$[M] \{\ddot{\delta}\} + [C] \{\dot{\delta}\} + [K^T] \{\delta\} = 0 \quad [3.2.13]$$

This is the standard form of equations of motion of undamped free vibrations of spinning structures, as the $[C]$ matrix obtained above represents the Coriolis rather than the damping terms. This eigenvalue problem can be solved by a standard procedure. This involves creation of a dummy variable $\{q\}$, the derivative of the displacements $\{\delta\}$

$$\{q\} = \{\dot{\delta}\}$$

$$\{\dot{q}\} = \{\ddot{\delta}\}$$

Then, the above equations of motion can be rewritten in the following form :

$$[M] \{q\} + [0] \{\delta\} + [0] \{\dot{q}\} - [M] \{\dot{\delta}\} = 0$$

$$[0] \{q\} + [K]^T \{\delta\} + [M] \{\dot{q}\} + [C] \{\dot{\delta}\} = 0$$

Or,

$$\begin{bmatrix} [M] & [0] \\ [0] & [K]^T \end{bmatrix} \begin{Bmatrix} \{q\} \\ \{\delta\} \end{Bmatrix} - \begin{bmatrix} [0] & [M] \\ -[M] & -[C] \end{bmatrix} \begin{Bmatrix} \{\dot{q}\} \\ \{\dot{\delta}\} \end{Bmatrix} = 0 \quad [3.2.14]$$

or,

$$[A] \{y\} - [B] \{\dot{y}\} = 0$$

where,

$$[A] = \begin{bmatrix} [M] & [0] \\ [0] & [K] \end{bmatrix}$$

$$[B] = \begin{bmatrix} [0] & [M] \\ -[M] & -[C] \end{bmatrix}$$

$$\{y\} = \begin{Bmatrix} \{q\} \\ \{\delta\} \end{Bmatrix} \quad [3.2.15]$$

Here, $[A]$ is a symmetric, and $[B]$ is an anti-symmetric matrix. Taking the solution to be of the form

$$y = e^{\lambda t},$$

$$[B]^{-1} [A] \{y\} = \lambda [I] \{y\}$$

3.2.1 Numerical Integration

In the present analysis, Gauss-Legendre quadrature has been used for numerical integration. In this, a linear transformation is used to convert from the global to the local co-ordinate system. In this study, the shape functions used are of maximum polynomial degree 2 for the rectangular 4-node linear plate element and of maximum polynomial degree 4 for the rectangular 9-node quadratic plate element. Thus they should be integrated exactly using 2 and 3-point integration, respectively. This integration is referred to as the full integration. It is seen that for thin plates, full integration of the shear deformation terms results in the phenomenon of **shear locking**, in which, the plate appears to become stiffer, resulting in under-prediction of deflections, and over-prediction of frequencies.

This phenomenon is attributed to the difference in the orders of magnitude between the bending and the shear terms. This results in an inaccurate representation of the shear terms. To circumvent this problem, reduced integration using one Gauss point less than the full integration is used on the shear coefficients. This is equivalent to reducing the degree of the interpolating polynomial by one for the shear coefficient terms. This appears to yield much better results in the analysis of thin

plates. However, as noted by Hughes, Taylor, and Konoknukulchai [14], reduced integration has the opposite effect for thick plates. In particular, in case of a body with rigid body modes, some spurious zero-energy modes are obtained as discussed later in Results and Conclusions.

4.0 RESULTS AND DISCUSSION

Here the problem of free vibration of isotropic and cross-ply laminated plates has been considered. The results for **non-rotating** isotropic cross-ply and angle-ply laminated plates are compared with the standard results available for various boundary conditions. Three types of boundary conditions have been considered, namely, Free, Simply Supported and Cantilever. Also a comparison has been made between the results obtained by using the 4-node linear rectangular plate element and the 9-node quadratic rectangular plate element.

For all problems, repeated frequencies have not been tabulated. Also, for symmetric plates, where the in-plane and the transverse deflections are uncoupled, only the frequencies corresponding to flexural modes of vibration have been tabulated. As observed by Leissa [21], repetition of frequencies is a result of using a square plate for which repeated frequencies have been seen to exist simultaneously.

For the **rotating** plate only the cantilever type of boundary conditions are considered as they are the only ones relevant to this study. Here, a study has been made of the relation between the angular velocity of the plate and its frequencies.

For the non-rotating plate the non-linear strains do not have any effect because of the absence of any force acting on the plate. Thus, in this study, the non-linear analysis has not been used for the case of the non-rotating plate. On the other hand, for the rotating plate, because of the presence of centrifugal forces, the non-linearity can have a significant effect on the results obtained, especially for thin plates. So, the non-linear analysis has been performed for the rotating plate.

For the isotropic plate, the material properties used are:

$$E = 10.92 \times 10^6 \text{ psi}$$

$$\nu = 0.3$$

$$\rho = 1.0 \text{ lb/in}^3$$

$$t = \text{thickness} = 1.0 \text{ in}$$

For the laminated composite plate, the material properties used are:

$$E_1 = 40.00 \times 10^6 \text{ psi}$$

$$E_2 = 1.00 \times 10^6 \text{ psi}$$

$$G_{12} = 0.60 \times 10^6 \text{ psi}$$

$$G_{13} = 0.60 \times 10^6 \text{ psi}$$

$$G_{23} = 0.50 \times 10^6 \text{ psi}$$

$$\nu_{12} = 0.25$$

$$\rho = 1.0 \text{ lb/in}^3$$

$$t = \text{thickness} = 1.0 \text{ in.}$$

4.1 *Non-Rotating Plates*

4.1.1 Free Plates

A free plate here has been defined as one without any constraints on it. The results for this plate are computed only for isotropic plates.

For this kind of problem, six rigid body modes would be expected, corresponding to the three translations and three rotations. However, as first observed by Hughes [15], for a first-order shear deformable rectangular plate element, some computational errors associated with reduced integration of shear coefficient terms, creep up resulting in seven zero energy modes. These zero energy modes correspond to five rigid modes and two spurious zero energy modes which do not correspond to rigid body modes. The extra zero energy mode is considered to be due to the use of reduced integration on transverse shear terms in the stiffness matrix.

As explained by Hughes [14], these spurious modes appear because the element is rank deficient, but this problem usually manifests itself only in very thick plates and only in some special cases. In this study it was observed that the spurious modes appeared only for a completely free plate. It has been accepted that one reason for this problem is the reduced integration performed on the transverse shear coefficient terms and this error can be corrected by modifying the reduced integration or by using constraints to prevent rigid body motion, when, it is observed, the problem disappears.

Also, because of the large number of identical zero eigenvalues, the eigenvalues subroutines may yield eigenvectors (mode shapes) which are linear combinations of two or more eigenvectors corresponding to the same eigenvalue. For this particular problem, there are three in-plane rigid body

modes, as is logically expected. But, there are four out-of-plane modes, which are linear combinations of the rigid body modes and the spurious mode shapes predicted by Hughes.

The results are compared with those obtained by Leissa [21]. During the development, the results were also compared with those obtained by Gorman [23], though they have not been tabulated here as the above two sources used different material properties for their analyses and only one is included here.

4.1.2 Simply-Supported Plates

The plate is simply supported on all four edges. For this problem, the tangential rotations and the out-of-plane displacements are constrained on the edges. As there is no in-plane constraint, this results in the expected three zero energy rigid body modes involving the two in-plane displacements and the in-plane rotation.

The first mode for the simply-supported plate is symmetric about lines parallel to the edges and about the diagonals. Similarly, the second and third modes have been obtained for the simply-supported plate.

The problem of an isotropic plate with all sides simply supported is a standard one and is one of the easiest to obtain an exact solution for. The exact solution obtained using the classical plate theory is (see [21,24]) :

$$\omega_{mn} = \left[\left(\frac{m\pi}{a} \right)^2 + \left(\frac{n\pi}{b} \right)^2 \right] \sqrt{\frac{D}{\rho}}$$

The nodal lines for an isotropic rectangular plate are straight lines parallel to the edges. For a square plate, two mode shapes may have the same frequency. The mode shapes for the simply-supported isotropic plate are shown in Figs. 5 - 10

Table 1. Vibration of Free Isotropic Plates

Isotropic Plate					
$\bar{\omega} = (\omega a^2)\sqrt{\rho h/D}$					
Mode	1	2	3	4	5
Exact (CPT)	13.473	19.596	24.270	35.156	35.156
8 x 8 Linear Mesh (FSDPT)	12.792	19.287	23.986	32.521	32.521
4 x 4 Quadratic Mesh (FSDPT)	12.729	18.999	23.429	32.052	32.052

$a = 10 \text{ in.}, b = 10 \text{ in.}, h = 1 \text{ in.}$

The problem of vibration of simply-supported laminated composite plates has been discussed by Reddy and Phan [25]. They have obtained results for this problem based on the first-order and the third-order transverse shear deformable plate theories. In the present study, the results have been obtained using the same material and geometric properties as in the above paper to provide a direct comparison between the two sets of results. As can be seen in Tables 2 and 3, there is an excellent agreement between the two sets of results. On the other hand, it can be seen that there is a great disparity between these results and those obtained from the classical plate theory. This may be explained by the fact that transverse shear effects manifest themselves more in laminated plates. The mode shapes for the $[0/90/90/0]$ laminate and isotropic plate are shown in Figures 11-16. The mode shapes have been plotted only for the $[0/90/90/0]$ laminate as this laminate is symmetric. So, it does not have bending-extension coupling and it is possible to obtain mode shapes and frequencies for the flexural vibration of the plate. Thus, Table 3 contains the flexural vibration frequencies for both the isotropic and the symmetric composite plate, and, only the lowest five frequencies have been tabulated for the anti-symmetric angle-ply laminated composite plate.

Interestingly both the present study and the above paper yield results which underpredict frequencies as compared to the results of 3-D elasticity. This is in contrast to the expectation that most approximate plate theories would overestimate frequencies because of the inadequate representation of the flexibility of the structure. It may be expected that the results obtained by this computation will converge to the expected over-prediction of frequencies and under-prediction of deflections.

4.1.3 Cantilever Plates

A rectangular plate with one edge (perpendicular to the longer side) clamped and the remaining sides free is known as a cantilever plate. For this problem, the transverse displacement, the two inplane displacements and the rotations normal to the edge are constrained. This results in suppression of rigid body modes and thus no zero eigenvalues are obtained for this problem. The first

Table 2. Vibration of Simply Supported Isotropic Plates

Isotropic Plate					
$\bar{\omega} = (\omega a^2)\sqrt{\rho h/D}$					
Mode	1	2	3	4	5
Exact (CPT)	19.739	49.348	78.957	98.696	128.31
Exact (FSDPT)	19.059	45.476	69.802	85.029	106.69
8 x 8 Linear Mesh (FSDPT)	19.375	48.103	73.722	81.751	87.352
4 x 4 Quadratic Mesh (FSDPT)	19.077	45.841	70.355	80.507	85.835

$a = 10, b = 10, h = 1$

Table 3. Vibration of Simply Supported Laminated Composite Plates

[0/90/90/0] Laminated Composite Plate					
$\bar{\omega} = (\omega a^2/h)\sqrt{\rho/E_2}$					
Mode	1	2	3	4	5
Exact (CPT)	18.738	33.148	63.518	67.268	73.196
Exact (FSDPT) (FSDPT)	15.143	27.162	36.848	43.342	46.624
8 x 8 Linear Mesh	15.333	28.398	38.125	44.655	51.606
4 x 4 Quadratic Mesh (FSDPT)	15.149	27.329	37.047	43.592	48.037

[45/-45] Laminated Composite Plate					
$\bar{\omega} = (\omega a^2/h)\sqrt{\rho/E_2}$					
Mode	1	2	3	4	5
Exact (CPT)	14.439	32.702	34.414	55.541	59.004
Exact (FSDPT)	13.044	26.938	34.414	41.341	44.530
8 x 8 Linear Mesh (FSDPT)	13.215	28.023	36.259	42.704	44.390
4 x 4 Quadratic Mesh (FSDPT)	13.047	27.078	34.546	41.146	41.532

$a = 10, b = 10, h = 1$

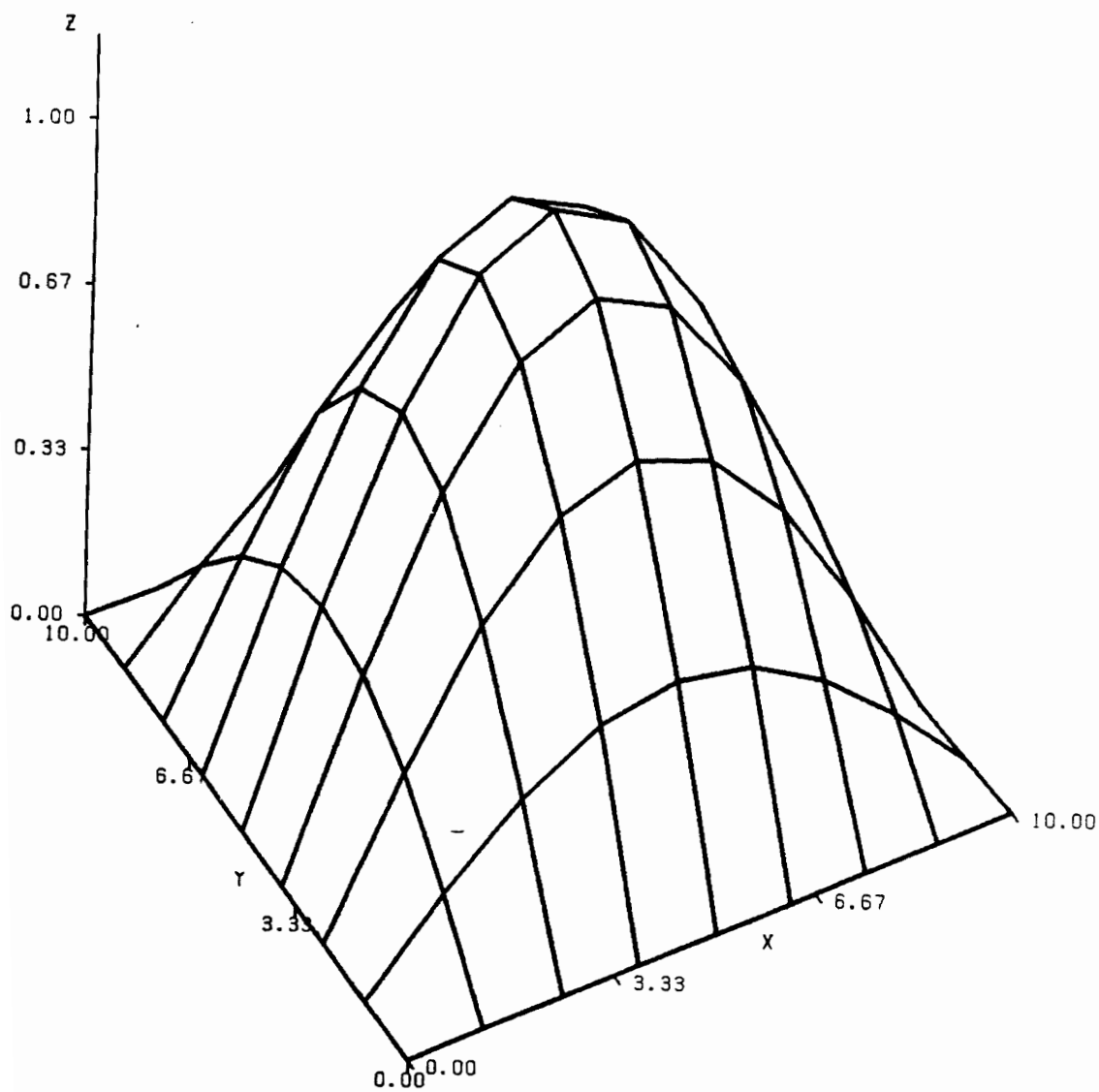


Figure 5. Simply Supported Isotropic Plate. Mode 1

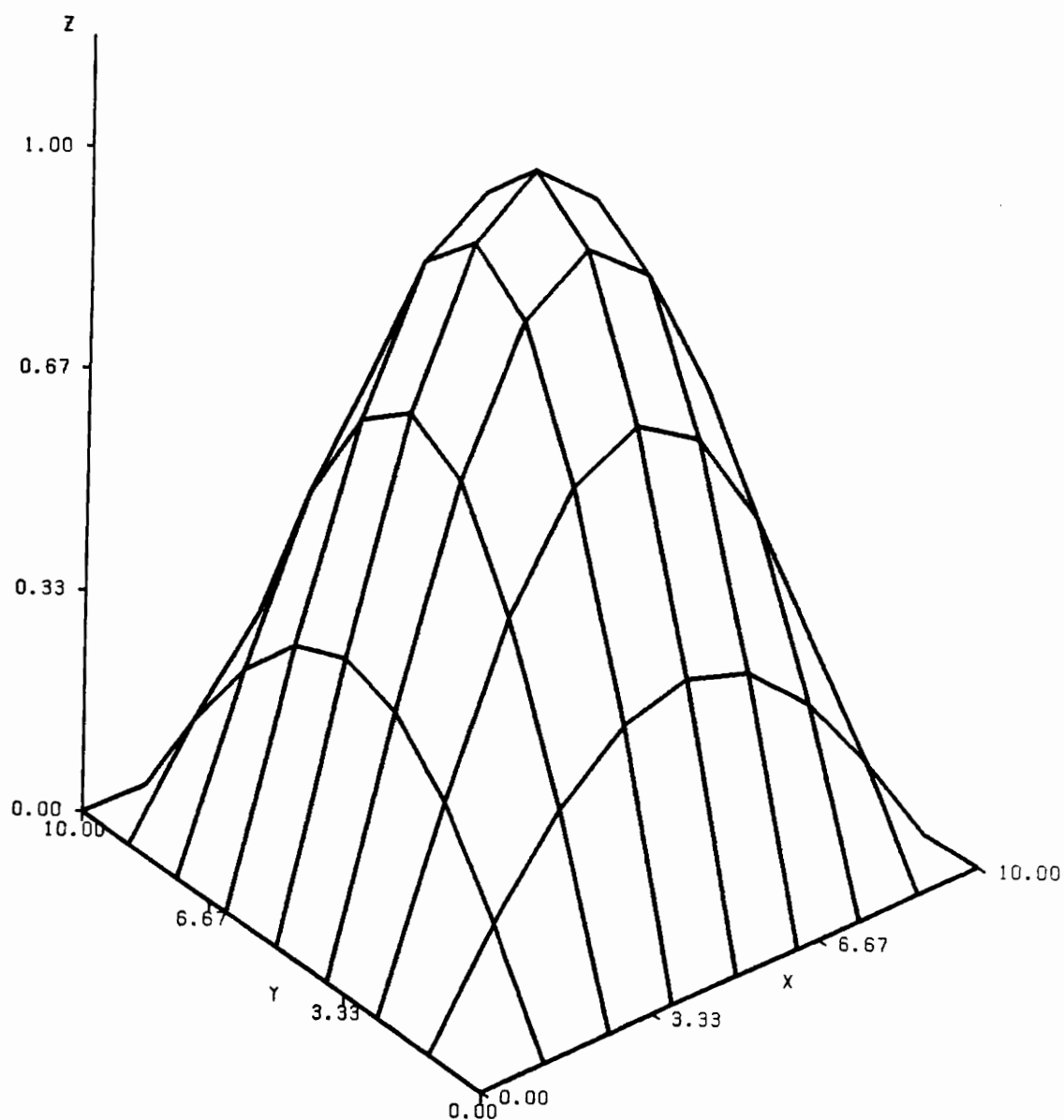


Figure 6. Simply Supported Isotropic Plate. Mode 1

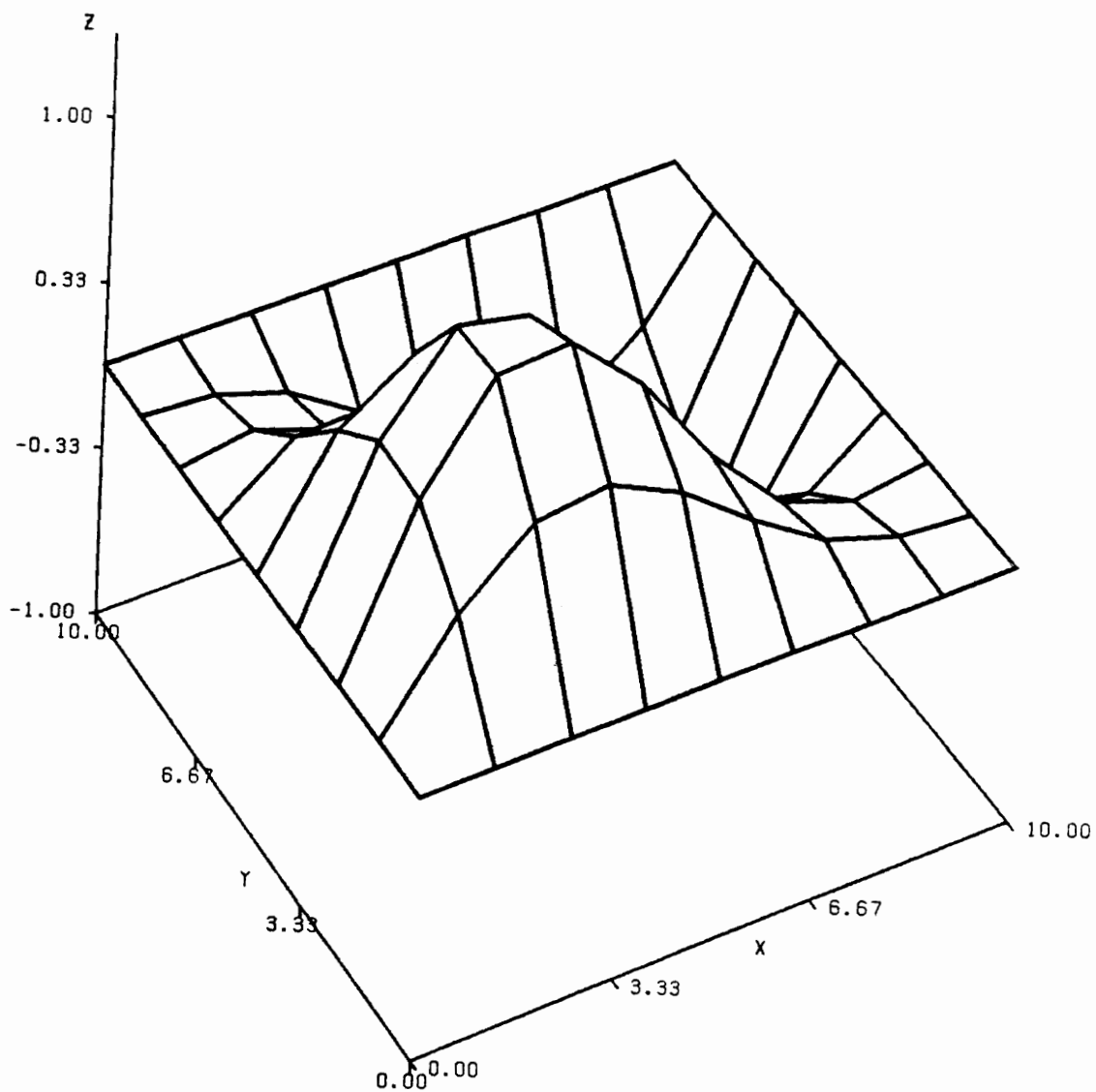


Figure 7. Simply Supported Isotropic Plate. Mode 2

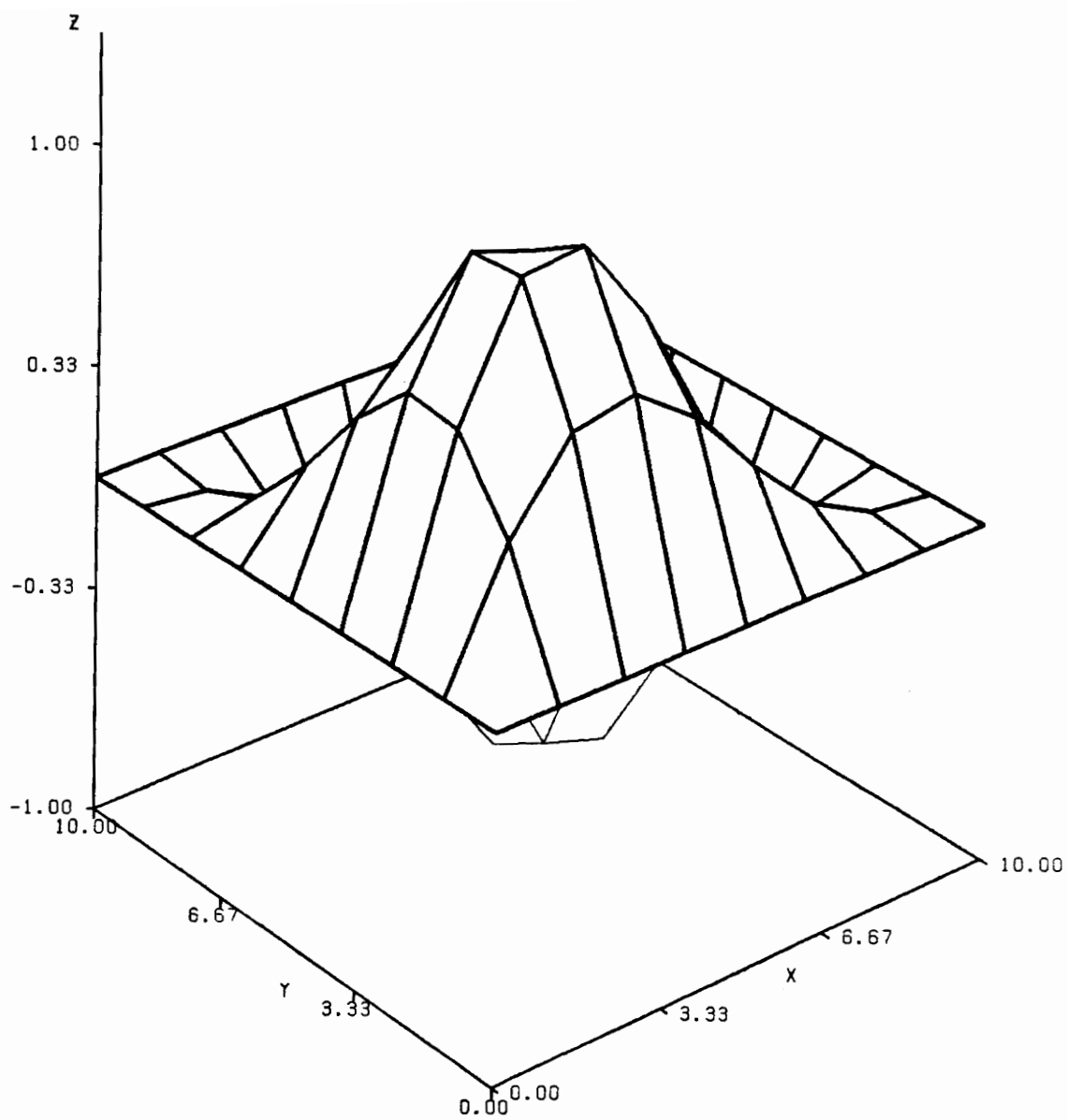


Figure 8. Simply Supported Isotropic Plate. Mode 2

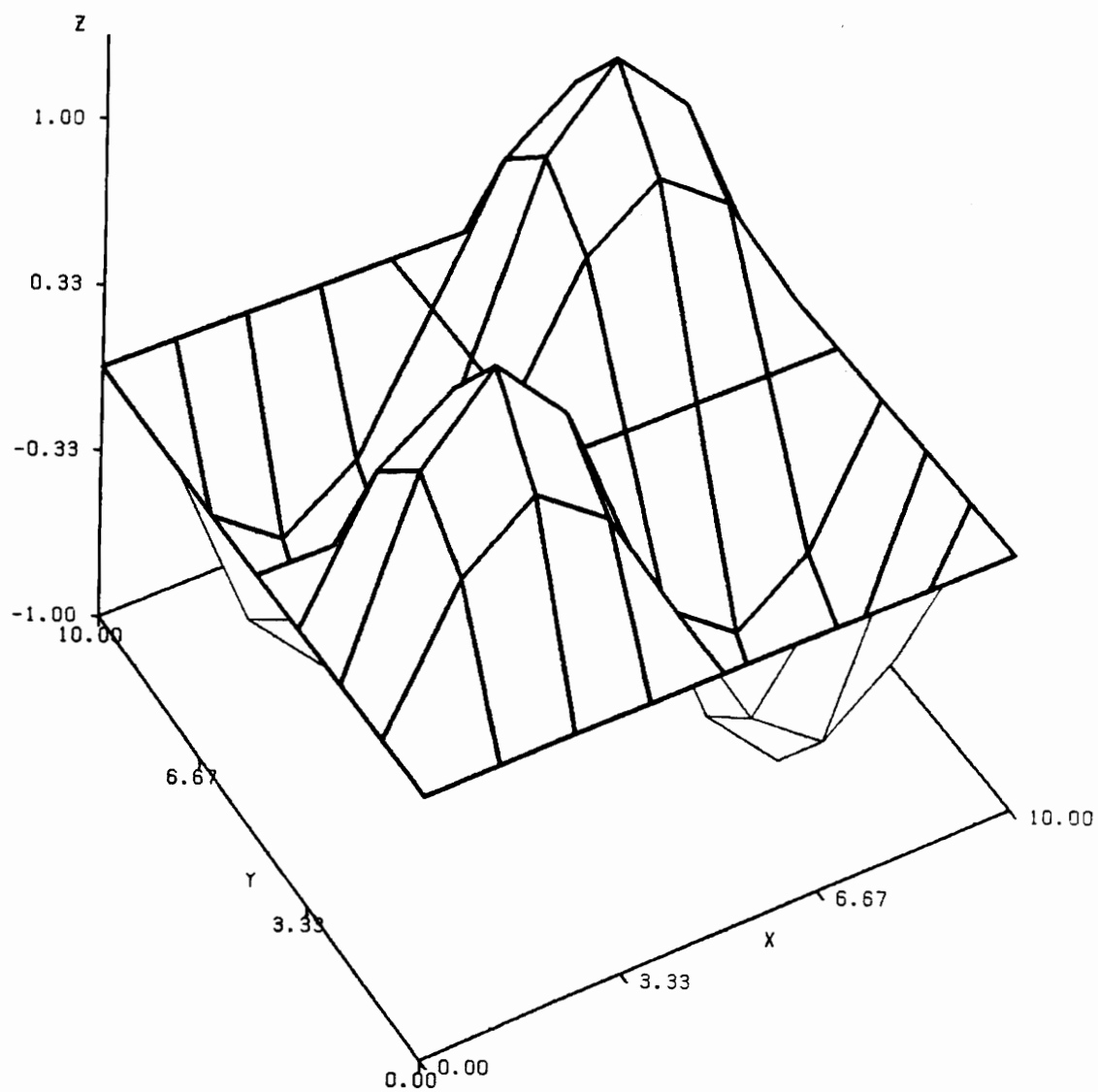


Figure 9. Simply Supported Isotropic Plate. Mode 3

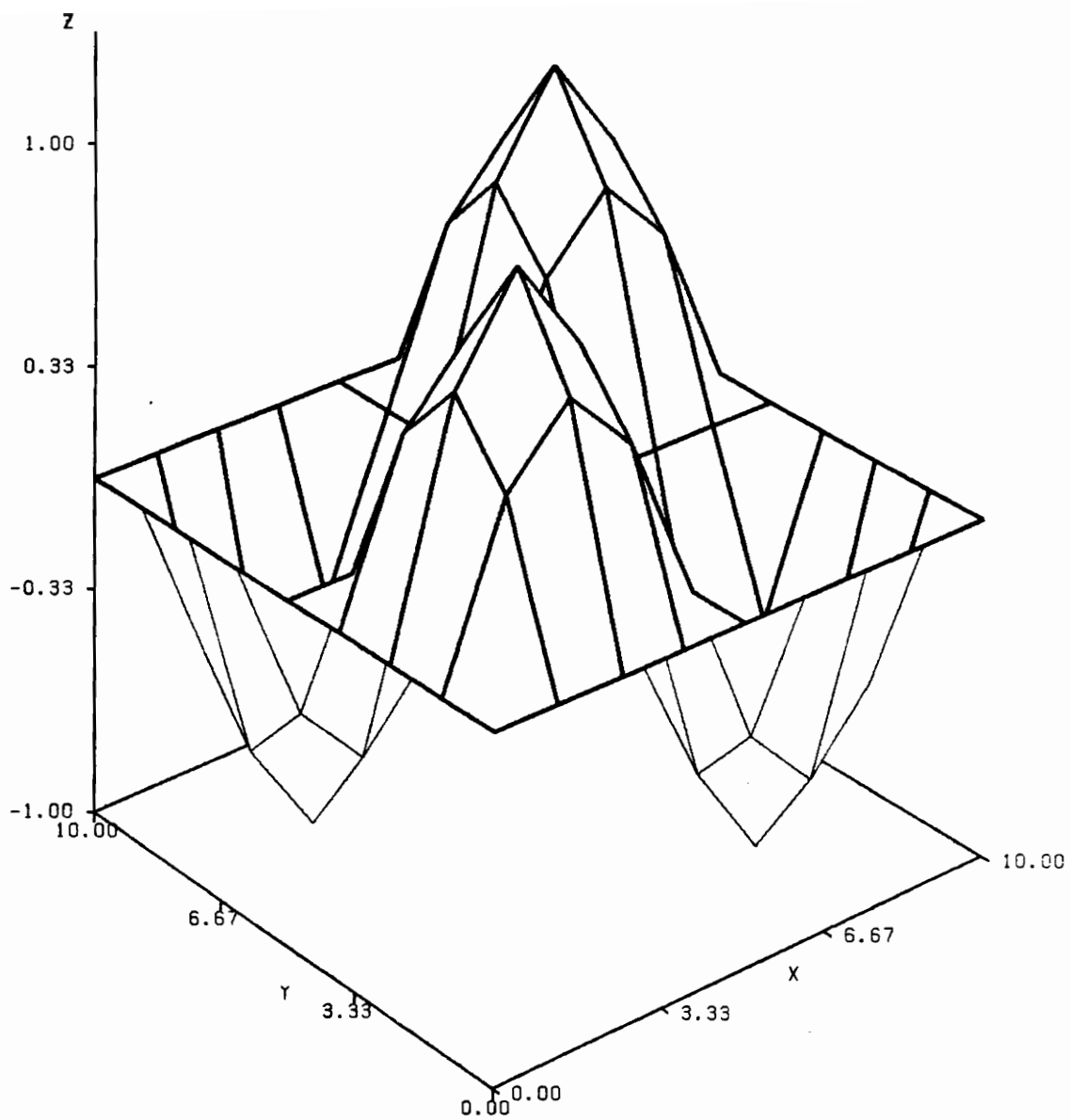


Figure 10. Simply Supported Isotropic Plate. Mode 3

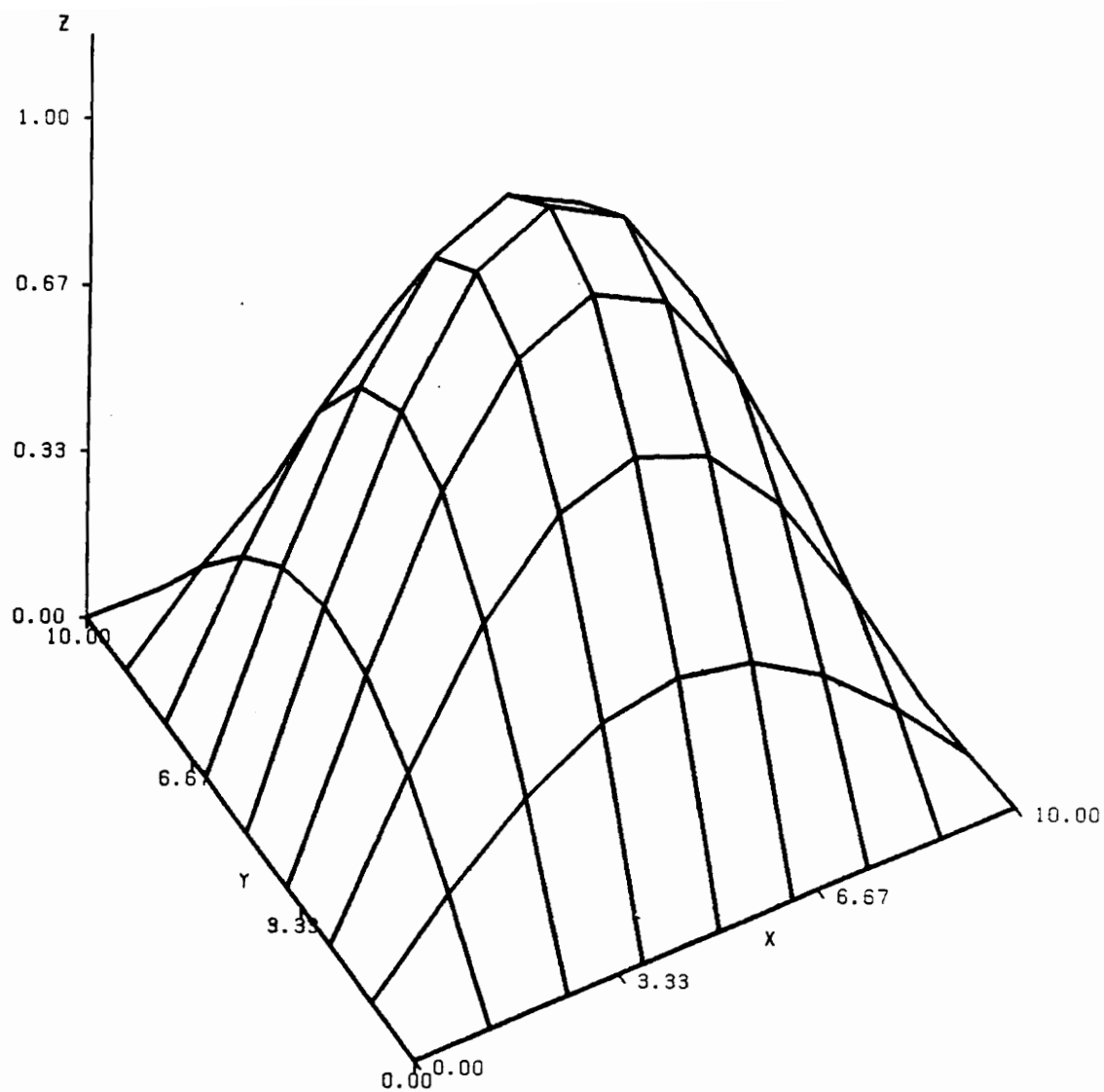


Figure 11. Simply Supported [0/90/90/0] Laminated Composite Plate. Mode 1

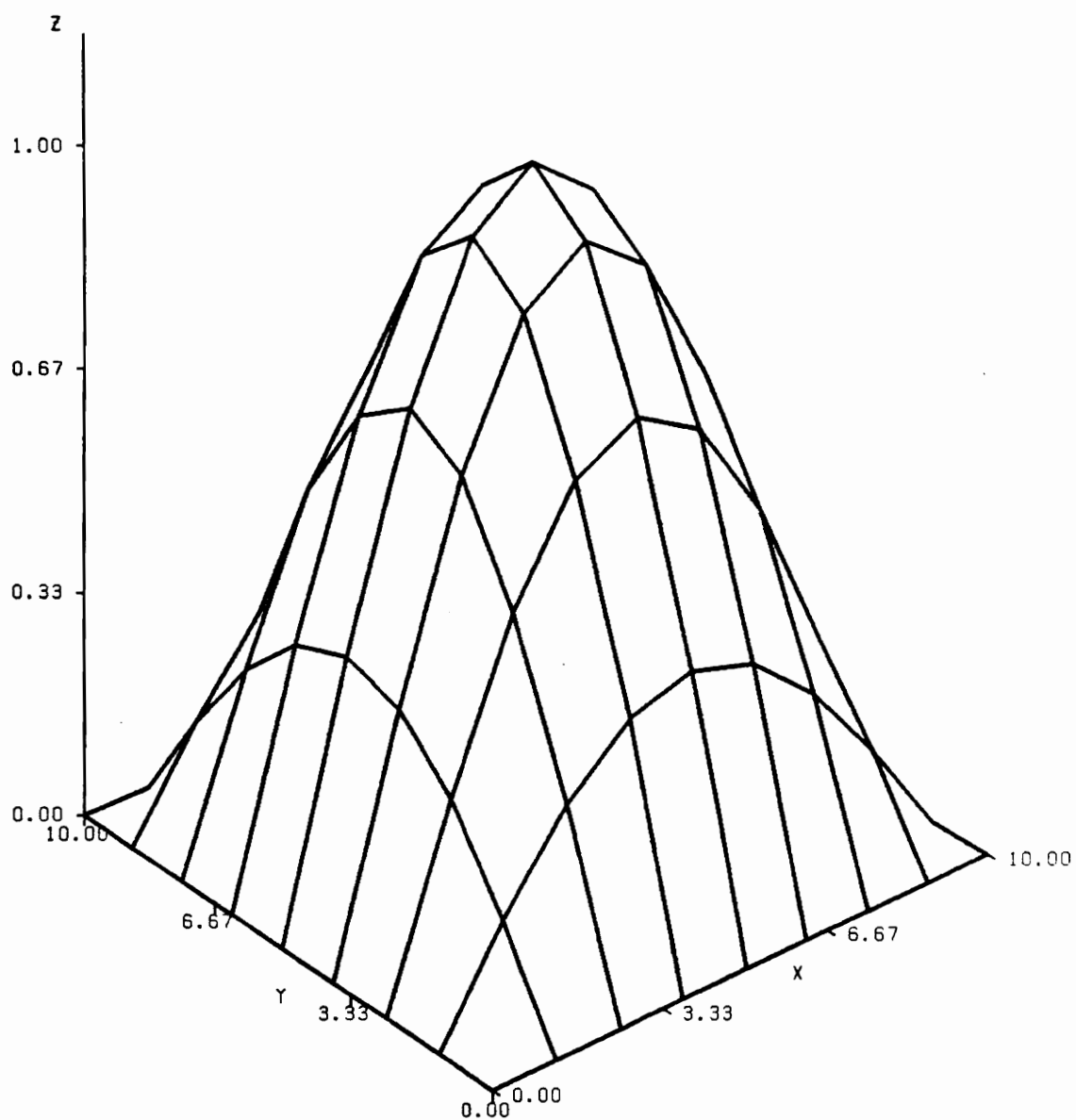


Figure 12. Simply Supported [0/90/90/0] Laminated Composite Plate. Mode 1

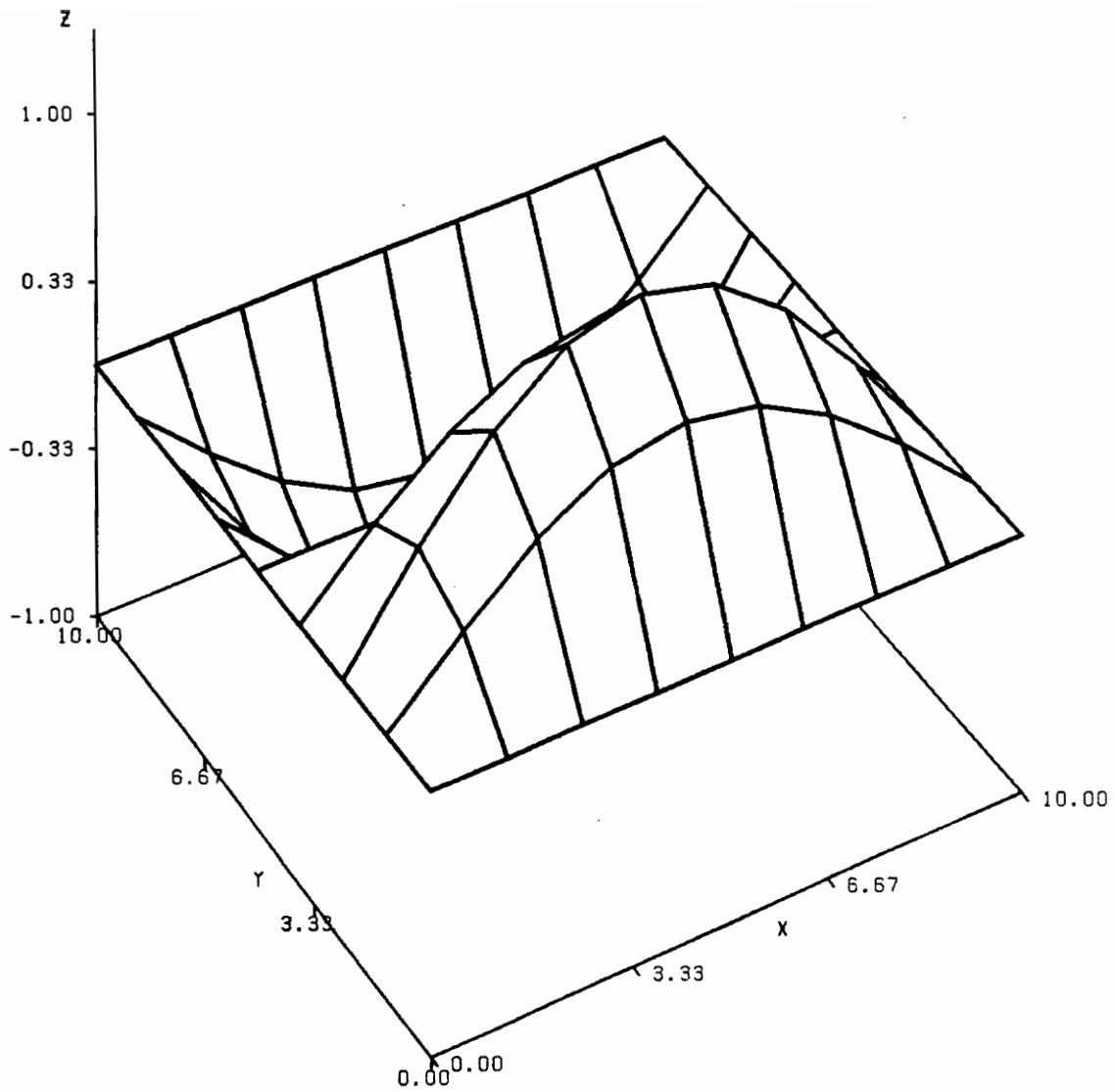


Figure 13. Simply Supported [0/90/90/0] Laminated Composite Plate. Mode 2

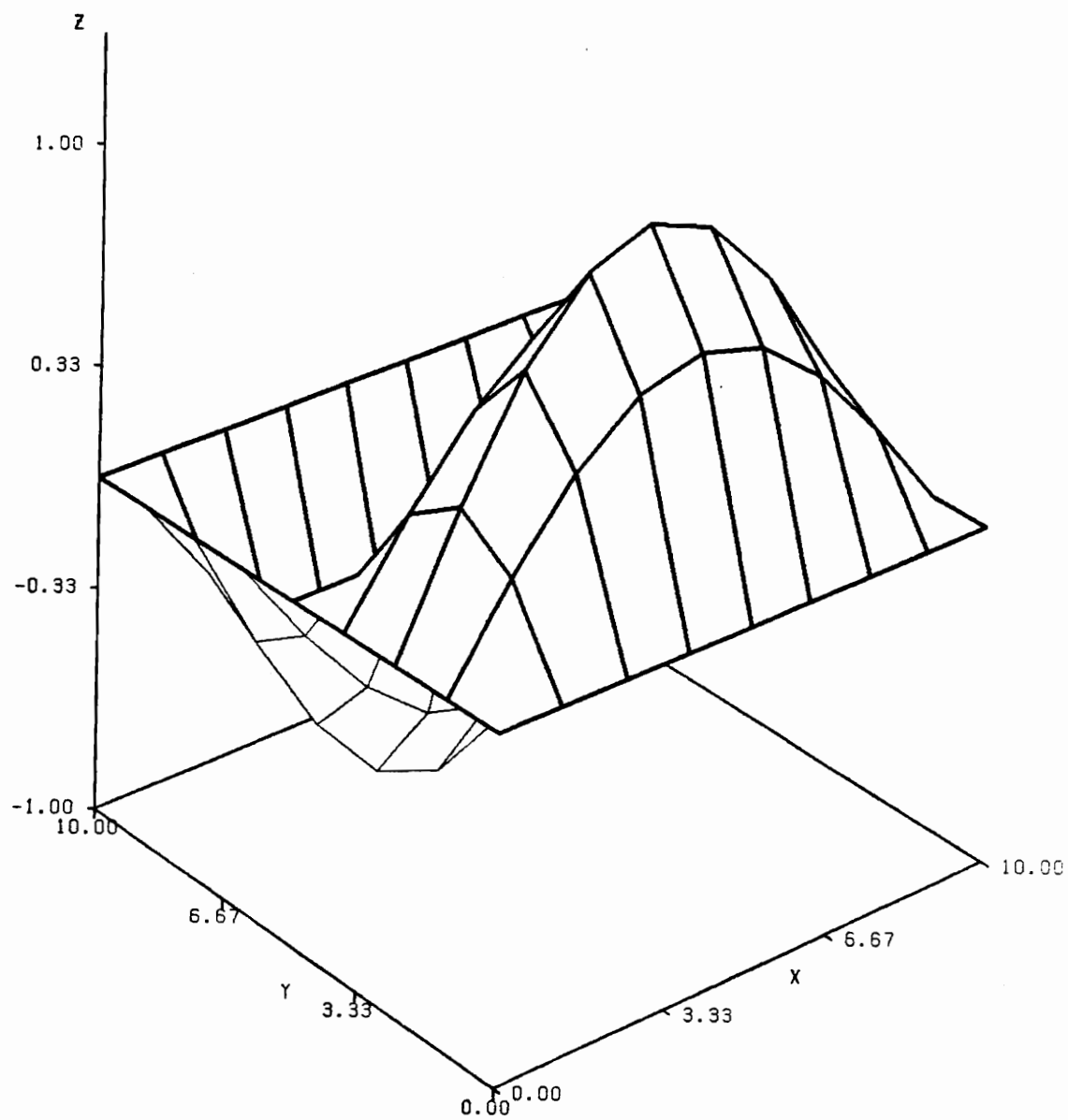


Figure 14. Simply Supported [0/90/90/0] Laminated Composite Plate. Mode 2

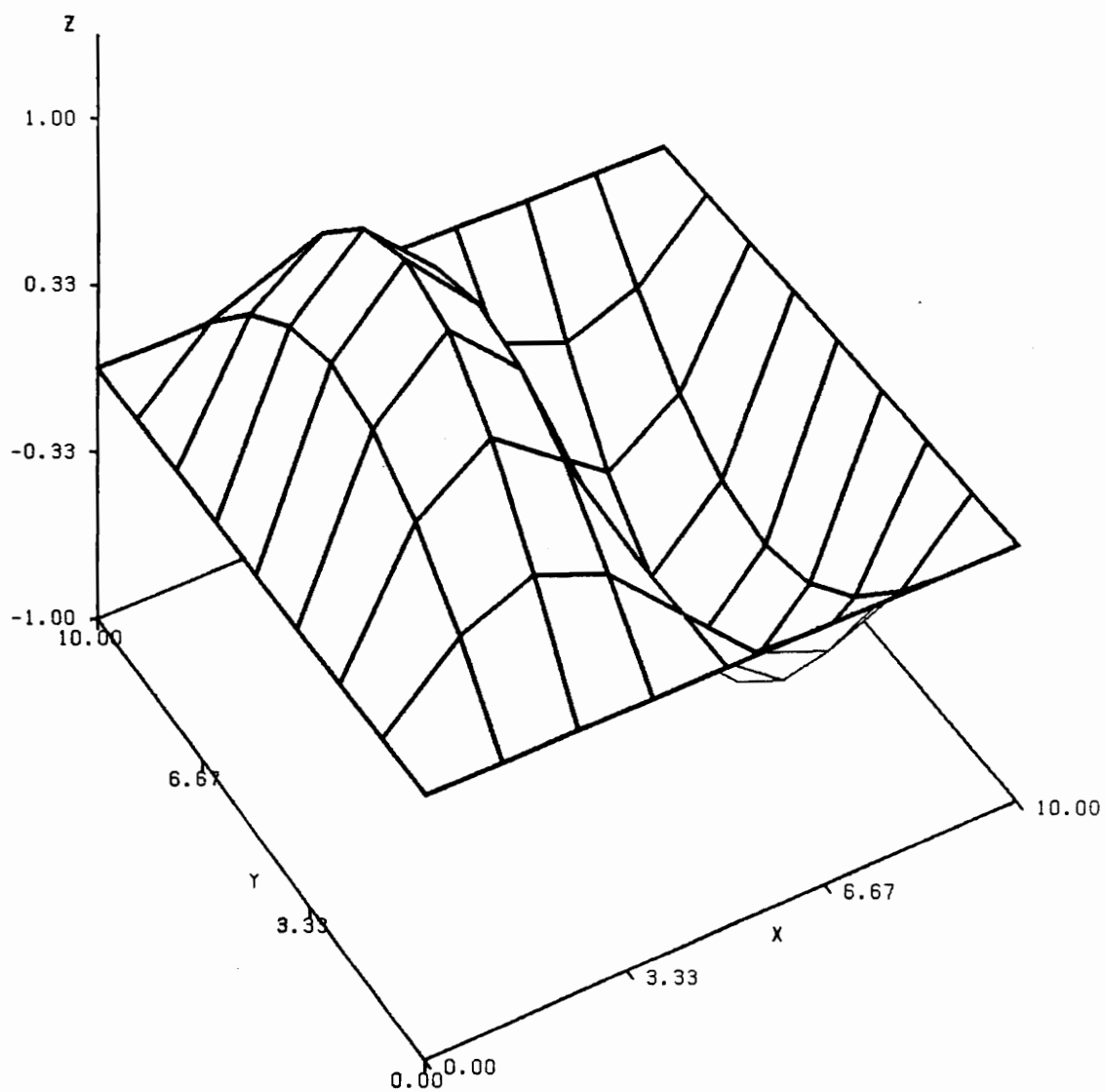


Figure 15. Simply Supported [0/90/90/0] Laminated Composite Plate. Mode 3

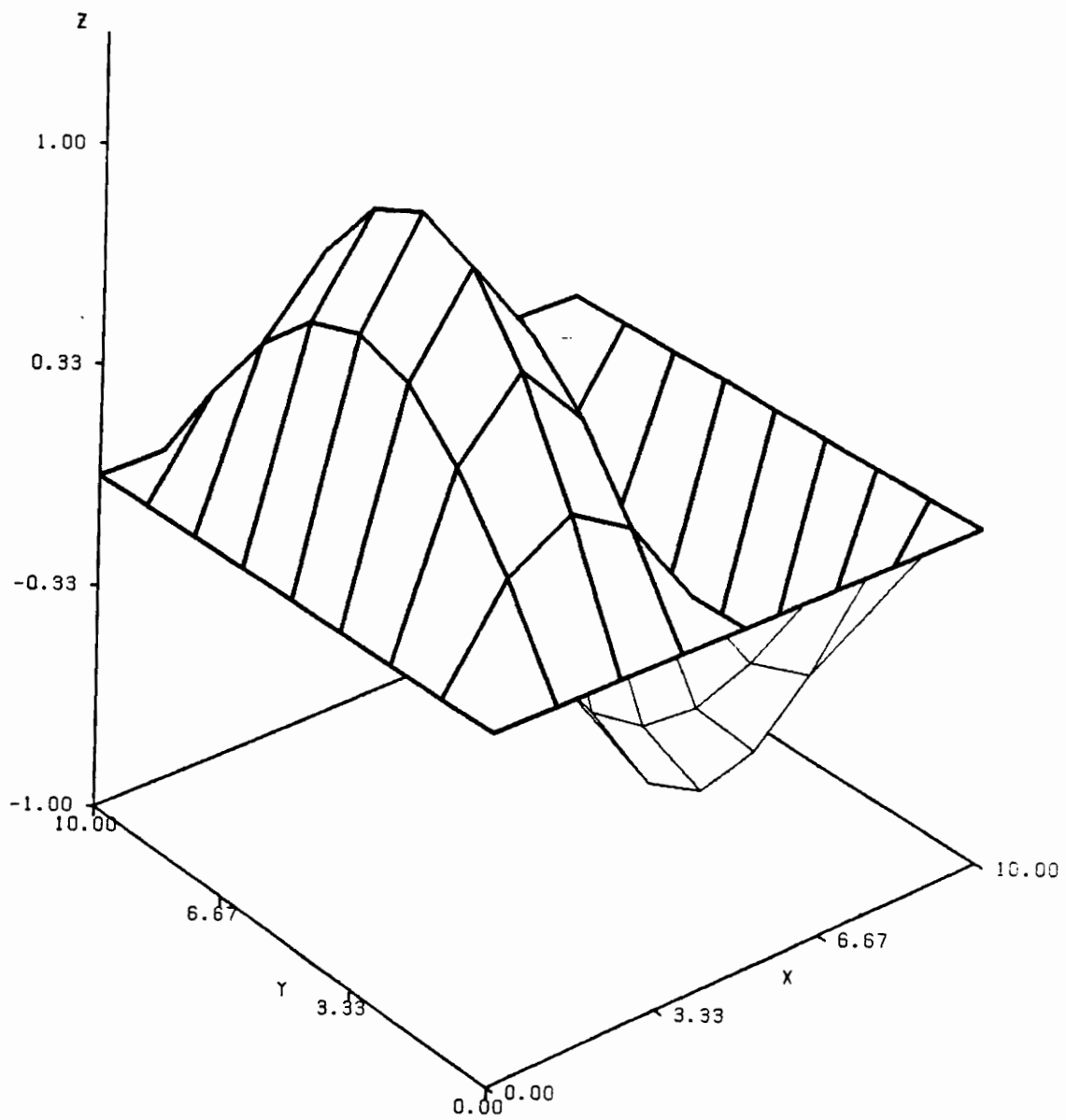


Figure 16. Simply Supported [0/90/90/0] Laminated Composite Plate. Mode 3

five frequencies of flexural vibration have been obtained for both the isotropic and the laminated composite plate in Tables 4 and 5. The mode shapes for the first three modes have been plotted for the isotropic cantilever plates in Figures 17 - 22. The mode shapes for the first three modes have also been plotted for the [0/90/90/0] laminated composite cantilever plates in Figures 23-28.

As in the case of simply-supported plates, the mode shapes have been plotted only for symmetric plates as these do not have bending-extension coupling and hence it is possible to obtain vibration modes for flexural vibration of the plates. Similarly, for the symmetric plates, the frequencies of flexural vibration of the plate have been tabulated, while, for the anti-symmetric angle-ply laminated plate the lowest frequencies of vibration have been tabulated.

The results for the cantilever isotropic plate have been compared with the exact results based on the classical plate theory, given by Leissa [21].

4.2 *Rotating Plates*

For rotating plates, only the cantilever boundary conditions have been considered.

The results for various angular velocities are tabulated for a plate. As shown in figure 29, the axis of rotation of the plate has been taken normal to the plate and lying at one corner of the plate. One of the edges adjacent to the axis of rotation is oriented along the radial direction. Thus in the present analysis, results have been obtained for a plate without any translational or rotational offsets from the axis of rotation.

The results for the rotating isotropic plate have been verified by comparing with those obtained by Dokainish and Rawtani [3], which used CPT to model the rotating plate and did not consider

Table 4. Vibration of Cantilever Isotropic Plates

Isotropic Plate					
$\bar{\omega} = (\omega a^2/h)\sqrt{\rho/D}$					
Mode	1	2	3	4	5
Exact (CPT)	3.4940	8.5470	21.440	27.460	31.170
8 x 8 Linear Mesh (FSDPT)	3.4338	8.0833	20.752	26.055	28.953
4 x 4 Quadratic Mesh (FSDPT)	3.4275	8.0545	20.144	25.576	28.307

$a = 10 \text{ in.}, b = 10 \text{ in.}, h = 1 \text{ in.}$

Table 5. Vibration of Cantilever Laminated Composite Plates

[0/90/90/0] Laminated Composite Plate					
$\bar{\omega} = (\omega a^2/h)\sqrt{\rho/E_2}$					
Mode	1	2	3	4	5
8 x 8 Linear Mesh (FSDPT)	1.7621	5.7851	9.8498	14.496	15.365
4 x 4 Quadratic Mesh (FSDPT)	1.7584	5.7590	9.5789	13.756	14.875

[45/-45] Laminated Composite Plate					
$\bar{\omega} = (\omega a^2/h)\sqrt{\rho/E_2}$					
Mode	1	2	3	4	5
8 x 8 Linear Mesh (FSDPT)	5.2784	5.2848	16.300	22.065	22.571
4 x 4 Quadratic Mesh (FSDPT)	5.2695	5.8310	16.067	21.670	22.294

$a = 10 \text{ in.}, b = 10 \text{ in.}, h = 1 \text{ in.}$

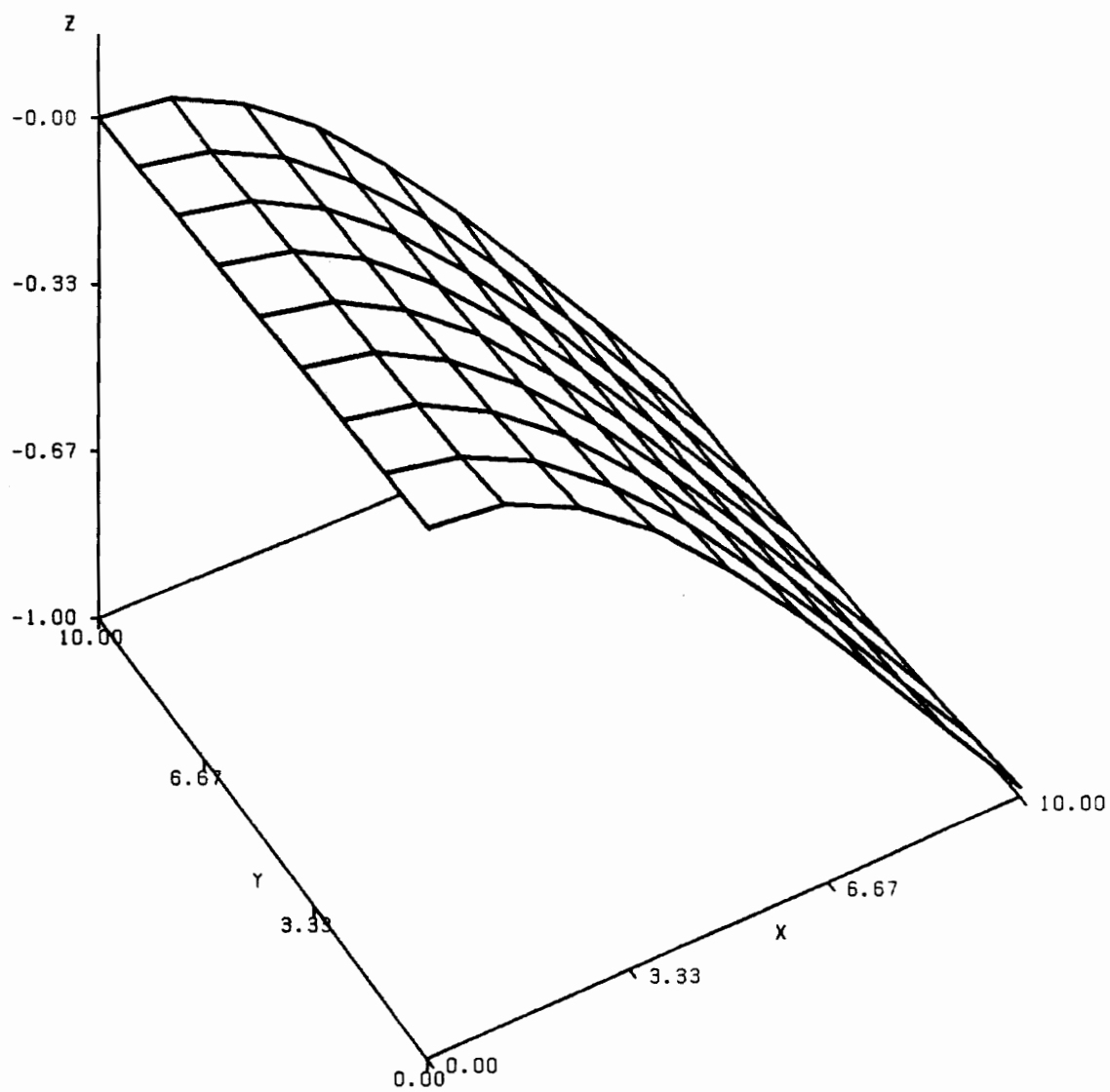


Figure 17. Cantilever Isotropic Plate. Mode 1

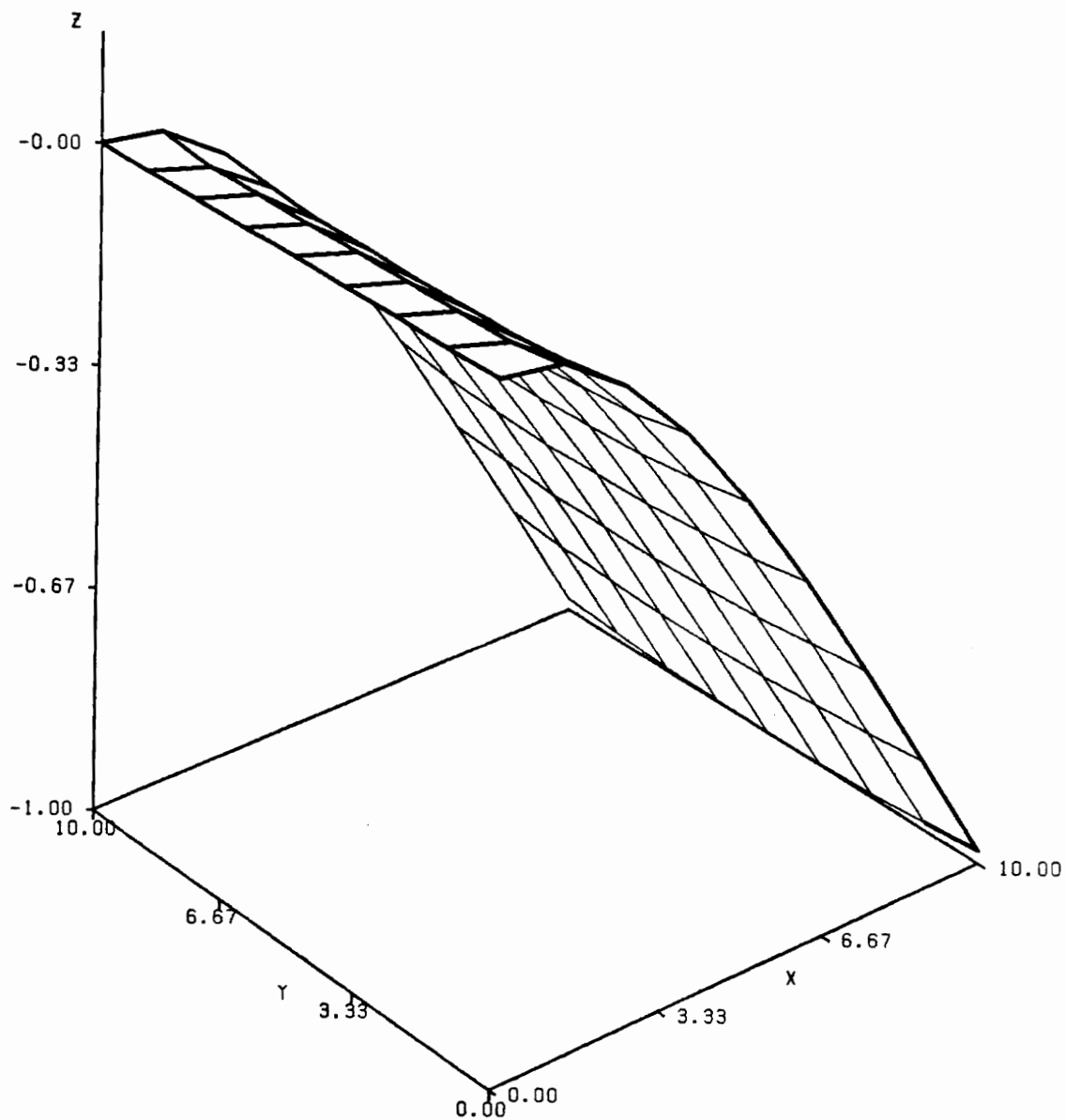


Figure 18. Cantilever Isotropic Plate. Mode 1

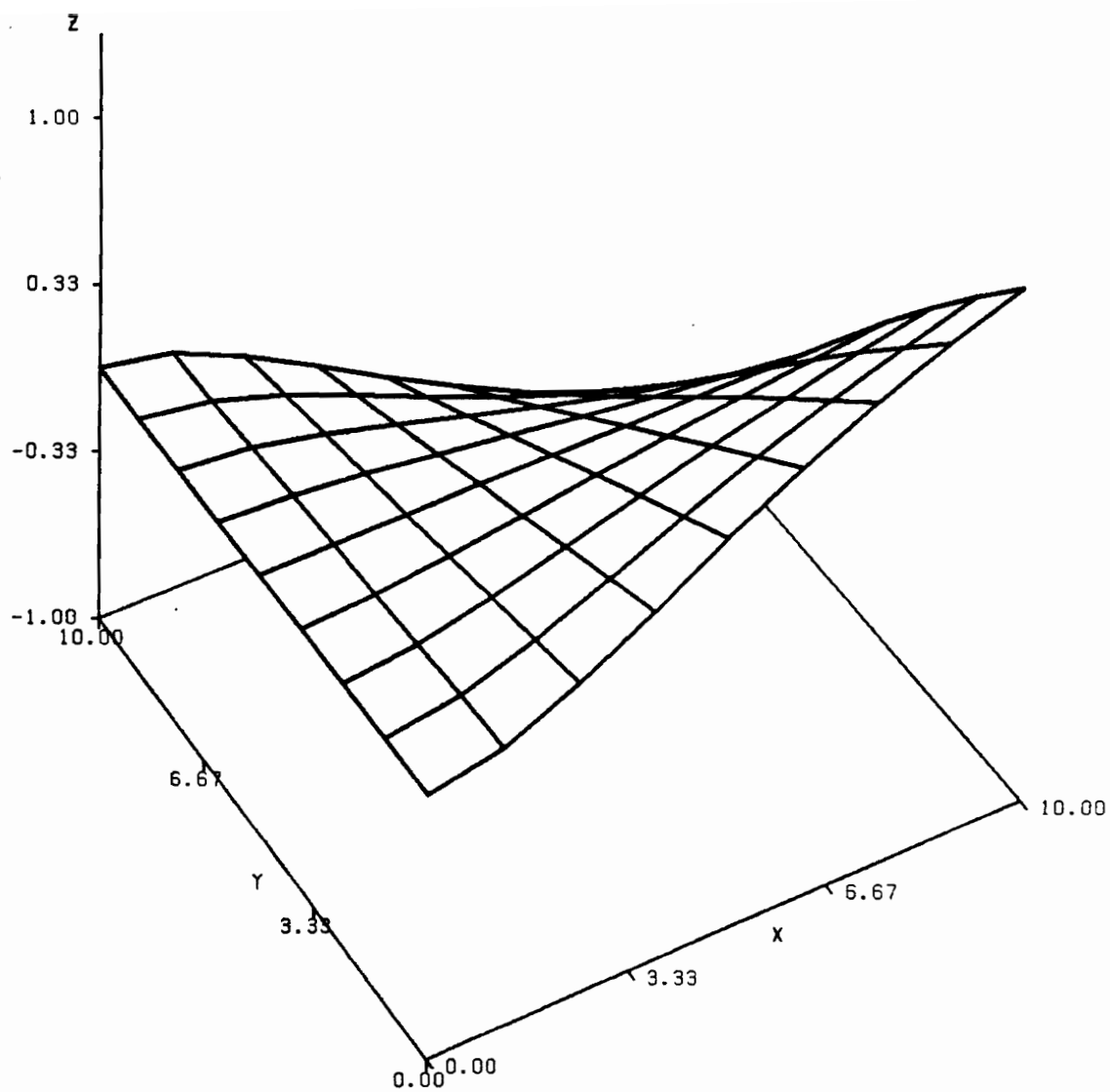


Figure 19. Cantilever Isotropic Plate. Mode 2

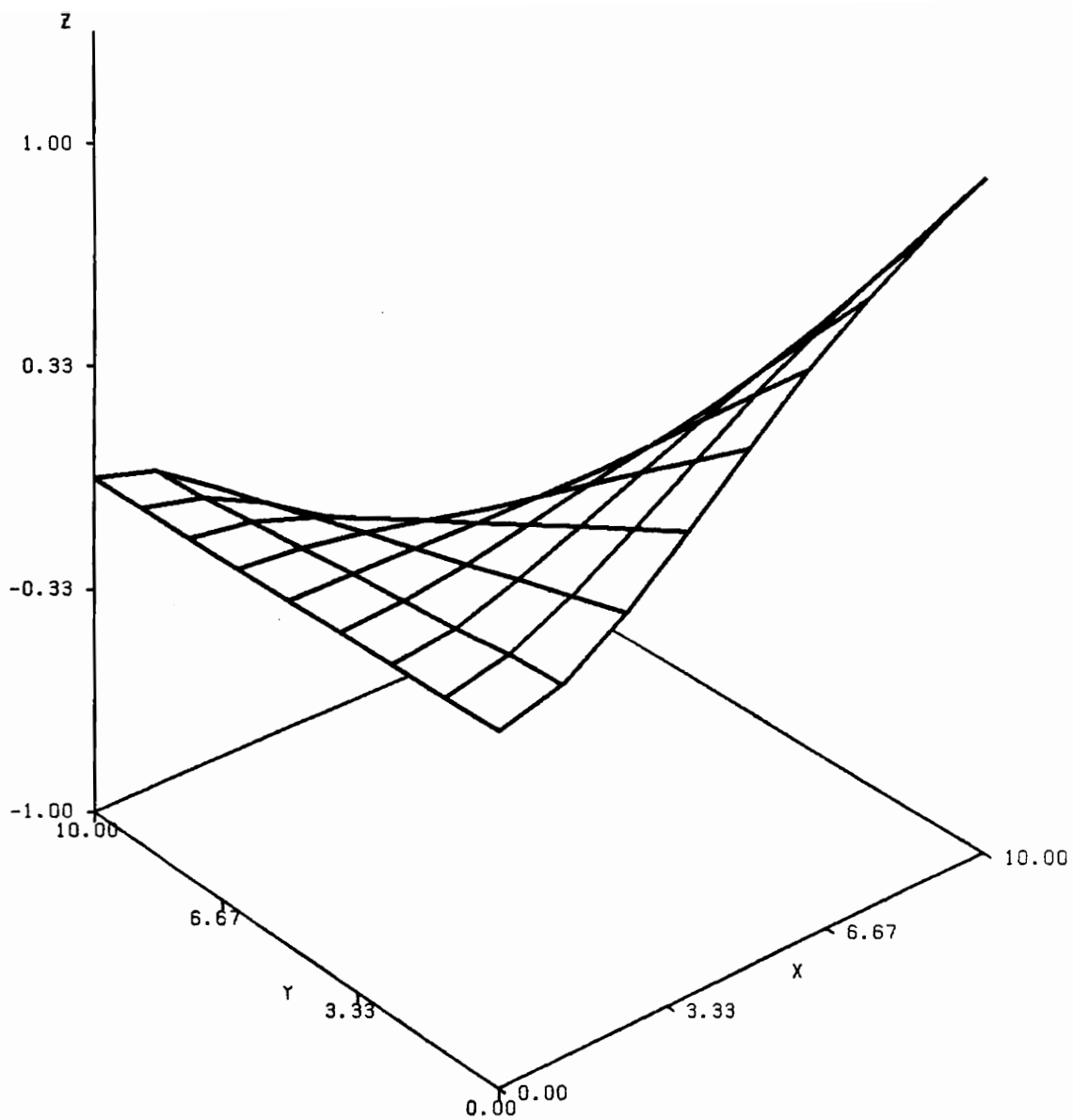


Figure 20. Cantilever Isotropic Plate. Mode 2

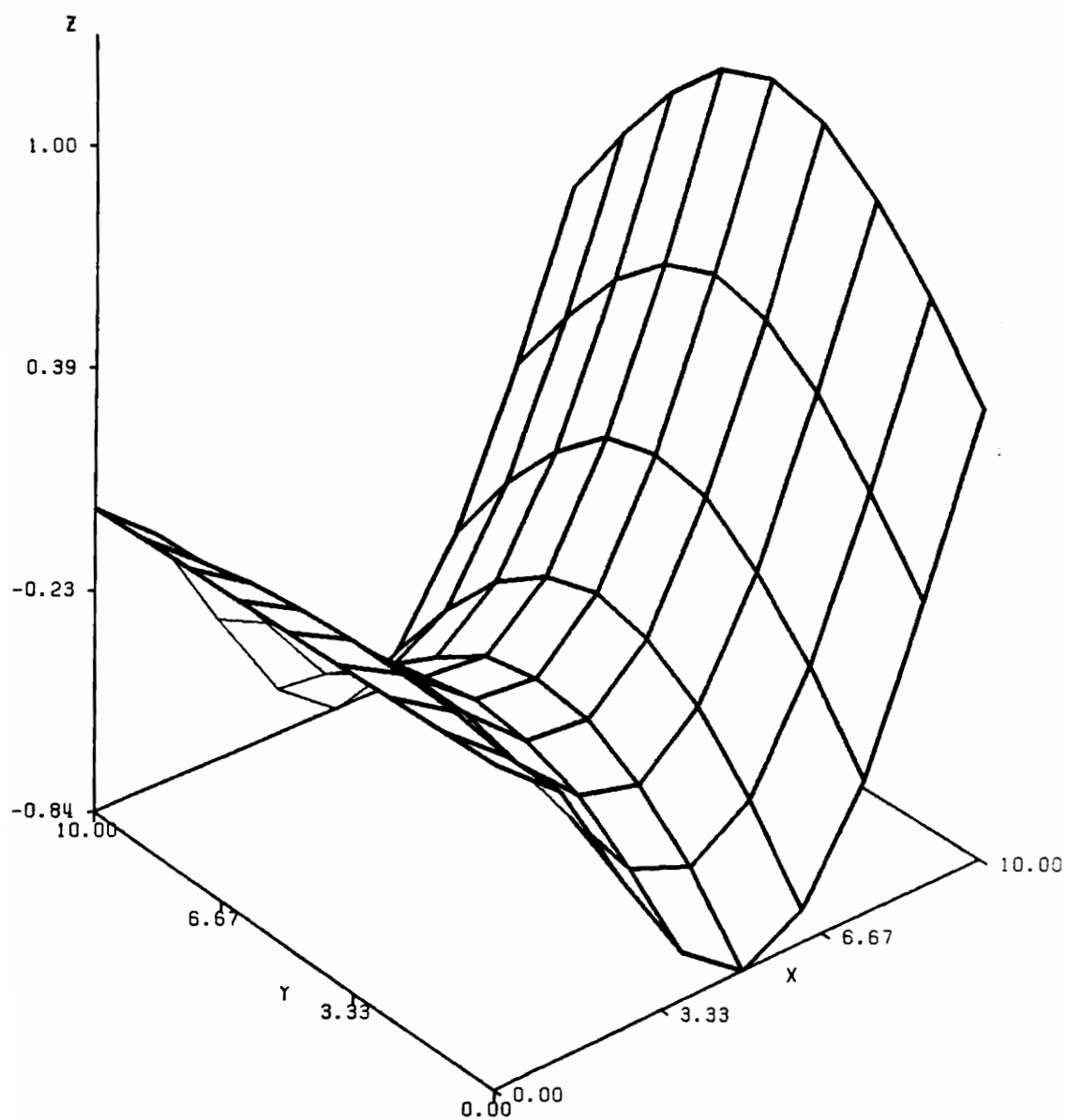


Figure 21. Cantilever Isotropic Plate. Mode 3

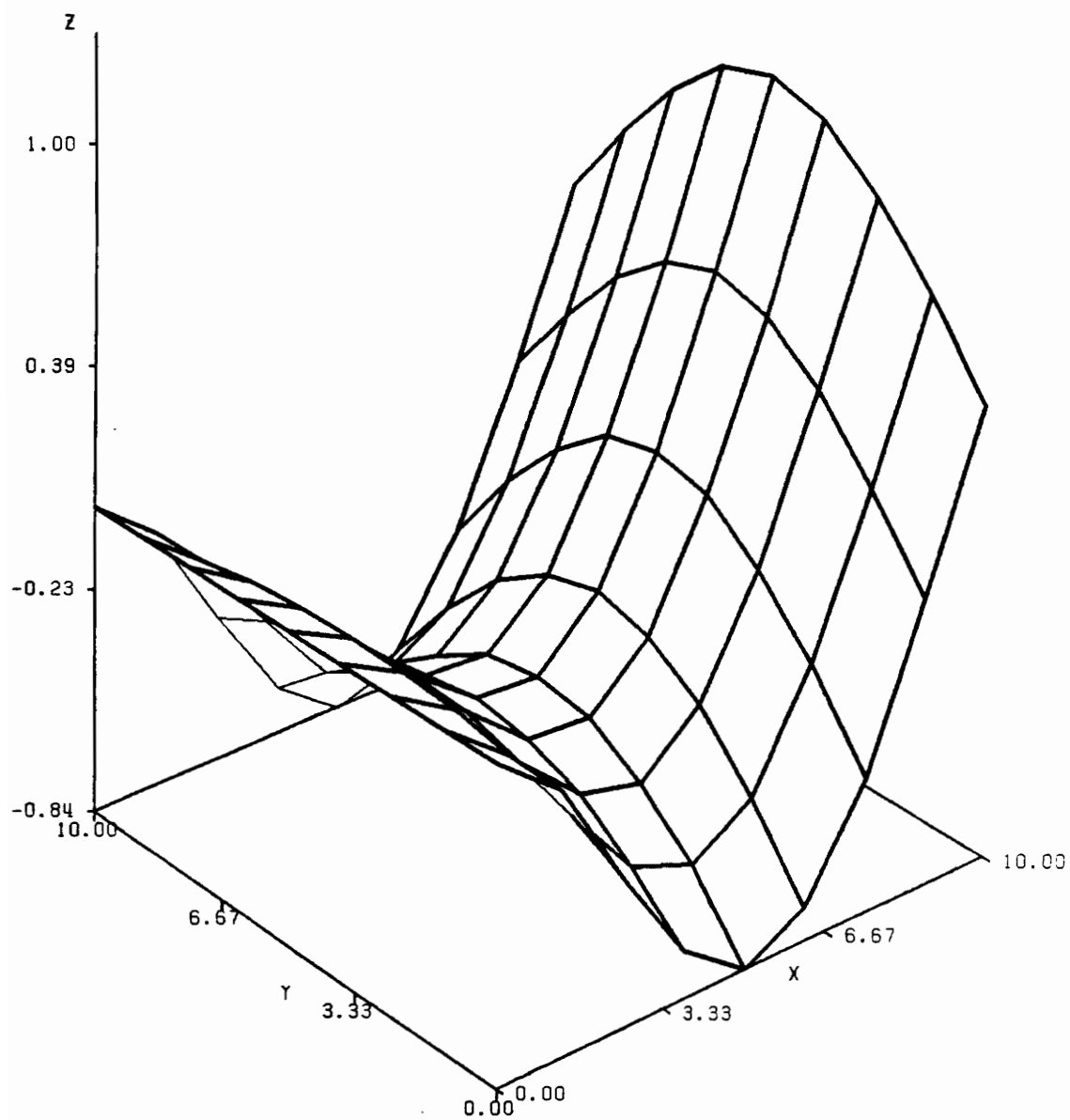


Figure 22. Cantilever Isotropic Plate. Mode 3

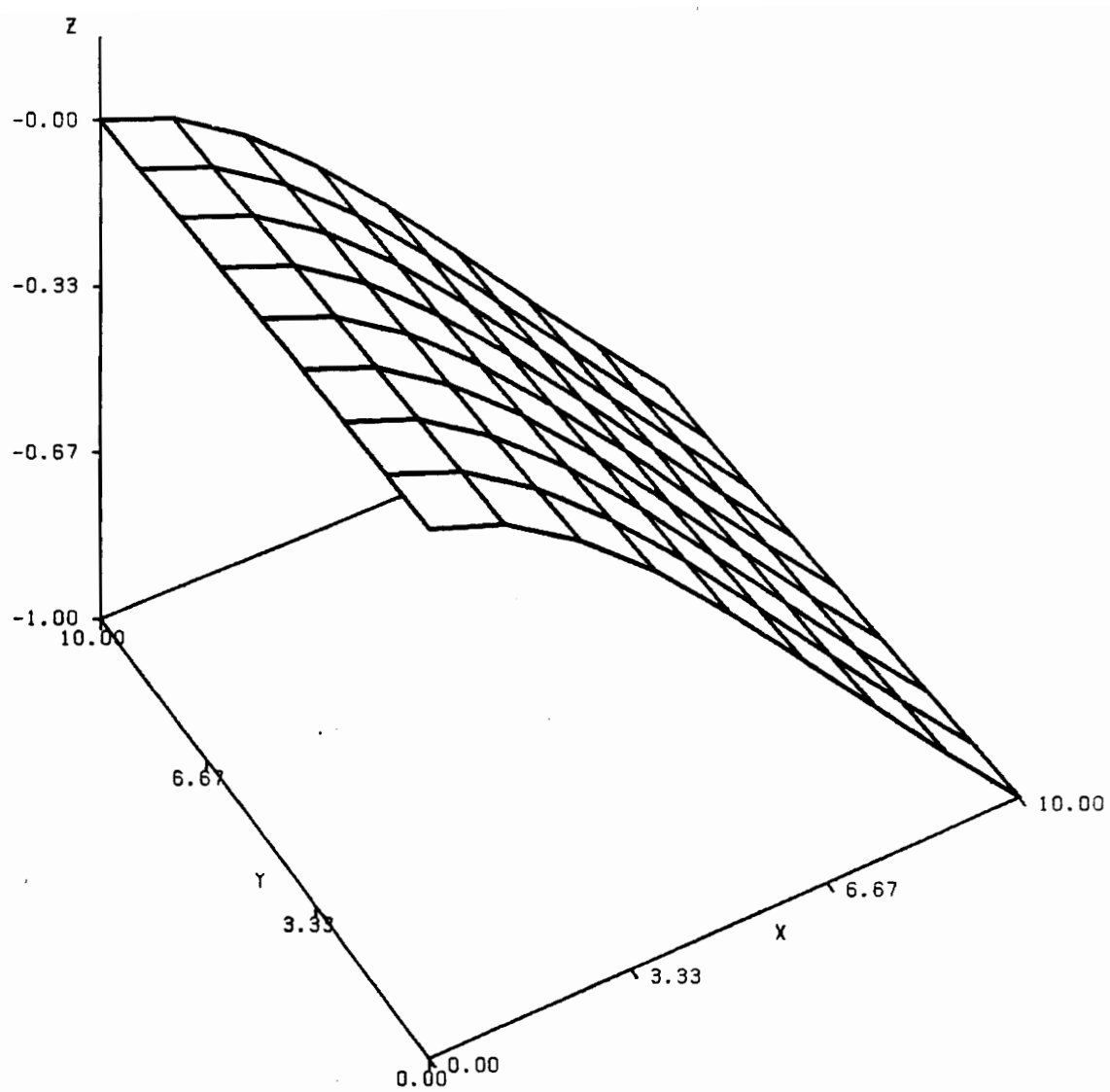


Figure 23. Cantilever Laminated Composite [0/90/90/0] Plate. Mode 1

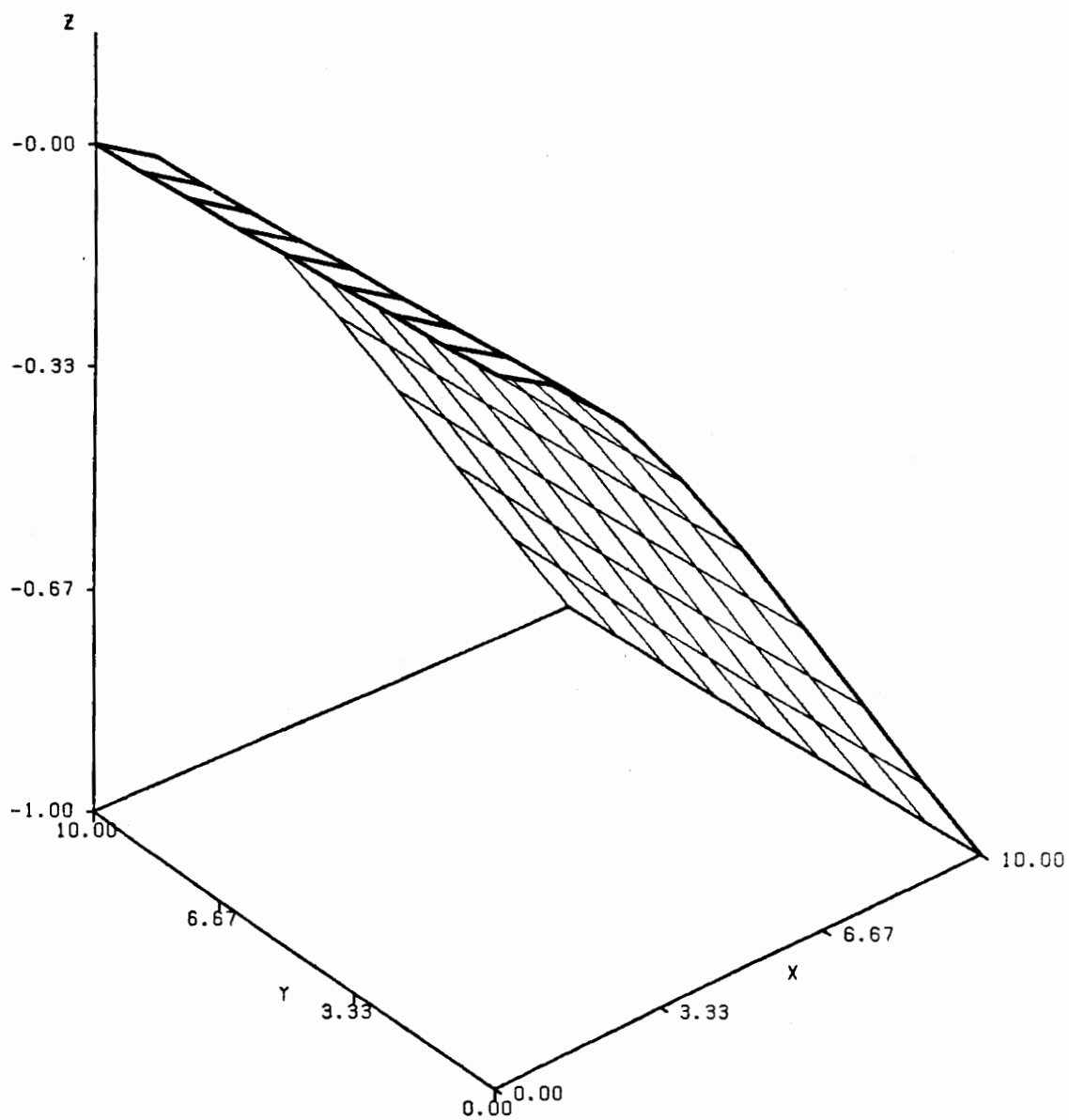


Figure 24. Cantilever Laminated Composite [0/90/90/0] Plate. Mode 1

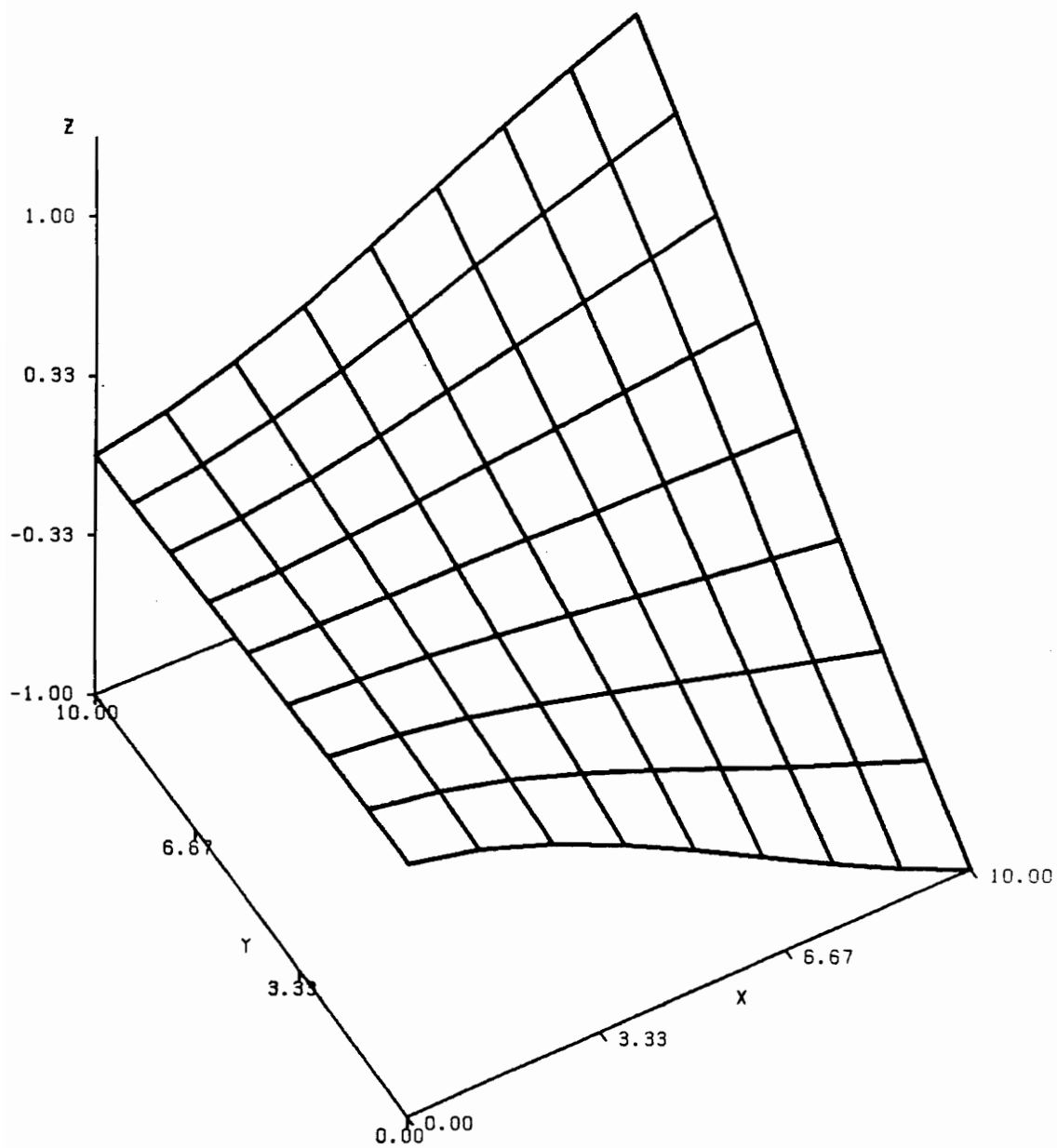


Figure 25. Cantilever Laminated Composite [0/90/90/0] Plate. Mode 2

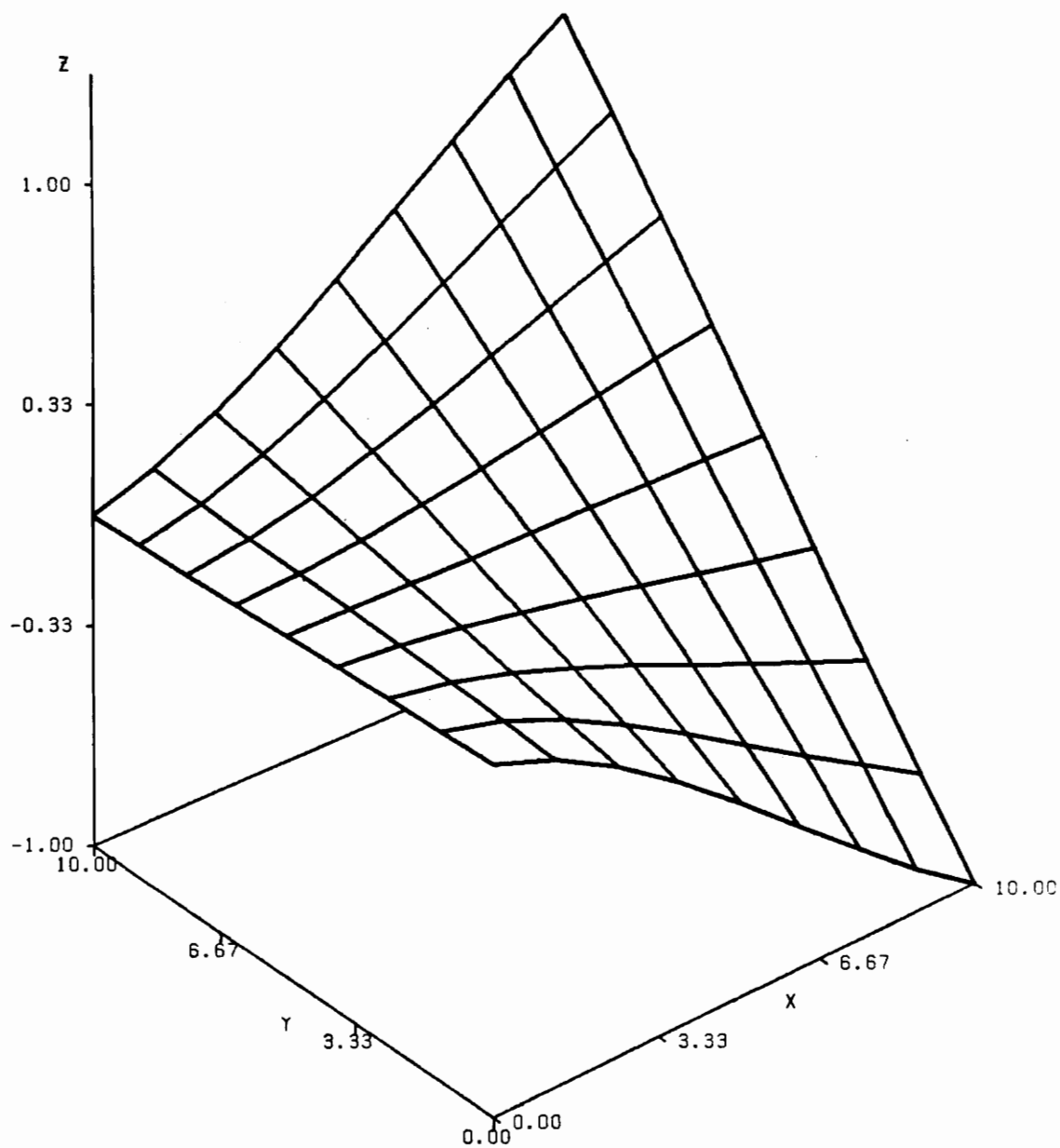


Figure 26. Cantilever Laminated Composite $[0/90/90/0]$ Plate. Mode 2

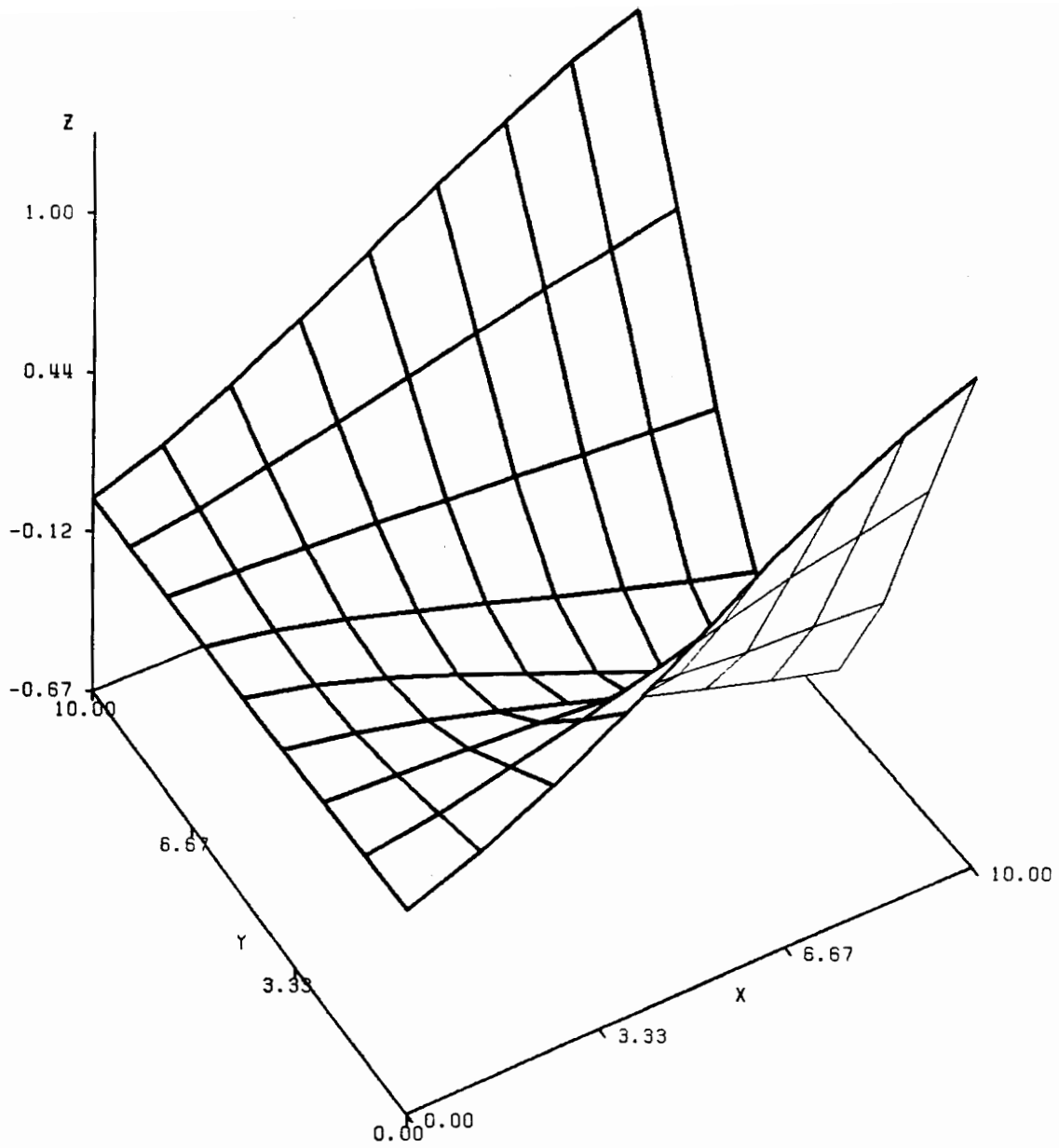


Figure 27. Cantilever Laminated Composite [0/90/90/0] Plate. Mode 3

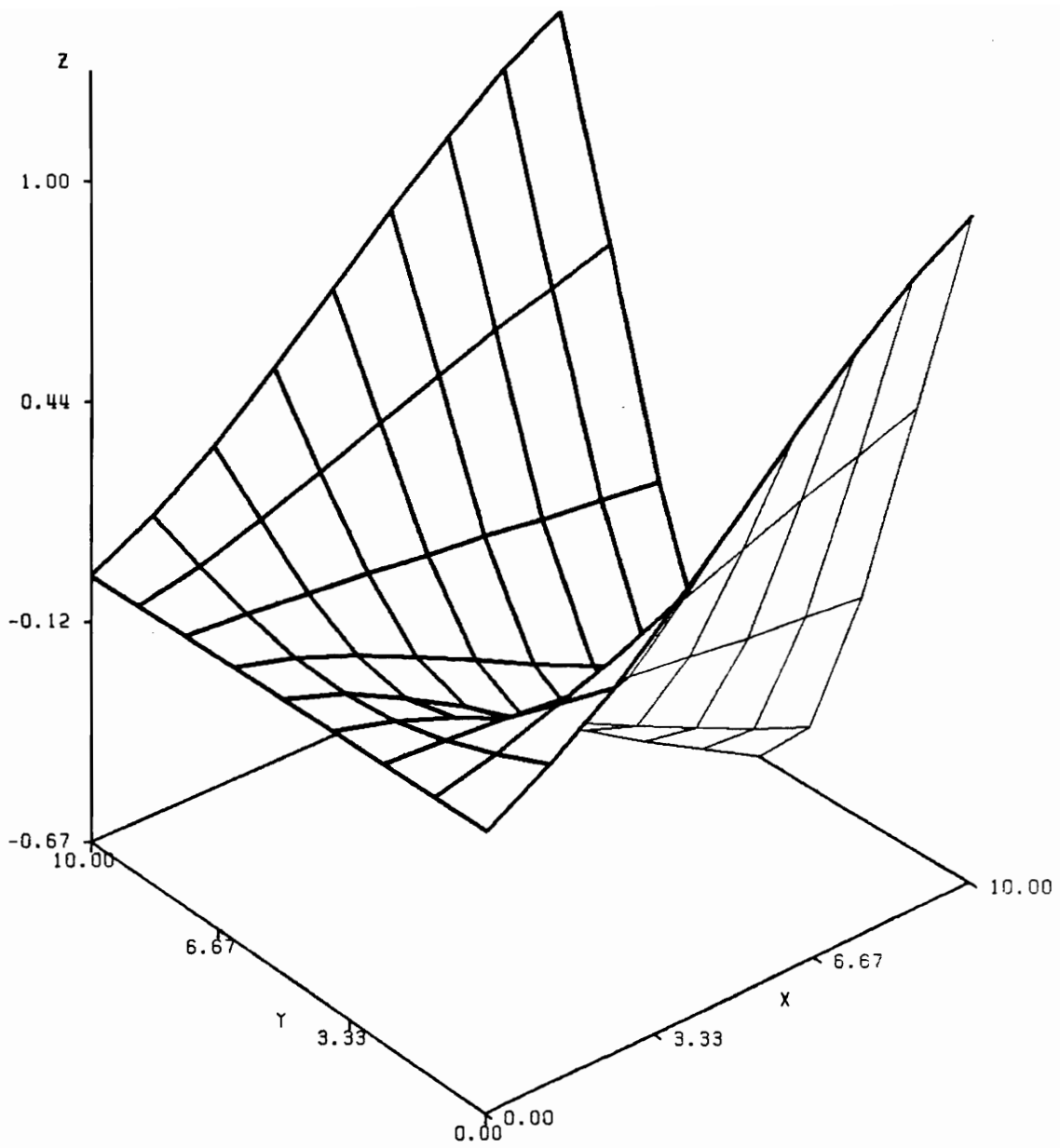


Figure 28. Cantilever Laminated Composite [0/90/90/0] Plate. Mode 3

non-linear strains. The comparison is given in Table 6 and in Figure 30. The angular velocity has been non-dimensionalized by dividing by the fundamental frequency of vibration of a non-rotating cantilever plate. It was seen that for the plate thickness used in the above reference, non-linear strains were not significant and the results obtained in the present study are very close to those obtained in the above reference. There was divergence of results for the higher modes of vibration, where, as has been observed earlier, the classical plate theory gives inaccurate results. Also, it was seen that for thin plates, non-linear strains are very significant and can not be neglected.

The results for the analysis are presented in Table 7 for isotropic and in Table 8 for laminated composite plates. As expected, the frequency of vibration increases with an increase in the angular velocity. Also, as predicted by Meirovitch [10], the fundamental frequency of free vibration of the plate remains greater than the angular velocity of the plate. There is a monotonic increase in the frequency of vibration with the increase in angular velocity. The same non-dimensionalization has been used for both the vibration frequency and the angular velocity.

The variation in the frequency of free vibration of plate with angular velocity has been plotted in Figure 31 for the isotropic plate and in Figure 32 for the laminated composite plate. It is seen both from the values obtained and from the corresponding plot that for the isotropic plate there is a slight decrease in the frequency with angular velocity for the third mode for one observation. For the laminated composite plate, it is seen that, in general, the frequency of vibration is lower, but there is a greater increase in the frequency with increase in angular velocity. Also, though the first and second modes, and, the fourth and fifth mode have frequency close to each other for the static case, they diverge with increase in angular velocity.

A study has been made of the effect of change of the side-to-thickness ratio of the [0/90/90/0] laminated composite plate on its fundamental frequency of free vibration, and the results are included in Table 9. For thick plates, it is observed that there is little change in the frequency with increase in angular velocity. This is explained by the fact that for thick plates the terms of the centrifugal stiffness matrix are much smaller than the linear and non-linear stiffness terms and hence

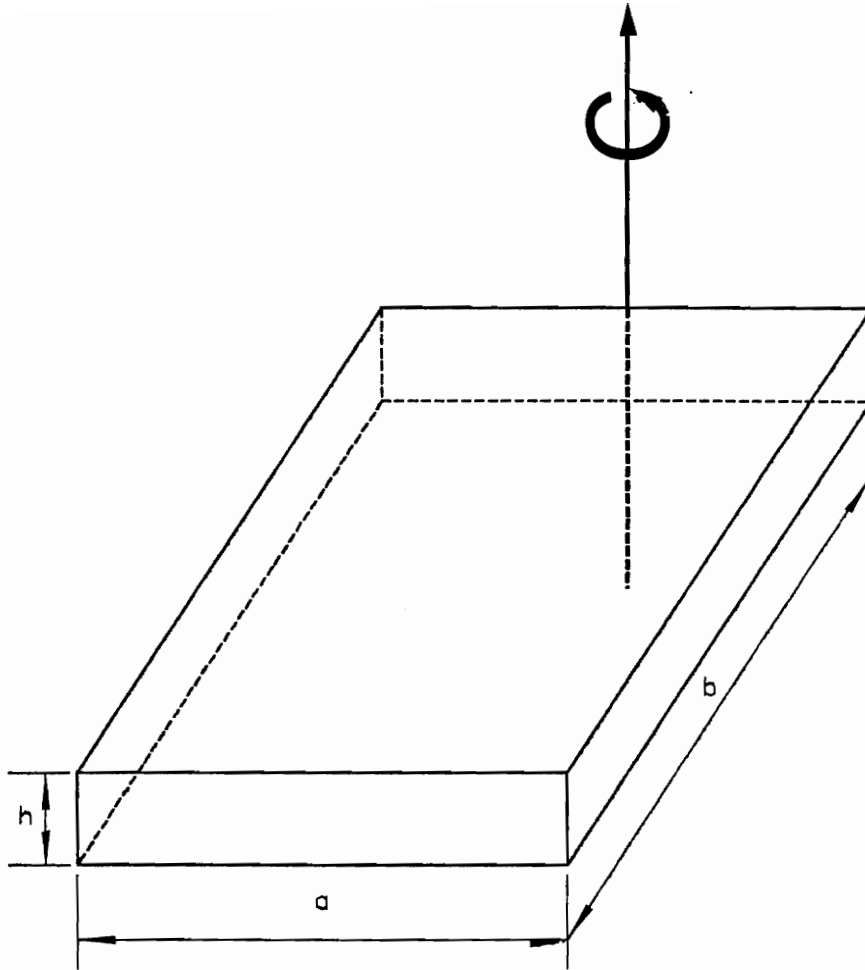


Figure 29. Orientation of Plate with Respect to Axis of Rotation

Table 6. Rotating Cantilever Isotropic Plates - Verification of Results

Isotropic Plate					
$\bar{\omega} = (\omega a^2)\sqrt{\rho h/D}$					
Mode	1	2	3	4	5
DOKAINISH	5.097	9.824	22.913	27.849	32.735
PRESENT STUDY	5.113	9.635	22.649	24.232	28.759

$a = 10 \text{ in.}, b = 10 \text{ in.}, h = 1 \text{ in.}$

Non-Dimensionalised Velocity = 1

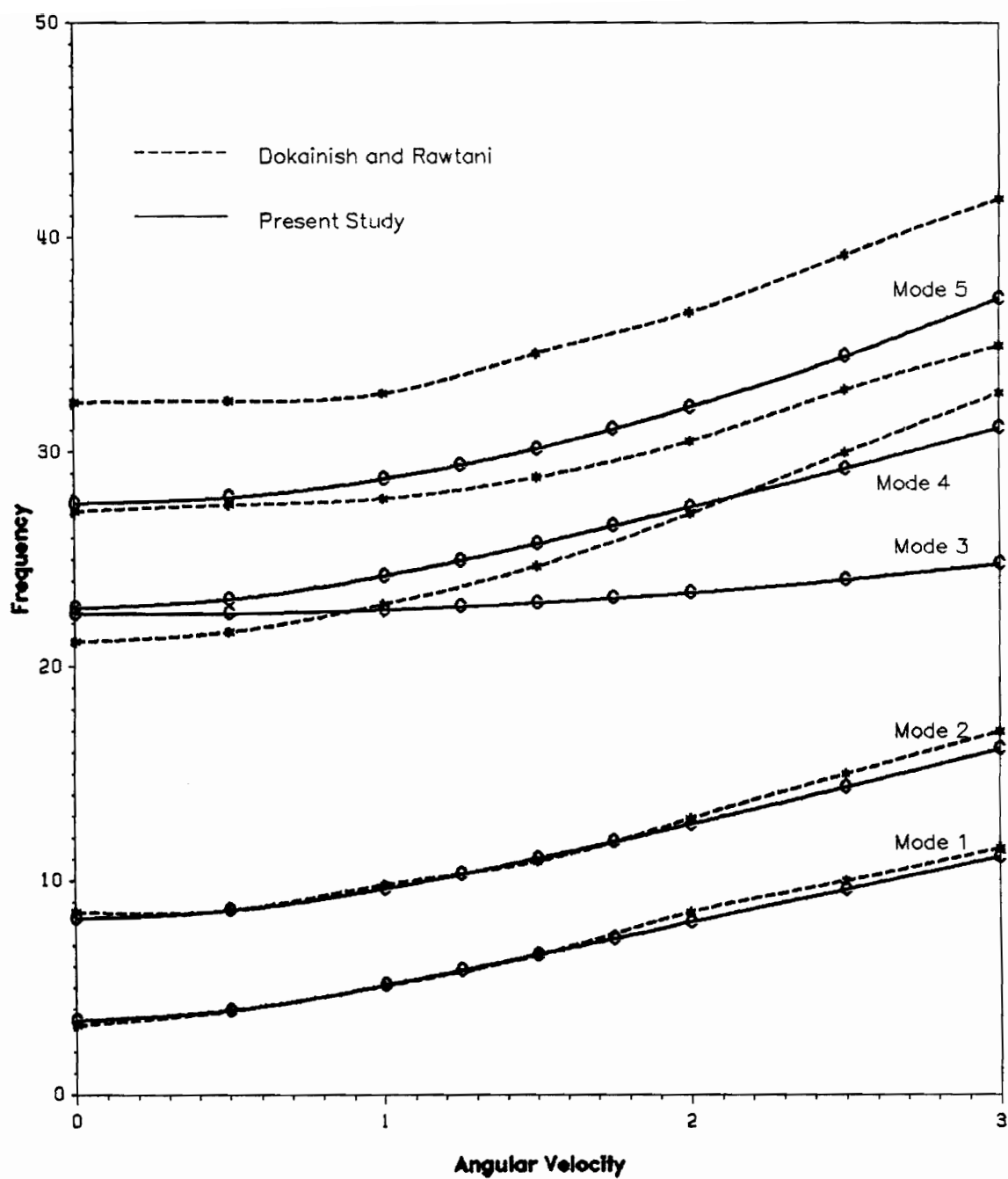


Figure 30. Rotating Cantilever Isotropic Plates - Verification of Results

Table 7. Vibration of Rotating Cantilever Isotropic Plates

Isotropic Plate					
$\bar{\omega} = (\omega a^2)\sqrt{\rho h/D}$					
Angular Velocity $\bar{\Omega} = (\Omega a^2/h)\sqrt{\rho/D}$	Mode				
	1	2	3	4	5
0.0	3.4275	8.0545	20.144	25.576	28.307
1.0	3.5949	8.1779	20.287	25.651	28.439
2.0	4.0491	8.5299	20.704	25.873	28.832
3.0	4.6921	9.0653	22.054	26.238	29.478
4.0	5.4414	9.7311	22.032	26.744	30.359
5.0	6.2456	10.842	22.369	27.407	31.446
6.0	7.0758	11.288	22.658	28.245	32.701

a = 10 in., b = 10 in., h = 1 in.

do not play a significant role. But, as the length-to-thickness ratio is increased, the effect of angular velocity on the frequency of the plate becomes more apparent. A plot of variation in fundamental frequency with angular velocity for various values of side-to-thickness ratio is shown in Figure 33.

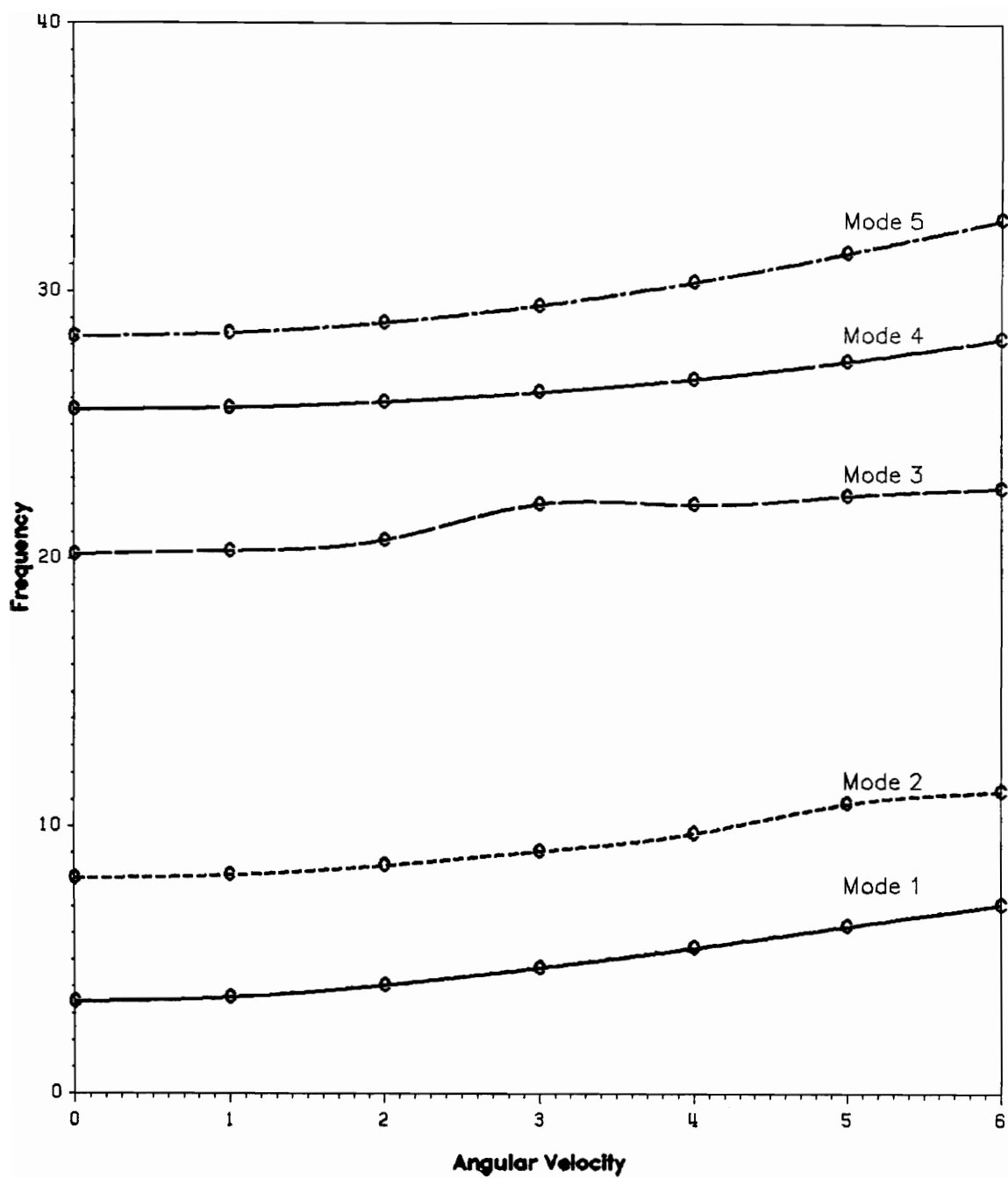


Figure 31. Variation in Frequency of Rotating Isotropic Plate with Angular Velocity for First 5 modes

Table 8. Vibration of Rotating Cantilever Laminated Composite Plates

[0/90/90/0] Laminated Composite Plate					
$\bar{\omega} = (\omega a^2/h)\sqrt{\rho/E_2}$					
Angular Velocity $\bar{\Omega} = (\Omega a^2/h)\sqrt{\rho/E_2}$	Mode				
	1	2	3	4	5
0.0	5.2695	5.8310	16.067	21.670	22.294
1.0	5.3639	6.0028	16.187	21.800	22.469
2.0	5.6304	6.4801	16.522	22.085	23.064
3.0	6.0338	7.1767	17.023	22.461	24.062
4.0	6.5368	8.0114	17.638	22.966	25.321
5.0	7.1062	8.9334	18.335	23.615	26.702
6.0	7.7144	9.9187	19.107	24.343	28.056

a = 10 in., b = 10 in., h = 1 in.

In Table 10, a study has been made of the effect of change of modulus ratio of the [0/90/90/0] laminated composite plate on its fundamental frequency. It is observed that the change in the

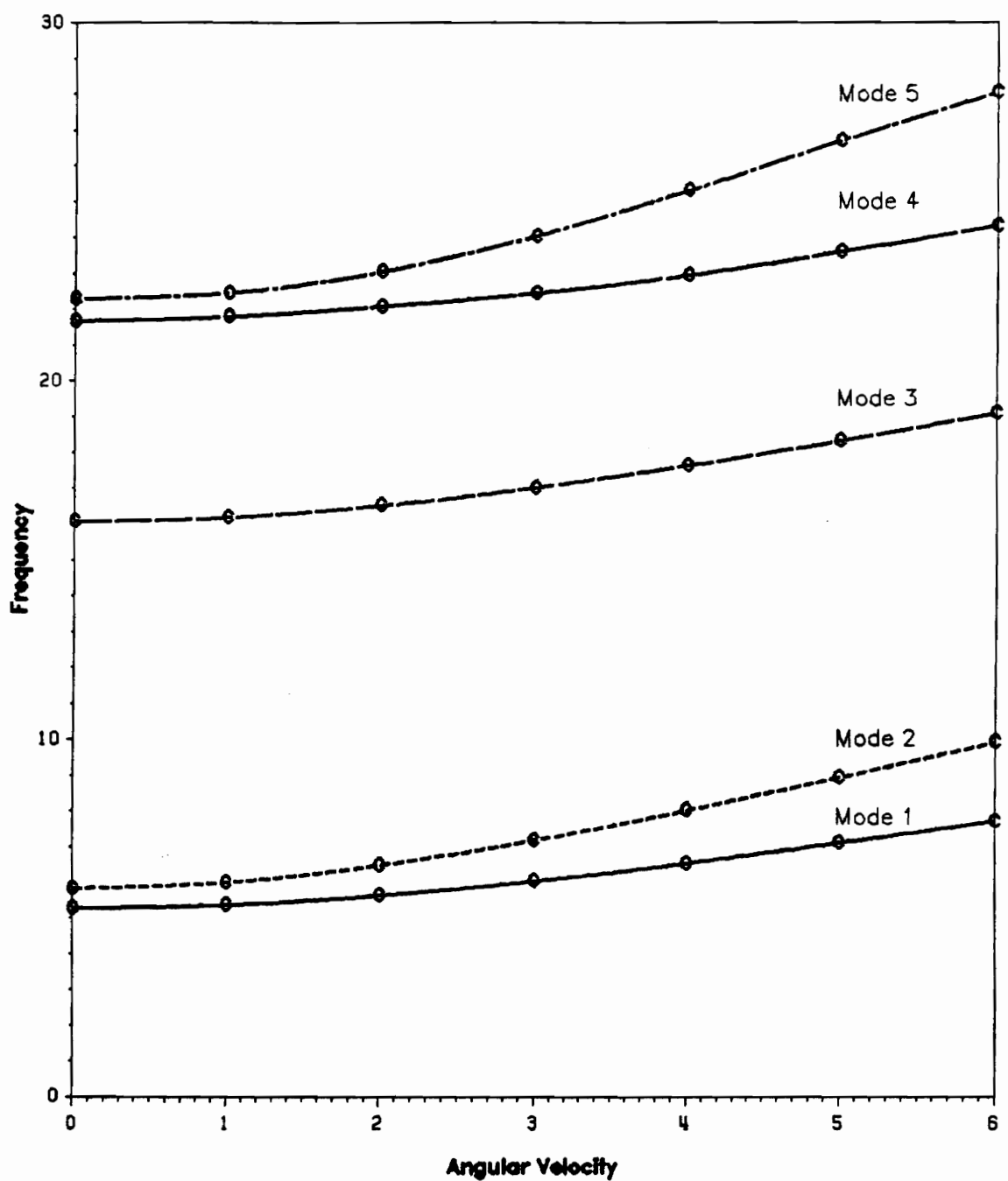


Figure 32. Variation in Frequency of Rotating Composite Plate with Angular Velocity for First 5 modes

Table 9. Variation in Fundamental Frequency of Rotating Plate with Side-to-Thickness Ratio

[0/90/90/0] Laminated Composite Plate					
$\bar{\omega} = (\omega a^2/h)\sqrt{\rho/E_2}$					
Angular Velocity $\bar{\Omega} = (\Omega a^2/h)\sqrt{\rho/E_2}$	a/h				
	4.0	10.0	20.0	50.0	100.0
0.0	3.5024	5.2761	5.8133	5.9935	6.0205
1.0	3.5047	5.3649	6.1737	7.9521	11.824
2.0	3.5142	5.6175	7.1091	11.749	19.854
3.0	3.5362	5.9994	8.3751	15.806	25.026
4.0	3.5753	6.4709	9.7946	19.676	-
5.0	3.6334	6.9956	11.262	23.043	-

a = 10 in., b = 10 in., h = 1 in.

E₁/E₂ = 40.0

fundamental frequency of the plate with angular velocity is maximum for low E₁/E₂ ratio and as the anisotropy increases, there is less change in the fundamental frequency with increase in angular

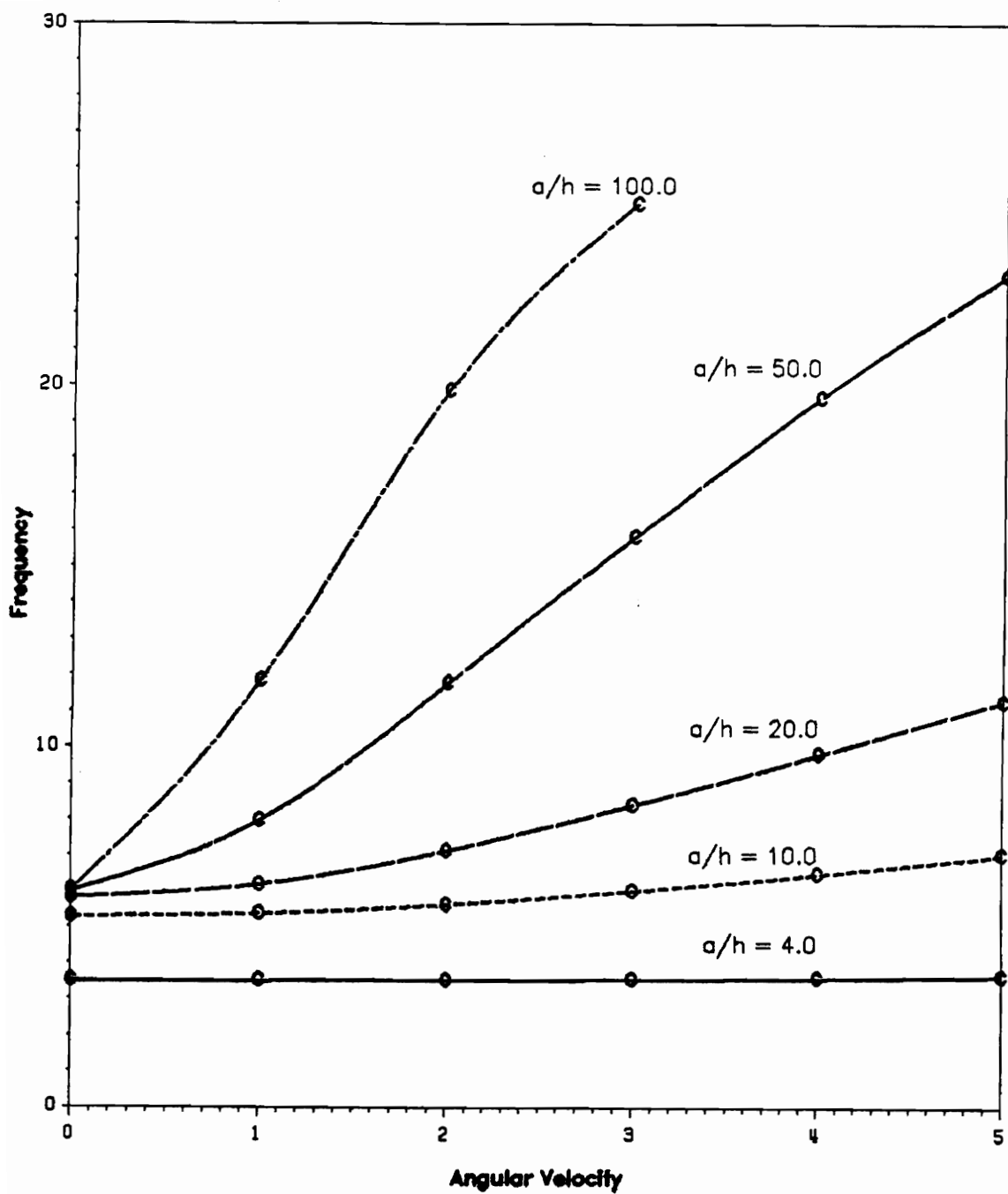


Figure 33. Variation in Fundamental Frequency of Rotating Plate with Angular Velocity for Different Side-to-Thickness Ratios

velocity of the plate. A plot of the variation of fundamental frequency of the plate with angular velocity for various values of the modulus ratio is shown in Figure 34.

Table 10. Variation in Fundamental Frequency of Rotating Plate with Modulus Ratio

[0/90/90/0] Laminated Composite Plate					
$\bar{\omega} = (\omega a^2/h)\sqrt{\rho/E_2}$					
Angular Velocity $\bar{\Omega} = (\Omega a^2/h)\sqrt{\rho/E_2}$	E_1/E_2				
	3.0	10.0	20.0	30.0	40.0
0.0	1.6749	2.9221	3.9776	4.7120	5.2761
1.0	1.9831	3.1027	4.1054	-	5.3649
2.0	2.6566	3.5686	4.4547	5.1054	5.6175
3.0	3.4254	4.1903	4.9958	5.5353	5.9994
4.0	4.1897	4.8777	5.5448	6.0562	6.4709
5.0	4.9106	5.5782	6.1737	6.6266	6.9956

$a = 10 \text{ in.}, b = 10 \text{ in.}, h = 1 \text{ in.}$

$a/h = 10$

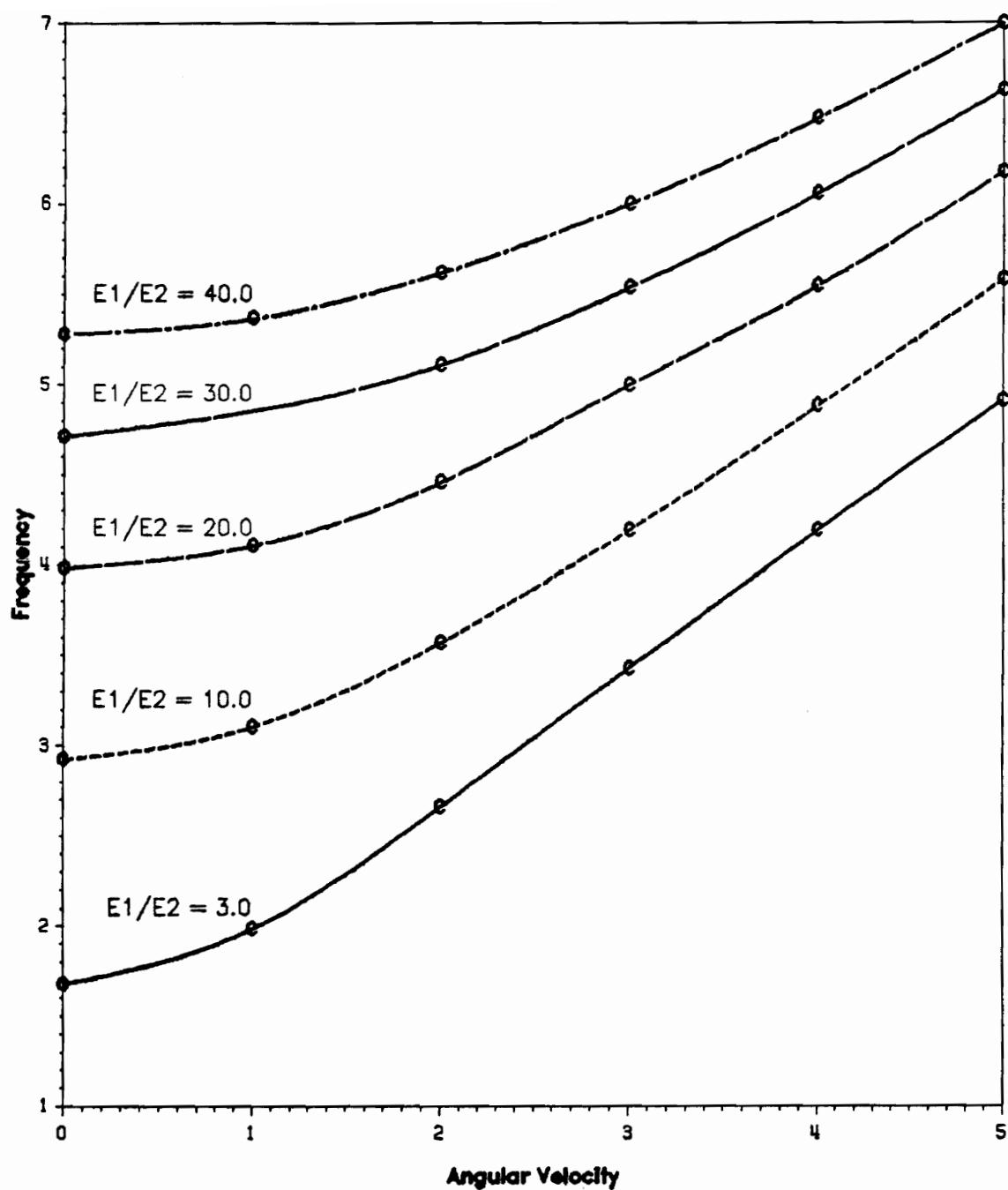


Figure 34. Variation in Fundamental Frequency of Rotating Plate with Angular Velocity for Different Modulus Ratios

5.0 CONCLUSIONS

A first-order shear deformation plate theory is used to analyze free vibrations in rotating plates. Results for some representative cases of plates rotating with cantilever boundary conditions are presented to serve as references for future experimental and analytical investigations.

There is an increase in the frequency of free vibration of rotating plates because of the stiffening of the plate caused by the centrifugal forces acting on it. The frequency of vibration is always seen to be higher than the angular velocity. There is a greater increase with angular velocity for laminated plates than for isotropic plates.

When the variation of frequency with angular velocity is studied for different plate thicknesses, it is seen that for thick plates, there is little change in frequency with angular velocity. The change is more rapid as the length-to-thickness ratio is increased. For different modulus ratios, it is seen that the frequencies of vibration are higher for plates with high modulus ratio though the increase with angular velocity is more rapid for plates with low modulus ratios.

This study can provide a basis for further studies in vibration of rotating plates with more complex geometries and incorporating aerodynamic loads. This can bring the problem closer to real-life situations involving vibrations of structures and their control.

REFERENCES

1. Chen, Lien-Wen and Chen Chung-Lu, "Vibration and Stability of Cracked Thick Rotating Blades", *Computers and Structures*, Vol. 28, No. 1, pp. 67-74 (1978)
2. Hodges, Dewey H. and Rutkowski, Michael J., "Free Vibration Analysis of Rotating Beams by a Variable-Order Finite Element Method", *AIAA Journal*, Vol. 19, No. 11 (Nov 1981)
3. Dokainish, M. A. and Rawtani, S., "Vibration Analysis of Rotating Cantilever Plates", *Int. J. Num. Meth. Eng.*, Vol. 3, pp. 233-248 (1971)
4. Gupta, K. K., "Recent Advances in Numerical Analysis of Structural Eigenvalue Problems"
5. Gupta, K. K., "Author's Reply - On a Combined Sturm Sequence and Inverse Iteration Technique for Eigenproblem Solution of Spinning Structures", *Int. J. Num. Meth. Engg.*, Vol. 9, pp. 488-489 (1975)
6. Gupta, K. K. "Development of a Block Lanczos Algorithm for Free Vibration Analysis of Spinning Structures", *Int. J. Numer. Meth. Eng.*, Vol. 26, pp. 1029-1037 (1988)
7. Gupta, K. K. "Development of a Unified Numerical Procedure for Free Vibration Analysis of Structures", *Int. J. Numer. Meth. Eng.*, Vol. 17, pp. 187-198 (1981)
8. Meirovitch, L., "A New Method for Solution of the Eigenvalue Problem for Gyroscopic Systems", *AIAA Journal*, Vol. 12, No. 10, (Oct 1974)
9. Bauchau, O. A., "A Solution of the Eigenvalue Problem for Underdamped Gyroscopic Systems with the Lanczos Algorithm", *Int. J. Numer. Meth. Eng.*, Vol. 23, pp. 1705-1713 (1980)
10. Meirovitch, L., "A Discussion of the Paper by K. K. Gupta", *Int. J. Num. Meth. Eng.*, Vol. 9, pp. 488-489 (1975)
11. Reissner, E., "The Effect of Transverse Shear Deformation on the Bending of Elastic Plates", *J. Appl. Mech.*, Vol. 12, pp. 69-77 (1945)

12. Mindlin, R. D., "Influence of Rotatory Inertia and Transverse Shear Deformation on the Flexural Motion of Isotropic, Elastic Plates", *J. Appl. Mech.*, Vol. 12, pp. 31-38 (1951)
13. Reddy, J. N., "A Review of the Literature on Finite-Element Modelling of Laminated Composite Plates", *Shock and Vibration Digest*, Vol. 17, No. 4, pp. 3-8 (April 1985)
14. Hughes, T. J. R., Taylor Robert L. and Kanoknukulchai, Worsak, "A Simple and Efficient Finite Element for Plate Bending", *Int. J. Num. Meth. Eng.*, Vol. 11, pp. 1529-1543 (1977)
15. Hughes, T. J. R. and Tezduyar, T. E., "Finite Elements Based upon Mindlin Plate Theory with Particular Reference to the Four-Node Bilinear Isoparametric Element", *J. App. Mech.*, Vol. 48, pp. 587-596 (Sept 1981)
16. Verhegghe, Benedict and Powell, Graham A., "Control of Zero-Energy Modes in 9-Node Element", *Int. J. Num. Meth. Eng.*, Vol. 23, pp. 863-869 (1986)
17. Levinson, M., "An Accurate Simple Theory of Statics and Dynamics of Elastic Plates", *Mech. Res. Commun.*, Vol. 7, No. 6, pp. 343-350 (1980)
18. Murthy, M. V. V., "An Improved Transverse Shear Deformable Theory for Laminated Anisotropic Plates", NASA Technical Paper (November, 1981)
19. Reddy, J. N., "A Refined Non-linear Theory of Plates with Transverse Shear Deformation", *Int. J. Solids Structures*, Vol. 20, No. 9/10, pp. 881-896 (1984)
20. Reddy, J. N., "A Simple Higher-Order Theory for Laminated Composite Plates", *J. App. Mech.*, Vol. 51., pp. 745-752 (1984)
21. Leissa, A. W., *Vibration of Plates*, NASA SP 160, Scientific and Technical Information Division, NASA, 1969
22. Jones, R. M., *Mechanics of Composite Materials*, Washington Scripta Book Company (1975)
23. Gorman, D. J., *Free Vibration Analysis of Rectangular Plates*, Elsevier, 1982
24. Reddy, J. N., *Energy and Variational Methods in Applied Mechanics*, Wiley (1984)
25. Reddy, J. N. and Phan, N. D., "Stability and Vibration of Isotropic, Orthotropic and Laminated Plates According to a Higher-Order Shear Deformation Theory", *J. Sound Vib.*, Vol. 98, No. 2, pp. 157-170 (1985)
26. Reddy, J. N., *An Introduction to the Finite Element Method*, McGraw-Hill Book Company (1984)
27. Thomson, W. T., *Theory of Vibration with Applications*, Prentice-Hall of India, 1982
28. Bathe, Klaus-Jurgen and Dvorkin, Eduardo N., "Short Communication A Four-Node Plate Bending Element Based on Mindlin/Reissner Plate Theory and a Mixed Interpolation", *Int. J. Num. Meth. Eng.*, Vol. 21, 367-383 (1985)
29. Brockman, R. A., "Dynamics of the Bilinear Mindlin Element", *Int. J. Num. Meth. Eng.*, Vol. 24, pp. 2343-2356 (1987)

30. Putcha, N. S. and Reddy, J. N., "A Refined Mixed Shear Flexible Finite Element for the Non-Linear Analysis of Laminated Plates", *Computers and Structures*, Vol. 22, No. 4, pp. 529-538 (1986)
31. Reddy, J. N., "A Small Strain and Moderate Rotation Theory of Elastic Anisotropic Plates", *J. App. Mech.*, Vol. 54, pp. 623-626 (Sept, 1987)
32. Reddy, J. N., "A Generalization of Two-Dimensional Theories of Laminated Composite Plates", *Comm. App. Num. Meth.*, Vol. 3, pp. 173-180 (1987)
33. Reddy, J. N. and Chandrashekhara, K., "Recent Advances in the Non-Linear Analysis of Laminates Composite Plates and Shells", *Shock and Vibration Digest*, Vol. 19, No. 4, pp. 3-9 (April 1987)
34. Reddy, J. N., "On the Solutions to Forced Motions of Rectangular Composite Plates", *J. App. Mech.*, Vol. 49, pp. 403-408 (June 1982)
35. Reddy, J. N. and Chao, W. C., "Large-Deflection and Large Amplitude Free Vibrations of Laminated Composite Plates", *Computers and Structures*, Vol. 13, pp. 341-347 (1981)
36. Reddy, J. N. and Sandiguel, D., "Mixed Finite Element Models for Laminated Composite Plates", *J. Engg. for Industry*, Vol.109, pp.39-45 (1987)

Appendix A. Element Matrices

Following the derivation of equations of motion and the derivation of the finite element equations for the dynamic analysis, the expressions for the element mass, stiffness and coriolis matrices have been derived. For the stiffness matrix, only the centrifugal stiffness matrix is given as the linear and the non-linear stiffness matrices are the usual ones for the rectangular plate element based on the first-order shear deformable plate theory.

I_1, I_2, I_3 are as defined in equation [2.3.23]. ϕ_i and ϕ_j are the interpolation functions as described in Appendix A.

The element stiffness, coriolis and mass matrices for the plate are given in terms of the element sub-matrices as follows :

A.1.1 Stiffness Matrix :

A.1.1.1 Linear Stiffness Matrix (K^L) :

$$[K^L] = \begin{bmatrix} (K_{ij}^{11})^L & (K_{ij}^{21})^L & (K_{ij}^{31})^L & (K_{ij}^{41})^L & (K_{ij}^{51})^L \\ (K_{ij}^{12})^L & (K_{ij}^{22})^L & (K_{ij}^{32})^L & (K_{ij}^{42})^L & (K_{ij}^{52})^L \\ (K_{ij}^{13})^L & (K_{ij}^{23})^L & (K_{ij}^{33})^L & (K_{ij}^{43})^L & (K_{ij}^{53})^L \\ (K_{ij}^{14})^L & (K_{ij}^{24})^L & (K_{ij}^{34})^L & (K_{ij}^{44})^L & (K_{ij}^{54})^L \\ (K_{ij}^{15})^L & (K_{ij}^{25})^L & (K_{ij}^{35})^L & (K_{ij}^{45})^L & (K_{ij}^{55})^L \end{bmatrix}$$

where $(K_{ij}^{\alpha\beta})^L$ are the element submatrices for linear stiffness components.

A.1.1.2 Non-Linear Stiffness Matrix (K^{NL}) :

$$[K^{NL}] = \begin{bmatrix} (K_{ij}^{11})^{NL} & (K_{ij}^{21})^{NL} & (K_{ij}^{31})^{NL} & (K_{ij}^{41})^{NL} & (K_{ij}^{51})^{NL} \\ (K_{ij}^{12})^{NL} & (K_{ij}^{22})^{NL} & (K_{ij}^{32})^{NL} & (K_{ij}^{42})^{NL} & (K_{ij}^{52})^{NL} \\ (K_{ij}^{13})^{NL} & (K_{ij}^{23})^{NL} & (K_{ij}^{33})^{NL} & (K_{ij}^{43})^{NL} & (K_{ij}^{53})^{NL} \\ (K_{ij}^{14})^{NL} & (K_{ij}^{24})^{NL} & (K_{ij}^{34})^{NL} & (K_{ij}^{44})^{NL} & (K_{ij}^{54})^{NL} \\ (K_{ij}^{15})^{NL} & (K_{ij}^{25})^{NL} & (K_{ij}^{35})^{NL} & (K_{ij}^{45})^{NL} & (K_{ij}^{55})^{NL} \end{bmatrix}$$

where $(K_{ij}^{\alpha\beta})^{NL}$ are the element submatrices for non-linear stiffness components.

A.1.1.3 Centrifugal Stiffness Matrix (K^{CF}) :

$$[K^{CF}] = \begin{bmatrix} (K_{ij}^{11})^{CF} & (K_{ij}^{21})^{CF} & (K_{ij}^{31})^{CF} & (K_{ij}^{41})^{CF} & (K_{ij}^{51})^{CF} \\ (K_{ij}^{12})^{CF} & (K_{ij}^{22})^{CF} & (K_{ij}^{32})^{CF} & (K_{ij}^{42})^{CF} & (K_{ij}^{52})^{CF} \\ (K_{ij}^{13})^{CF} & (K_{ij}^{23})^{CF} & (K_{ij}^{33})^{CF} & (K_{ij}^{43})^{CF} & (K_{ij}^{53})^{CF} \\ (K_{ij}^{14})^{CF} & (K_{ij}^{24})^{CF} & (K_{ij}^{34})^{CF} & (K_{ij}^{44})^{CF} & (K_{ij}^{54})^{CF} \\ (K_{ij}^{15})^{CF} & (K_{ij}^{25})^{CF} & (K_{ij}^{35})^{CF} & (K_{ij}^{45})^{CF} & (K_{ij}^{55})^{CF} \end{bmatrix}$$

where $(K_{ij}^{\alpha\beta})^{CF}$ are the element submatrices for centrifugal stiffness components.

A.1.2 Coriolis Matrix :

$$[C] = \begin{bmatrix} C_{ij}^{11} & C_{ij}^{21} & C_{ij}^{31} & C_{ij}^{41} & C_{ij}^{51} \\ C_{ij}^{12} & C_{ij}^{22} & C_{ij}^{32} & C_{ij}^{42} & C_{ij}^{52} \\ C_{ij}^{13} & C_{ij}^{23} & C_{ij}^{33} & C_{ij}^{43} & C_{ij}^{53} \\ C_{ij}^{14} & C_{ij}^{24} & C_{ij}^{34} & C_{ij}^{44} & C_{ij}^{54} \\ C_{ij}^{15} & C_{ij}^{25} & C_{ij}^{35} & C_{ij}^{45} & C_{ij}^{55} \end{bmatrix}$$

where $C_{ij}^{\alpha\beta}$ are the element submatrices for coriolis components.

A.1.3 Mass Matrix :

$$[M] = \begin{bmatrix} M_{ij}^{11} & M_{ij}^{21} & M_{ij}^{31} & M_{ij}^{41} & M_{ij}^{51} \\ M_{ij}^{12} & M_{ij}^{22} & M_{ij}^{32} & M_{ij}^{42} & M_{ij}^{52} \\ M_{ij}^{13} & M_{ij}^{23} & M_{ij}^{33} & M_{ij}^{43} & M_{ij}^{53} \\ M_{ij}^{14} & M_{ij}^{24} & M_{ij}^{34} & M_{ij}^{44} & M_{ij}^{54} \\ M_{ij}^{15} & M_{ij}^{25} & M_{ij}^{35} & M_{ij}^{45} & M_{ij}^{55} \end{bmatrix}$$

where $M_{ij}^{\alpha\beta}$ are the element submatrices for mass components.

A.2 Centrifugal Stiffness Matrix (K^{CF})

The sub-matrices of the element stiffness matrix can be expressed in the following form :

$$(K_{ij}^{11})^{CF} = \int_{\Omega^e} -I_1 (\Omega_y^2 + \Omega_z^2) \phi_i \phi_j dx dy$$

$$(K_{ij}^{12})^{CF} = \int_{\Omega^e} I_1 (\Omega_y \Omega_x) \phi_i \phi_j dx dy$$

$$(K_{ij}^{13})^{CF} = \int_{\Omega^e} I_1 (\Omega_z \Omega_x) \phi_i \phi_j dx dy$$

$$(K_{ij}^{14})^{CF} = \int_{\Omega^e} -I_2 (\Omega_y^2 + \Omega_z^2) \phi_i \phi_j dx dy$$

$$(K_{ij}^{15})^{CF} = \int_{\Omega^e} I_2 (\Omega_y \Omega_x) \phi_i \phi_j dx dy$$

$$(K_{ij}^{21})^{CF} = \int_{\Omega^e} I_1 (\Omega_x \Omega_y) \phi_i \phi_j dx dy = (K_{ij}^{12})^{CF}$$

$$(K_{ij}^{22})^{CF} = \int_{\Omega^e} - I_1 (\Omega_z^2 + \Omega_x^2) \phi_i \phi_j dx dy$$

$$(K_{ij}^{23})^{CF} = \int_{\Omega^e} I_1 (\Omega_z \Omega_y) \phi_i \phi_j dx dy$$

$$(K_{ij}^{24})^{CF} = \int_{\Omega^e} I_2 (\Omega_x \Omega_y) \phi_i \phi_j dx dy$$

$$(K_{ij}^{25})^{CF} = \int_{\Omega^e} - I_2 (\Omega_z^2 + \Omega_x^2) \phi_i \phi_j dx dy$$

$$(K_{ij}^{31})^{CF} = \int_{\Omega^e} I_1 (\Omega_x \Omega_z) \phi_i \phi_j dx dy = (K_{ij}^{13})^{CF}$$

$$(K_{ij}^{32})^{CF} = \int_{\Omega^e} I_1 (\Omega_y \Omega_z) \phi_i \phi_j dx dy = (K_{ij}^{23})^{CF}$$

$$(K_{ij}^{33})^{CF} = \int_{\Omega^e} - I_1 (\Omega_x^2 + \Omega_y^2) \phi_i \phi_j dx dy$$

$$(K_{ij}^{34})^{CF} = \int_{\Omega^e} I_2 (\Omega_x \Omega_z) \phi_i \phi_j dx dy$$

$$(K_{ij}^{35})^{CF} = \int_{\Omega^e} I_2 (\Omega_y \Omega_z) \phi_i \phi_j dx dy$$

$$(K_{ij}^{41})^{CF} = \int_{\Omega^e} - I_2 (\Omega_y^2 + \Omega_z^2) \phi_i \phi_j dx dy = (K_{ij}^{14})^{CF}$$

$$(K_{ij}^{42})^{CF} = \int_{\Omega^e} I_2 (\Omega_x \Omega_y) \phi_i \phi_j dx dy = (K_{ij}^{24})^{CF}$$

$$(K_{ij}^{43})^{CF} = \int_{\Omega^e} I_2 (\Omega_x \Omega_z) \phi_i \phi_j dx dy = (K_{ij}^{34})^{CF}$$

$$(K_{ij}^{44})^{CF} = \int_{\Omega^e} - I_3 (\Omega_y^2 + \Omega_z^2) \phi_i \phi_j dx dy$$

$$(K_{ij}^{45})^{CF} = \int_{\Omega^e} I_3 (\Omega_x \Omega_y) \phi_i \phi_j dx dy$$

$$(K_{ij}^{51})^{CF} = \int_{\Omega^e} I_2 (\Omega_y \Omega_x) \phi_i \phi_j dx dy = (K_{ij}^{15})^{CF}$$

$$(K_{ij}^{52})^{CF} = \int_{\Omega^e} - I_2 (\Omega_z^2 + \Omega_x^2) \phi_i \phi_j dx dy = (K_{ij}^{25})^{CF}$$

$$(K_{ij}^{53})^{CF} = \int_{\Omega^e} I_2 (\Omega_y \Omega_z) \phi_i \phi_j dx dy = (K_{ij}^{35})^{CF}$$

$$(K_{ij}^{54})^{CF} = \int_{\Omega^e} I_3 (\Omega_x \Omega_y) \phi_i \phi_j dx dy = (K_{ij}^{45})^{CF}$$

$$(K_{ij}^{55})^{CF} = \int_{\Omega^e} -I_3 (\Omega_x^2 + \Omega_z^2) \phi_i \phi_j dx dy$$

A.3 Coriolis Matrix (C)

The sub-matrices of the element coriolis matrix can be expressed in the following form :

$$C_{ij}^{11} = 0$$

$$C_{ij}^{12} = \int_{\Omega^e} -2I_1 \Omega_z \phi_i \phi_j dx dy$$

$$C_{ij}^{13} = \int_{\Omega^e} 2I_1 \Omega_y \phi_i \phi_j dx dy$$

$$C_{ij}^{14} = 0$$

$$C_{ij}^{15} = \int_{\Omega^e} -2I_2 \Omega_z \phi_i \phi_j dx dy$$

$$C_{ij}^{21} = \int_{\Omega^e} 2I_1 \Omega_z \phi_i \phi_j dx dy = -C_{ij}^{12}$$

$$C_{ij}^{22} = 0$$

$$C_{ij}^{23} = \int_{\Omega^e} -2I_1 \Omega_x \phi_i \phi_j dx dy$$

$$C_{ij}^{24} = \int_{\Omega^e} 2I_2 \Omega_z \phi_i \phi_j dx dy$$

$$C_{ij}^{25} = 0$$

$$C_{ij}^{31} = \int_{\Omega^e} -2I_1 \Omega_y \phi_i \phi_j dx dy = -C_{ij}^{13}$$

$$C_{ij}^{32} = \int_{\Omega^e} -2I_1 \Omega_x \phi_i \phi_j dx dy = -C_{ij}^{23}$$

$$C_{ij}^{33} = 0$$

$$C_{ij}^{34} = \int_{\Omega^e} -2I_2 \Omega_y \phi_i \phi_j dx dy$$

$$C_{ij}^{35} = \int_{\Omega^e} 2I_2 \Omega_x \phi_i \phi_j dx dy$$

$$C_{ij}^{41} = 0$$

$$C_{ij}^{42} = \int_{\Omega^e} -2I_2 \Omega_z \phi_i \phi_j dx dy = -C_{ij}^{24}$$

$$C_{ij}^{43} = \int_{\Omega^e} 2I_2 \Omega_y \phi_i \phi_j dx dy = -C_{ij}^{34}$$

$$C_{ij}^{44} = 0$$

$$C_{ij}^{45} = \int_{\Omega^e} -2I_3 \Omega_z \phi_i \phi_j dx dy$$

$$C_{ij}^{51} = \int_{\Omega^e} 2I_2 \Omega_z \phi_i \phi_j dx dy = -C_{ij}^{15}$$

$$C_{ij}^{52} = 0$$

$$C_{ij}^{53} = \int_{\Omega^e} -2I_2 \Omega_x \phi_i \phi_j dx dy = -C_{ij}^{35}$$

$$C_{ij}^{54} = \int_{\Omega^e} 2I_3 \Omega_z \phi_i \phi_j dx dy = -C_{ij}^{45}$$

$$C_{ij}^{55} = 0$$

A.4 Mass Matrix (M)

The sub-matrices of the element mass matrix can be expressed in the following form :

$$M_{ij}^{11} = \int_{\Omega^e} I_1 \phi_i \phi_j dx dy$$

$$M_{ij}^{12} = 0$$

$$M_{ij}^{13} = 0$$

$$M_{ij}^{14} = \int_{\Omega^e} I_2 \phi_i \phi_j dx dy$$

$$M_{ij}^{15} = 0$$

$$M_{ij}^{21} = 0$$

$$M_{ij}^{22} = \int_{\Omega^e} I_1 \phi_i \phi_j dx dy$$

$$M_{ij}^{23} = 0$$

$$M_{ij}^{24} = 0$$

$$M_{ij}^{25} = \int_{\Omega^e} I_2 \phi_i \phi_j dx dy$$

$$M_{ij}^{31} = 0$$

$$M_{ij}^{32} = 0$$

$$M_{ij}^{33} = \int_{\Omega^e} I_1 \phi_i \phi_j dx dy$$

$$M_{ij}^{34} = 0$$

$$M_{ij}^{35} = 0$$

$$M_{ij}^{41} = \int_{\Omega^e} I_2 \phi_i \phi_j dx dy$$

$$M_{ij}^{42} = 0$$

$$M_{ij}^{43} = 0$$

$$M_{ij}^{44} = \int_{\Omega^e} I_3 \phi_i \phi_j dx dy$$

$$M_{ij}^{45} = 0$$

$$M_{ij}^{51} = 0$$

$$M_{ij}^{52} = \int_{\Omega^e} I_2 \phi_i \phi_j dx dy$$

$$M_{ij}^{53} = 0$$

$$M_{ij}^{54} = 0$$

$$M_{ij}^{55} = \int_{\Omega^e} I_3 \phi_i \phi_j dx dy$$

Vita

Ravinder Bhumbra was born on February 13, 1965 in Hissar, India. He graduated from Delhi Public School, R. K. Puram, New Delhi in May, 1982. He obtained a Bachelor of Engineering in Mechanical Engineering and a Master of Science in Mathematics from Birla Institute of Technology and Science, Pilani, India in May 1987. He joined the Engineering Science and Mechanics Department in Virginia Polytechnic Institute and State University (Virginia Tech) in September 1987 to pursue a Master's degree.

Ravinder Bhumbra